ISSN: 2331-1959 Volume 6, Number 3, July 2018

Scientific Research Publishing

Archaeological Discovery

ISSN: 2331-1959

9 772331 195007 03

www.scirp.org/journal/ad

Journal Editorial Board

ISSN Print: 2331-1959 ISSN Online: 2331-1967

http://www.scirp.org/journal/ad

Archaeological Discovery, 2018, 6, 187-277
http://www.scirp.org/journal/ad
ISSN Online: 2331-1967
ISSN Print: 2331-1959

Table of Contents

Volume 6 Number 3 July 2018

Archaeological Discovery (AD)
Journal Information

SUBSCRIPTIONS

The *Archaeological Discovery* (Online at Scientific Research Publishing, www.SciRP.org) is published quarterly by Scientific Research Publishing, Inc., USA.

Subscription rates:
Print: $39 per issue.
To subscribe, please contact Journals Subscriptions Department, E-mail: sub@scirp.org

SERVICES

Advertisements
Advertisement Sales Department, E-mail: service@scirp.org

Reprints (minimum quantity 100 copies)
Reprints Co-ordinator, Scientific Research Publishing, Inc., USA.
E-mail: sub@scirp.org

COPYRIGHT

PRODUCTION INFORMATION

For manuscripts that have been accepted for publication, please contact:
E-mail: ad@scirp.org

Archaeological Discovery, 2018, 6, 187-195
http://www.scirp.org/journal/ad
ISSN Online: 2331-1967
ISSN Print: 2331-1959

Discussion on the Reinforcement Technology of the Fragile Bronze Ware Unearthed in the Archaeological Process

Xingang Tan

University of Chinese Academy of Sciences, Beijing, China
Email: tanxingang@163.com

How to cite this paper: Tan, X. G. (2018). Discussion on the Reinforcement Technology of the Fragile Bronze Ware Unearthed in the Archaeological Process. *Archaeological Discovery, 6,* 187-195.
https://doi.org/10.4236/ad.2018.63010

Received: March 26, 2018
Accepted: May 18, 2018
Published: May 31, 2018

Abstract

During the archaeological excavation process, the reinforcement of the unearthed fragile bronze ware concerns the long-term preservation and subsequent protection of the bronze wares. Therefore, the reinforcement technology must be scientific, safe and effective. Starting from the protection and restoration work of the fragile bronze ware unearthed at the excavation site, this paper first introduces the background of bronze ware, and then introduces the characteristics of vulnerable bronze ware. Finally, from the point of protection of fragile bronze ware, this paper studies the related reinforcement technologies in order to provide reference for the protection and restoration of archaeological excavation culture.

Keywords

Archaeology, Bronze Ware, Corrosion, Reinforcement Technology

1. Introduction

Bronze ware plays an important role in the history of material civilization in ancient China. It is the wisdom of our ancestors, and it has a place in the history of world art. Bronze ware first appeared in the late Neolithic period to the Qin and Han dynasties, and reached its peak in the late Shang and early western Zhou dynasties. Among them, the Shang and Zhou utensil designs are the most exquisite. Until the late spring and autumn period to the early warring states period, the heavy use of iron made the bronze ware less and less. As the bronze ware had been buried underground for too long, there were different degrees of corrosion when unearthed, which made some bronzes very fragile. Especially in southern

China, the underground burial conditions are very poor due to the weather and geographical factors. So, all the bronze wares unearthed in the archaeological process are very fragile, and some have even been mineralized, which makes the excavation and protection very tricky. If not careful, people will destroy the cultural relics, and cause a defect that cannot be fixed permanently. This paper studies and summarizes the reinforcement technology of the fragile bronze ware unearthed at the archaeological site by analyzing the excavations of multiple archaeological sites (Li & Jin, 2014).

2. The Relevant Historical Background of Bronze Ware

From an archaeological point of view, the bronze ware in China refers to the bronze wares of the Shang, Western Zhou dynasties and the spring and autumn period. These objects are mainly made of copper, with a small amount of tin and lead. The color of the objects is steel grey and hence its name. Its main types are tools, weapons, cooking utensils, food container, wine container, water container, harness, etc. It has a variety of shapes and exquisite patterns. Its inscription is a treasure of calligraphy. The bronze wares of the Shang dynasty and the early western Zhou dynasty are dignified and elaborate. The ornamentations are mostly the gluttony, Kui dragon grain, animal prints and geometric patterns. The inscription is simple with few words.

From mid-western Zhou dynasty to mid-spring and autumn period, the styles of bronze wares tend to be simple, and the shape is casual. Ornamentation is also a geometric pattern of fine lines. But there are more bronze wares with the long inscriptions. This may be because of the development of the word. From late spring and autumn period to the warring states period, the bronze wares are light and thin. Besides the animal prints and geometric patterns, they are also decorated with a pattern of hunting, war, and banquets with fine lines.

The invention of bronze ware was an epoch-making creation. The three historical periods of Chinese Shang, western Zhou and spring and autumn period belong to the Bronze Age. But when did Chinese bronzes first appear? There is a legend called "Chi You Lead soldiers". It is said that Chi You led the army to attack the Huangdi tribe. The two sides fought in the field of Zhuo Lu. At the beginning of the war Chi You army was victorious. Because they have five kinds of weapons, which are dagger-axe, bamboo weapon, halberd, Monsieur beaucaire spear and Yi spear. These weapons are estimated to be made of copper. Later, Huangdi made the south-pointing chariot for war and turned the tide. At last, Huangdi subdued Chi You.

The book *Zi Hua Zi* also recorded that Huangdi sent people to a copper mine and transported the copper ore to the foot of Jing Mountain and cast a tripod as a victory in war. As described above, bronze ware is of great importance to the study of our history and culture. Therefore, we should try our best to protect them.

3. The Corrosion and Characteristics of Bronze Wares

3.1. The Corrosion of Bronze Ware

Bronze is an alloy which is mainly composed of copper, tin and lead, and also contains very small amounts of iron, zinc, manganese, silicon, arsenic and phosphorus and so on. The bronze relics of the bronze age in China are mainly tin bronze and lead bronze (Yuan & Hou, 2013).

In relatively suitable conditions (such as low temperature, low humidity, no uv irradiation, no harmful gas, etc.), the corrosion layer of bronze ware can generally be stable. If the environment changes, especially affected by temperature and humidity, it is easy to produce bronze powdery rust. The researchers studied the atmospheric corrosion of copper in different areas, and believed that the influence of external environment is an important factor leading to the corrosion of bronze ware. Therefore, the anoxic environment before the excavation of the bronze ware has entered the enriched oxygen environment, which is the most important cause of its corrosion.

Bronze artifacts usually adhere to a large amount of corrosion products when unearthed. The corrosion products can be divided into harmful rust and harmless rust.

Harmless rust can enhance the artistic value of bronze cultural relics and has a certain protective effect. Harmless rust is the protective layer formed by the change of the bronze surface after the bronze ware is immersed in the water, buried by soil and corroded by the atmosphere, which can protect the cultural relics from suffering corrosion. Its chemical constituents include black copper oxide, red oxide, green or blue-green alkali carbonate. Blue copper is sometimes mixed with black copper sulfide, white tin oxide and so on. These are the stable, colorful and finely formed elements of the bronze rust. However, harmful rust will powder and destroy bronze cultural relics, and even shorten their life. When it is serious, the whole bronze wares will be pulverized, or even completely destroyed. In addition, it can damage other bronzes. It is contagious between the bronzes themselves and with other bronzes. Its chemical composition is mainly cuprous chloride and basic copper chloride. Alkaline copper chloride is the main component of the powdery rust of bronze. Harmful rust is a kind of copper rust which develops rapidly and has a malignant expansion. It is the copper rust which has the main effects on the bronze ware.

3.2. The Characteristics of Bronze Wares

China's bronze wares are not only abundant, but also rich in shape and variety. Each one has a different style in each era. The same object of the same age has a variety of styles. And bronze varies from region to region, which likes a hundred flowers in bloom. Therefore, bronze ware has very high ornamental value. From the point of view of cultural relic appraisal, it certainly adds to the difficulty of identifying. It is difficult to identify, which in turn makes the study more interesting, and makes bronze more attractive.

The reputation of ancient bronze ware in China is not in the quantity, but the quality. There are a lot of high-quality bronze wares in ancient China, especially at the end of the Shang dynasty, when Chinese bronze ware manufacturing was at its peak. The bronze ware at this time is exquisitely made, beautifully patterned and magnificent. Of course, the spring and autumn and warring states periods also had a number of special novel bronzes. In the existing Shang and Zhou bronze wares, the Si Mu Wu Square Ding (Figure 1) is famous for its huge size. It is 133 centimeters high and weighs 875 kilograms. It is majestic in appearance. In the slave society of Shang dynasty, it was not easy to make such a huge bronze tripod. It embodies the high level of bronze casting technology in ancient China. The Tiger Cannibalism You, a wine vessel, is a rare art treasure. The general body sits in like a tiger in a sitting position. The two back claws and tail of the tiger are three supporting points. And the tiger's front claws are forcefully holding a person with a discordant foot and makes a eating form. The modelling is very vivid. And from the girder to the three branches are all decorative patterns. The casting is exquisite and gives the person beauty enjoyment. In addition, like He Zun, Wall Dish, Li GUI and Big Grams Tripod in the western Zhou dynasty, the lotus flower pot in the spring and autumn period, and banquet and percussion pot in the warring states period and so on are all treasures of the country and of the arts. So, bronzes are different from bones. It has complex shapes and colorful patterns, which increased the appreciation of art.

4. Protection of Fragile Bronzes

4.1. The Maintenance Method of Bronze Ware

The destroyer of bronze ware is chloride ion, water vapor and other harmful gases. Green powdery rust (Figure 2) is the archenemy for bronzes. The ways to deal with it: One is mechanical method. Clean the powdery embroidery on the surface of the bronze ware and the gray-white cuprous chloride covered below

Figure 1. The Si Mu Wu Square Ding.

Figure 2. A bronze ware with green powdery rust

carefully by using stainless steel needles, hammers and steel knives. Two is chemical method. Chemical reagents are used to prepare the derusting solution. Then expose the harmful bronze to the derusting liquid and make them react in a chemical way. In this way, the harmful rust of the bronze is converted into a stable substance without chloride ion (Mo, 2014).

Three is the electrochemical reduction method. Electrochemical reduction can restore the corrosion of bronzes to uncorroded state. The reduction metal should be made of zinc powder or aluminum powder. The electrolyte solution is 10% sodium hydroxide solution. But in order to preserve the beautiful mineralization layer of ancient bronze ware, the electrochemical reduction can only be used for the local treatment of the harmful rust of bronzes. Thus, the ornamentation and inscriptions are clearly displayed. Four is the closed method. It is still difficult to convert the copper chloride completely and thoroughly. Therefore, we can seal the cuprous chloride with chemical and physical methods to isolate it from oxygen, chlorine, water vapour and other harmful gases in the air and stabilize the bronzes. Five is comprehensive protection method. In order to better and more effectively protect the corrosion of bronze ware, we can adopt the protection method of combining silver oxide, benzotriazole and surface seal. First, we clean the corroded bronzes with distilled water, then close the corrosion zone "bronze disease" with the silver oxide method and seal its surface with benzotriazole solution. This comprehensive protection method by using benzotriazole is one of the most ideal protection methods to date.

4.2. The Repair Technology of Bronze Ware

Bronze repair purpose is to restore the broken or deformed bronze to its original shape through various repair methods, for example, welding method, the method of pin, mould, pounding, sawing method and filling method. The welding

method is the basic method to combine the broken pieces of bronze ware or the matching pieces with the main body. In the process of welding, the first step is to find a few pieces of debris adjacent to the residual, then press the edge of the nibble to close the welding. After most of the debris is welded, and the shape and pattern position are accurate, then carry out the solid welding. Then find the tiny pieces and splice them together. However, it is worth noting that as the temperature of the welding method is too high, and the harm of weld junctions have great persecution to copper, we should minimize the use of it. Sometimes some bronze fragments are very thin and suitable for bonding. In the process of bonding, the adhesive should be evenly applied to the interface. The glue is fully integrated into the section so that the gap is completely bonded. If the paste is not even, it will produce bubbles and reduce the strength. In order to strengthen the adhesion, we also can feel the gap between the sections and bond it with copper strip. The ratio of copper powder to viscose is 1:1. For larger objects, due to the width and thickness of the mouth, the adhesive strength is not enough, and the pin can be added at the edge of the mouth (Chen, Tian, Li., Gao, Xie, Liang, Ma, Li, & Yang, 2013).

5. Researches on Strengthening Technology of Fragile Bronze Ware

5.1. Archaeological Site Reinforcement

Because the fragile bronze ware is extremely fragile, it holds the basic shape of the bronze ware, but it cannot be directly extracted from the archaeological site. However, due to the restrictions of temperature and humidity of the archaeological site and operating space, the technology of improving the ontology strength is limited by strengthening the ontology method on site. So, we must change our thinking way. Protecting the vulnerable bronzes by strengthening the support is to extract the bronze ware with the surrounding soil.

According to the size and soil conditions of the fragile bronzes and considering the working time and work cost in the actual situation at the same time, different overall extraction techniques should be adopted. The overall extraction technology includes box method, gypsum method and polyurethane foam method. As to the big fragile bronze wares and the complicated situation of many fragile bronze ware overlying, we should adopt the case method to carry out the whole extraction. The *Archaeological Work Manual* published by Institute of Archaeology, Chinese Academy of Social Sciences in 1982 introduced the overall extraction method of cases in detail (Institute of Archaeology, Chinese Academy of Social Sciences, 1982). When the bronze ware is large, the weight may be several tons. It may use the cranes and the cost is relatively high.

Gypsum and polyurethane foam are specially designed for small and fragile objects. They are used frequently and the operation is relatively simple. The two methods of field extraction are to reserve the earth table for the fragile bronze ware at the archaeological site. After the surface is set up with Xuan paper and

polyethylene film, the soil table is extracted using gypsum or polyurethane foam. Gypsum is cheaper and easier to get in daily life. After the cast, the extraction part of the quality increased, and the gypsum will be easily broken. So, there is also the addition of hemp inside gypsum to enhance its toughness. Polyurethane foam is also very convenient and light. Its greatest drawback is that it has certain toxicity. And the cost is higher than the gypsum.

5.2. Laboratory Reinforcement Techniques

The first is the traditional reinforcement method. Reinforce the fragile bronze body and increase its strength. The traditional method is to adopt decompression permeation or surface painting other permeable polymer materials. To strengthen the fragile bronzes in the laboratory, first of all, in the process of surface soil cleaning, a part revealed of the fragile noumenon should be reinforced immediately. According to the degrees of vulnerability, the color changes of composite reinforcement materials, temperature, humidity and other factors, 1% - 5% B72 trimethyl resin acetone solution could be used to strengthen it, or fluorine rubber 2311 used by Nanjing museum Wan Li research could be used. Finally, the requirements for the entire surface of the vulnerable bronze vessels are reinforced. Due to the different corrosion degrees of the fragile bronze vessels, the number of penetrated reinforcement could not be accurately confirmed. Therefore, in the process of decompression penetration or surface coating, repeat operations over time until the object absorbs. In the surface coating operation process, when the amount of brushing exceeds the capacity to absorb, a membranous substance will be formed on the surface of the object. In this case, stop osmosis and clean the superfluous membrane materials in order to meet the requirement of not changing the color of cultural relics.

The second method is the backlining reinforcement treatment. Due to the poor preservation conditions of some bronzes, the reinforcement method of surface permeable polymer material has some certain limitations. The strength of most large and vulnerable bronzes is still very low through by penetrating surface polymer materials. The strength of the object itself cannot meet the mechanical requirements of standing. Therefore, in order to achieve better reinforcement effect, we adopt the technique of backlining reinforcement (Wang, 2010).

Use AAA glue to harmonize mineral pigment. Reinforce the inner lining of the utensil with a glass fiber cloth as the support, when the glue is dry, a certain color processing is done to let the color be similar to the color of the object. The reinforcement process is in the interior of the utensil, so, it will not affect the appearance of cultural relics and cover the pattern or text of the object. The thickness of the backing layer is less than 1 mm. It plays a decisive role in strengthening the whole fragile cultural relics.

The process of backing reinforcement: with the support of peripheral gypsum or polyurethane foam to the cultural relics, remove the soil from the mouth of

the utensil first, and immediately reinforce the inside of the mouth of the device. The mouth is the import and export of the soil inside. Tools and soil are frequently in and out. It is inevitable to have repeated collision between mouth and mouth edge. Slight inadvertences will completely destroy the mouth and mouth edge. After the glue in the mouth is dried, clean the soil deeper inside the bronzes and strengthen the back lining accordingly. Do not remove the soil from the inside of the utensil at once, because the bronze ware with serious corrosion will be in danger of collapse.

The third method is to remove gypsum or polyurethane foam. After the backing is hardened, remove all the gypsum or polyurethane foam. As to the bronze ware which are well preserved, only the foot is relatively thin, the foot strength could not bear the weight of the relic, only the inner lining of the fragile circle is treated with the same backing.

6. Conclusion

To sum up, historical relics are important cultural assets of China. It is an important symbol of the economic development of the times. The development, research and preservation of historical relics will help us to study the culture and history of the past. China attaches great importance to the protection of historical relics. However, the protection of vulnerable bronze vessels should be taken seriously from the excavation site. It is necessary to make a preplan for the protection of the fragile bronze ware before the excavation. In previous archaeological excavations, the protection of cultural relics was rarely involved. The phenomenon of paying attention to excavation and neglecting protection is widespread. Most of the cultural relics in the archaeological site cannot be timely and effectively protected, which caused irreparable damages. In recent years, with the continuous improvement of China's archaeological technology, the archaeological site protection of unearthed cultural relics is gradually taken into account. The earlier the conservation force is involved in archaeological excavations, the more powerful the protection of vulnerable cultural relics will be.

References

Chen, H., Tian, J., Li, X. F., Gao, J. Z., Xie, Y. G., Liang, Y. Z., Ma, W. J., Li, L., & Yang, X. F. (2013) Progress in Restoration and Protection of Bronze Relics. *Corrosion and Protection, 9,* 4-9.

Institute of Archaeology, Chinese Academy of Social Sciences (1982) *Archaeological Work Manual,* 3-15.

Li, R. L., & Jin, P. (2014) A Brief Discussion on the Inheritance and Development of the Traditional Restoration Techniques of the Bronze Ware in the South—Take Anhui Museum for Example. *Identification and Appreciation of Cultural Relics, 3,* 09.

Mo, P. (2014) Protection and Restoration of Vulnerable Bronze Ware Unearthed in Pre-Qin Period in Guangdong Province. *Restoration and Research of Cultural Relics, 1,* 3-8.

Wang, F. Z. (2010) Large Bronze Cultural Relics in Pre-Qin Period. *Casting Equipment*

and Technology, 4, 11-18.

Yuan, X. H., & Hou, X. M. (2013) The Scientific Analysis and Corrosion Mechanism and Protection Methods of Bronze Cultural Relics Are Briefly Described. *Luoyang Archaeological, 3,* 10.

Archaeological Discovery, 2018, 6, 196-215
http://www.scirp.org/journal/ad
ISSN Online: 2331-1967
ISSN Print: 2331-1959

Two French Oil Terminals in the WWII

Giancarlo T. Tomezzoli

Etno-Archaeological Observatory, Munich, Germany
Email: gt21949@gmx.de

How to cite this paper: Tomezzoli, G. T. (2018). Two French Oil Terminals in the WWII. *Archaeological Discovery, 6,* 196-215.
https://doi.org/10.4236/ad.2018.63011

Received: April 19, 2018
Accepted: June 5, 2018
Published: June 8, 2018

Abstract

Often, literature suggests that the Atlantic Wall was a set of support points (*Stützpunkte*) and fortresses (*Festungen*) extended from Norway up to Spain. This concept is not completely wrong but it masks the logistics involved in its defence activity. In this article the parallel destiny of the Talards and Bouchemaine oil terminals active in France during the German occupation and both having failed a complete destruction is considered. Original air recognition images, archive documents, information from experts and visits on the terrain helped a lot in clarifying their history, organization and preservation states. From previous publications and the present article, it appears now clear that the Atlantic Wall study must be addressed as an interdisciplinary matter with the contributions of experts in different fields.

Keywords

WWII, Atlantic Wall, Saint-Malo, Talards, Angers, Bouchemaine, Oil, Kerosene, Terminal, France

1. Introduction

Previous publications provided some hint about the Atlantic Wall logistics by presenting two structures involved in its construction (Tomezzoli, 2015; Tomezzoli & Marzin, 2015) and a logistic base (Tomezzoli, 2016). Now sufficient material has accumulated concerning two other structures involved, this time, in its fuel supply. United by the common destiny to be active in France during the German occupation and both having failed a complete destruction, the Talards and the Bouchemaine oil terminals respectively in Saint-Malo and near Angers had parallel stories which are here considered.

2. The Talards Oil Terminal (Saint-Malo)

The Talards oil terminal was built on a side of an internal basin of the

Saint-Malo harbour, named Mare aux Canards (Ducks Pond). It was skirted by a branch of the railway coming from the nearby Saint-Malo *SNCF* station and by the metric railway line Rennes - La Mazière - Saint-Malo of the TIV (Tramways d'Ille et Villaine). From 1939 the oil terminal was operated by Les Pétrole de l'Ouest founded on 20th January 1936, head office at 2 rue Joseph Sauveur, Rennes and the Societé Armoricaine des Carburants, head office at 8 quai de Richemond, Rennes. From 1940 the terminal was operated by Societédes Dépôts de Petrole de Cherbourg, head office at 42 rue de Washington, Paris 8 (Élysée District) together with Societé des Dépôts Côtiers, head office at the same address in Paris, which was also the head office address of the Societé Shell (Pottier, 2013) (**Figure 1**). The rapid German offensive in France on May-June 1940 caused the defeat of the French army and the retreat of the British Expeditionary Force toward the French ports for embarking toward Great Britain. A letter dated 27th July 1989 of the Rear Admiral Howard-Johnson, let evocate those days in the following terms. On June 1940, tenth of thousands British soldiers were in Saint-Malo harbour, waiting for embarking. The Rear Admiral demolition group arrived in Saint-Malo on 17th June 1940 from Portsmouth on board of HMS Wild Swan, after a brief stop at Saint Helier (Jersey Island). During the stop, a meeting took place with the Commodore of the Saint Helier Yacht Club in which the Rear Admiral explained him that the Wild Swan has not to remain to Saint-Malo and, because of the orders, after the work, the group had to leave Saint-Malo on foot toward West. If the Yacht Club sent boats to Saint-Malo the departure of the group would have been simplified. After the embarking of most of the British soldiers, further disbanded soldiers arrived at the harbour often without weapons and sometime with cognac bottles generously offered by Frenchs. The group was formed by the Rear Admiral and 25 voluntaries and had eight tons of explosives for the demolition of the harbour facilities. They were all sailors with the exception of a military officer of the Royal Engineers; the only

Figure 1. Talards oil terminal—pre-war image, on the left oil tanks, on the right entrance gate, on the foreground left the still existing square tower of the Civic Centre of the Louis Martin Avenue in front of the Commerce Chamber (Pottier, 2013; Archive Saint-Malo, 1940).

expert in demolitions. The group had nothing to do with the soldiers' embarking, but in absence of gendarmes and French military units it taken all in the hands comprising the destruction of the cognac bottles. A group of disbanded soldiers arrived one day followed by a Belgian taxi with four British officers two of which injured. At the last moment Belgian nurses arrived on board of a magnificent ambulance. During the night they encountered German tanks on the road to Rennes. Up to that moment nobody knows that the Germans were so close. They told that the Germans were at Dôle. The only Dôle known by the Rear Admiral was on the way to Switzerland. Just at the moment of the Germans arrival, he realised that Dôle was actually Dol-de-Bretagne, 20 km from Saint-Malo.

Before to leave London the Rear Admiral received three hundred pounds in banknotes and the order to proceed to the demolitions under the orders of the French authorities. At the group arrival, the situation was chaotic, but the French Navy Commander in Saint-Malo was found. The Commander received no information from Paris or the Naval Prefecture in Normandy concerning the group mission. He beware the group and the explosives. He was Vessel Captain and the Rear Admiral a Frigate Captain at that time; therefore, the Commander was the French authority sought. After two days, the Commander authorised the Rear Admiral to put explosives at the basin sluices and at the oil tanks. Cars and trucks, often completely new British trucks, were parked in the city hippodrome. French guards all around the hippodrome prevented the group to bring these vehicles toward a beach and in the water. The group had no baggage and slept where it was possible, often on pavements. The group fed in a bistrot of a dock and this reduced the pounds received. The general De Gaulle appeal was diffused by the bistrot radio, but the Commander received no order Paris or elsewhere about how to react. At the end, the Commander convened the Rear Admiral urgently at the town hall together with other city authorities to receive the Germans. He ordered the Rear Admiral to do what he could. The group had no time for well demolish the harbour sluices, but just the time to burn the gasoline tanks. The German flag waved on the city hall when the group leaved the harbour thanks to the boats and the courage of the of Saint Helier Yacht Club members (Pottier, 2013). A further letter of the Rear Admiral of 28th July 1989 let still to evocate those days in the following terms. Lines of railway wagons with military supplies and clothing were on the harbour docks. The HMS Wild Swan crew provided the Rear Admiral with eight smoke floats which he lit in the narrow streets of Saint-Malo. A westerly breeze propagates a dense smoke screen which he hoped would have delayed the German entrance. He wondered if it did that. When Saint-Malo crowds were plundering all the stores, he remarked a chap who said in French "we will only be left with our eyes to cry". Without the Saint Helier Yacht Club he supposed not to be alive today (Pottier, 2013). The Wild Swan was lost on 17th June 1942 because of an air bomb in the Gascoigne Gulf.

A thick column of smoke from the burning terminal tanks remained visible for days. Avro Ansons of 48th RAF Squadron patrolling off the French coast documented columns of smoke and flames from the Talards oil tanks (**Figure 2**, **Figure 3**) set on fire by the Howard-Johnson's demolition group. However, the terminal was not completely destroyed and it was rapidly put back in operation (Brichet & Peyle, 2005) for the supply of kerosene to the Luftwaffe fighters and bombers stationed at the nearby airfield of Dinard-Pleutuit (Lippmann, 2012; Tomezzoli et al., 2013; Tomezzoli, 2014; Dahiot et al., 2009), participating to the battle of Britain (10th July - 31st October 1940). A daily supply of kerosene to the airfield was possible by road, crossing the Saint-Hubertus bridge 15 km south of Saint-Malo or by using the ferry Saint-Malo-Dinard. In both the cases this would have caused unacceptable delivery delays. To overcome this problem, the German *Luftwaffe* decided the requisition of the self-propelled barges in the harbour. Each barge filled its bunkers at the Talards terminal, leaved Saint-Malo harbour, reached the mouth of the Rance river and docked at a mooring peer near La Richardais. There a pumping station extracted the kerosene from the barges and sent it to the airfield by means of a pipeline. The barges were a dozen comprising Esso, Naphta I, Naphta II, Marie-Therese, Chantilly, Galem and Molan (Brichet & Peyle, 2005).

The oil terminal (48˚38'38.34"N, 2˚00'41.61"W) (**Figure 4**) was definitively dismantled at the beginning of the years two thousands. Several visits in the harbour in looking for possible terminal surviving components provided no result.

3. The Bouchemaine Oil Terminal (Angers)

The Bouchemaine oil terminal construction began on 1939, following a French law which obliged the edification of oil terminals outside sea harbours. The platforms construction and the tanks mounting were completed at the beginning

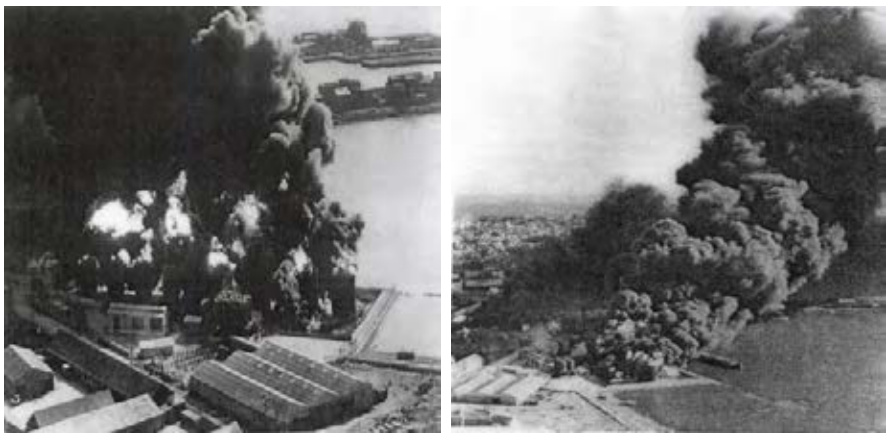

(a) (b)

Figure 2. Talards oil terminal—(a) tanks on fire (Imperial War Museum, RAF Coastal Command); (b) smoke column above the tanks (Imperial War Museum, RAF Coastal Command) on the right a tanker at the mooring peer.

Figure 3. Talards oil terminal on fire (Imperial War Museum, RAF Coastal Command, Cat.: C 1802).

Figure 4. Talards oil terminal organization—a: 1st area—main tanks burned by the Howard-Johnson's demolition group; b: 2nd area; c: 3rd area; d: 4th area, e: mooring peer; f: degaussing station (Tomezzoli & Pottier, 2016); g: moored barges; h: movable bridge; i: Bouvet basin; j: Jacques Cartier basin - Mare aux Canards; k: railway; l: bombarded zone; m: railway; n: Talards casern. (Mission identification: C1115-0331_1944_106G1614_4005, cliché n 4005, scale: 1/10313, cliché type: Argentique, Date de prise de vue: 24/07/1944).

of 1940. The oil terminal comprised four tanks coded A, B, D and E, each 16.1 m in diam., 10.5 m height, 2140 m^3 in capacity, ten tanks coded 1 to 10 each of 50 m^3 in capacity, a dock with a pumping station on the board of the Maine river, a pipeline, a pipeline metal bridge on the *SNCF* railway, a rail depot for receiving tank trains, a charging station for tank trucks, a site canalization net and an anti-fire station (Figure 5). The refuelling of the oil terminal was assured by self-propelled barges and tankers coming from the refinery of Donge at the mouth of the Loire river and by tank trains. The pumping station extracted the

Figure 5: Bouchemaine—b: damaged suspended bridge; d: oil dock; r: railway; t: oil terminal; B:Bouchemaine; L: Loire river; M: Maine river.(Mission identification: C93PHQ8041_1948_CDP3032_0010, cliché n˚ 10, scale: 1/5034, cliché type: Argentique, Date de prise de vue: 17/09/1948).

fuel from the tankers and pumped it in the pipeline. Responsible of the oil terminal was Mr J-E. Chaffot president and director general (*PDG*) of Les Pétroles de l'Ouest (the same company operating the Talards oil terminal), *PDG* of Béton Cellulaire and manager of Les Sablières de Bretagne. Administrators were Mr M. Laussel, war prisoner on 1941, and Mr Denoual. The tanks A-B were managed by Les Pétroles de l'Ouest, the tanks D-E were sold on 31st July 1942 to Pétrole Jupiter (Shell). The personnel comprised 18 workers and employees. In period of the terminal reconstruction (March 1945 - November 1946) their salaries varied between 10.5 and 30 *Frs* per hour with a taxation up to 67%.

An assurance policy was negotiated on 29th Mai 1940 for the risk of burning. The administration council of 6th September 1940 confirmed the normal functioning of the oil terminal notwithstanding the war. From 12th June 1941 to 8th August 1944 the oil terminal was under requisition of the German *Kriegsmarine*.

A 1943 administrative report made apparent that the incomes from the fuel sale was practically nothing and that the only benefits came from the rent of the fuel tanks, the fees payed by the *Kriegsmarine* for the terminal requisition and from other minor activities. On 1944 a sum of 49,726 *Frs* was affected to a provision chapter for the war risks (Oil Terminal Archive, 2018).

During the requisition were built: an octagonal concrete wall 10.5 m height with a variable thick of 1 m at the base to 0.80 m at the top around each tank A-E, a six side wall around the tanks 1 to 10, a bunker at the terminal entrance, a further bunker and a building. The *Kriegsmarine* proceeded to new installations comprising some groups of motor-cycle pumps *Renault-Guinard* of 180 m^3 and tubes larger in diameter (8", 10").

The damages to the oil terminal came from the *Kriegsmarine* requisition and from allied bombardments on July 1944 in which about 24 - 29 bombs hit the terminal site. Three damages reports of 7th November 1944, 2nd April 1945 and 12th March 1946 estimated the damages as follows: tank A damaged at 60%, tank B at 30%, footbridge between the two tanks and accessing stair completely destroyed, tank E about 40 holes on the cap, tank D about 20 holes on the cap, footbridge between the two tanks and accessing stairs slightly distorted by projectile impacts, 1 to 10 tanks 66 perforations on nine tanks, three houses (offices, concierge, WC) damaged, the pipeline metal bridge partially destroyed, 209 m of pipes on the site partially destroyed, 1 hangar damaged at 80%, entrance portal and barriers destroyed at 100%.

At its retreat the *Kriegsmarine* brought away a charging post for trucks, three electro-pumps *Mouvex* of 28 m^3, two of the three counters *Thémis* of 2500 litres of capacity, pipes either in place or in stock for a length of 1221 m, a basin of 5 × 3 m, an oil remover, bronze valves, soldering material and other materials.

On 24th November 1944 a sum of 3,540,000 *Frs* was authorized for the terminal reconstruction, which started on March 1945 and terminated on November 1946 (Oil Terminal Archive, 2018). Les Petrole de l'Ouest was definitively acquired by the group Elf on 1989.

3.1. The Oil Dock

The oil dock visit took place on 4th January 2018. The identified components were the following.

The dock platform (Figure 6), about 126 × 27 m, completely covered by grass, about 450 m far from the oil terminal. Nine well preserved minor columnar bollards, each formed by a concrete prismatic column about 0.5 m large and 1.5 m height with a small metallic bollard at the top, were aligned on its river side. Five main columnar bollards a, b, d, e, f, each having a concrete square base about 5 m large with a superimposed concrete octagonal column of about 3 m in long diagonal and 3 m height with a metallic railing and a metallic bollard at the top, were aligned in its middle. Some well preserved concrete supports of an original metallic barrier and two prismatic, concrete, white columns marking a dock entrance were aligned in its land side (Figure 7(b), Figure 7(c), Figure 7(e)).

Bollard a (47˚25'0.72"N, 0˚36'44.98"W, 16.53 m) (Figure 7(b)) was in good preservation state with possible traces of white painting. Its square base was covered by grass. It presented two steps on four opposed column sides, a metallic stair on two opposed column sides, a railing and a blue painted bollard on its top. Two tubes of a possible ground system were fixed on two column sides.

Bollard b (47˚24'59.91"N, 0˚36'45.57"W, 16.45 m) (Figure 7(c), Figure 7(d)) was in good preservation state with possible traces of white painting. Its square base was covered by grass. It presented two steps on four opposed column sides, a metallic stair on four opposed column sides, a railing and a grey painted bollard on its top. One mooring ring, about 30 cm in diameter was attached on four opposed column sides.

Bollard c and the superimposed pumping station have disappeared (Figure 7(e)).

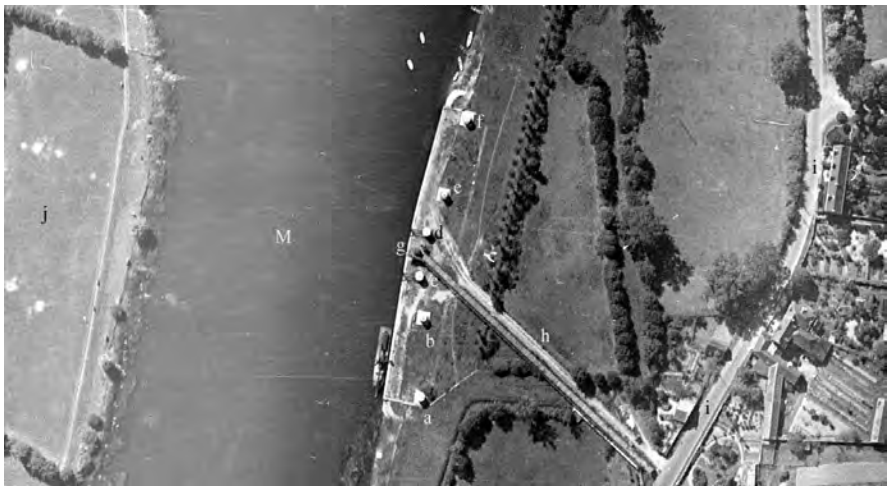

Figure 6. Bouchemaine oil dock—a, b: main columnar bollards; c: disappeared main columnar bollard; d, e, f: main columnar bollards; g: pumping station; h: dock's access road—pipeline road; i: actual rue Chevrière; j: possible bomb impact craters, M: Maine river. (Mission identification: C93PHQ8041_1948_CDP3032_0010, cliché n˚10, scale: 1/5034,cliché type: Argentique, Date de prise de vue: 17/09/1948).

(a)

(b)

(c)

(d)

(e)

(f)

(g)

(h)

(i)

(j)

Figure 7. Bouchemaine oil dock—(a) suspended bridge; (b) platform and columnar bollard a, on the foreground the columnar bollard (b), (d), (e) and the supports of an original metallic barrier; (c) platform and columnar bollard b on the foreground the columnar bollard (d), (e) and supports of the barrier; (d) columnar bollard (b), details; (e) platform, location of the disappeared columnar bollard (c) with superimposed pumping station, on the left and on the foreground left the minor columnar bollards, on the foreground right entrance, concrete white columns and columnar bollard (d); (f) columnar bollard d with two small square holes at a stair lower side; (g) columnar bollard (e); (h) columnar bollard (e), on the fore-ground the columnar bollard (d); (i) columnar bollard (f); (j) unpaved pipeline road.

Bollard d (47˚24'59.03"N, 0˚36'46.24"W, 16.49 m) (**Figure 7(e)**, **Figure 7(f)**) was in good preservation state with possible traces of a white painting. Probably deprived of a square base (**Figure 7(f)**), it presented a metallic stair on four opposed column sides, a railing and a grey bollard on its top. Minor mooring rings were present on the column sides and two small square holes at a stair lower side let suspect that its interior was empty.

Bollard e (47˚24'58.75"N, 0˚36'46.81"W, 16.44 m) (**Figure 7(g)**, **Figure 7(h)**) was in good preservation state without traces of painting. Its square base was covered by grass. It presented two steps on four opposed column sides, a metallic stair on four opposed column sides, a railing and a white painted bollard on its top. One small mooring ring, about 5 cm in diameter was present on four opposed column sides.

Bollard f (47˚24'58.08"N, 0˚36'47.71"W, 16.40 m) (**Figure 7(i)**) was in good preservation state, with possible traces of white painting. Its square base

emerged from the grass. It presented two steps on four opposed column sides, no metallic stair on the column sides, a railing and a white painted bollard on its top. Two tubes of a possible ground system were fixed on two column sides.

3.2. The Oil Pipeline

The oil pipeline connected the oil dock d to the oil terminal t (Figure 8). The pipeline began at the pumping station initially located between the bollards c, d. Subsequently, the pumping station was elevated on the top surface of bollard c and, in recent years a metallic platform was added for facilitating oil barges and tankers discharging (Figures 9(a), Figures 9(b)). From the pumping station, the pipeline, partly buried, continued on one side of an unpaved road and then it turned west along the actual rue Chevrière, before to bend at a right angle to cross cultivated fields up to a metal bridge on the *SNCF* railway and enter the oil terminal. The bollard c, the pumping station and the metallic platform were demolished in 2012 (Figures 9(a)-(d)). The pipeline was probably dismantled or remains buried in the terrain and no longer visible.

3.3. The Oil Terminal

Figure 10 shows the oil terminal organization and is particularly touching because its high quality permits, by enlargement, to distinguish a train formed by a puffing steam locomotive towing 35 wagons crossing the Bouchemaine stations and transiting under the pipeline metal bridge on the faraway day of 17th September 1948.

The oil terminal visit took place on 4th January 2018. The terminal identified components were the following.

The main terminal entrance g, comprising a well preserved white painted German small rectangular bunker (47˚25'9.32"N, 0˚37'1.24"W) (Figure 11(a))

Figure 8. oil pipeline—c: rue Chevrière; d: oil dock; s: pumping station on bollard c; p: pipeline; j: pipeline metal bridge on the *SNCF* railway; r: *SNCF* railway; t: oil terminal. (Mission identification: C1522_0281_1954_CDP860_0358, cliché n˚358, scale: 1/4090, cliché type: Argentique, Date de prise de vue: 12/04/1954).

(a) (b)

(c) (d)

Figure 9. Pumping station and bollard c demolition—(a) side view, on the left the added metallic platform with oil discharging tubes, on the foreground right the columnar bollards d, e (courtesy Mr F. Guillaume, 07th November 2006); (b) side view, on the foreground left the columnar bollard b, on the right the metallic platform with oil discharging tubes (courtesy Mr F. Guillaume, 07th November 2006); (c) platform and pumping station demolition (courtesy Mr F. Guillaume); (d) bollard c demolition (courtesy Mr F. Guillaume).

Figure 10. Bouchemaine oil terminal—a: 1st area; b: 2nd area; c: six side wall with tanks 1 to 10; A, B, D, E labelled octagonal walls and corresponding oil tanks; d: possible disappeared structure; e: damaged building; f: protected passage to the building e or anti-tank trench; g: terminal main entrance/exit; h: bunker; i: bunker; j: pipeline metal bridge; k: Bouchemaine freight station; l: Bouchemaine passenger station; m: excavation; n: train; o: entrance/exit p: minor construction; q: hangar; r: *SNCF* railway line, s: railway depot. (Mission identification: C93PHQ8041_1948_CDP3032_0010, cliché n˚10, scale: 1/5034, cliché type: Argentique, Date de prise de vue: 17/09/1948).

(a) (b)

Figure 11. Bouchemaine oil terminal—(a) small German bunker h at the entrance; (b) after war electrical distribution cabin.

about 9 × 4 m. The nearby electrical distribution cabin, not present in **Figure 10**, was built well after the war.

A well preserved oval concrete platform (47˚25'9.44"N, 0˚37'3.63"W) (**Figure 12**) about 7 × 3 m, 30 cm high with two bases for vertical structures on its surface.

Octagonal wall A (47˚25'8.45"N, 0˚37'3.82"W) (**Figure 13**) about 20 m in long diagonal, still protecting the original tank refurbished several times after the war. It presented a three steps external structure with some large concrete superficial failures that left uncovered rods of the internal armour. On one side was a slightly eroded white board with the label A G8 1897 M^3 indicating a tank capacity inferior to the above mentioned capacity of 2140 m^3. On another side a circular, yellow metallic cover marked with a black label A closed the access to the tank protected by the wall.

Octagonal wall B (47˚25'8.84"N, 0˚37'4.81"W) (**Figure 12**) about 20 m in long diagonal, still protecting the original tank refurbished several times after the war. It presented a three steps external structure with some local concrete superficial failures leaving uncovered rods of the internal armour. On one side was an eroded white board with the label B G8 1897 M^3. On another side a circular, yellow metallic cover marked with a black label B closed the access to the tank protected by the wall.

Octagonal wall D (47˚25'7.44"N, 0˚37'4.71"W) (**Figure 14**) about 20 m in long diagonal, still protecting the original tank refurbished several times after the war. It presented a three steps external structure with some local concrete superficial failures, leaving uncovered rods of the internal armour, and projectile impact cavities due to air attack. On one side was a white board whose label B G8 1897 M^3 was abraded and covered by a blue, square board with a white label Er. On another side a circular, yellow metallic cover marked with a black label D closed the access to the tank protected by the wall.

Octagonal wall E (47˚25'7.85"N, 0˚37'5.7"W) (**Figure 15**) about 20 m in long diagonal, still protecting the original tank refurbished several times after the war. It presented a three steps external structure with some local concrete superficial

Figure 12. Bouchemaine oil terminal 1st area—on the left the six sides wall, in the middle octagonal wall A, on the right octagonal wall B, near the octagonal wall B, on the ground, the oval platform.

(a) (b)

Figure 13. Octagonal wall A—(a) three steps external structure with white board; (b) local concrete superficial failures.

(a) (b)

Figure 14. octagonal wall D—(a) external structure with white board covered by a square, blue board; (b) concrete pit with connection pipes.

failures leaving uncovered rods of the internal armour and projectile impact cavities due to air attack. On one side was a white board whose label B G8 1897 M3 was abraded and covered by a blue, square board with a square, white label. On another side was a circular, yellow metallic cover marked with a black label E closed the access to the tank protected by the wall. The access was a circular, metallic passage in the wall, about 1 m in diameter. The wall internal structure was vertical with no steps and in perfect preservation stage showing the traces of

(a)

(b)

(c)

(d)

(e)

(f)

(g)

(h)

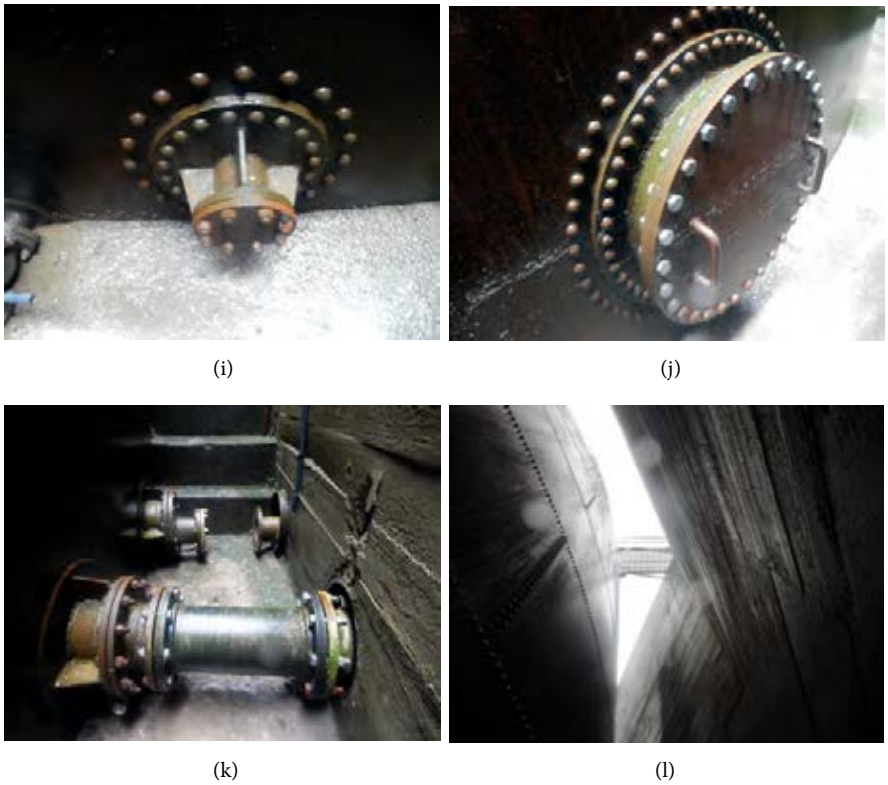

(i) (j)

(k) (l)

Figure 15. Octagonal wall E—(a) abraded white board covered by a square blue board; (b) garage leaning against the wall; (c) projectile impact cavities; (d) projectile impact cavity; (e) circular, yellow metallic cover; (f) wall internal structure; (g) metallic pin in the wall; (h) hydraulic valve; (i) riveted tank access; (j) riveted tank access; (k) connection pipes; (l) wall internal structure and tank riveted structure.

the construction formwork elements (**Figure 15(f)**), typical of the German masonry, confirming its German construction. The tank presented a black, riveted surface with connection pipes crossing the wall.

Six sides wall c (47˚25'7.01"N, 0˚37'3.79"W) (**Figure 16(a)**) about 17 × 13 m, which encircled the disappeared tanks 1 to 10. It presented a well preserved external three step structure without concrete superficial failures and projectile impact cavities.

A manifold (47˚25'8.85"N, 0˚37'3.25""W) (**Figure 16(b)**) about 7 × 3 m of polygonal, irregular shape, about two m deep, near octagonal wall A, containing pipes for the distribution of oil among the tanks. Not present in **Figure 10**, it was built well after the war. From one of its sides a long pipe gone towards the Bouchemaine freight station.

Bunker i (47˚25'8.84"N, 0˚37'6.11"W) (**Figure 17(a)**, **Figure 17(b)**) about 7 × 3 m, buried in the terrain. The coverage, crossed by pipes and a light bridge, appeared in a good preservation state without damages due to concrete failures or projectile impact cavities. On the coverage were circular holes of about 5 cm in diameter. The entrance was obstructed by the terrain so that the inspection of the interior was not possible.

(a) (b)

Figure 16. Bouchemaine oil terminal—(a) six sides wall; (b) after war manifold.

(a) (b)

(c) (d)

Figure 17. Bouchemaine oil terminal—(a) bunker i crossed by pipes, west view; (b) bunker i crossed by pipes, east view; (c) possible buried bunker under pipes; (d) pipes exit toward the freight station, in the foreground left the Bouchemaine passenger station.

The entrance/exit o (**Figure 18**) already presents during the period of the German occupation and now main entrance of the oil terminal. Its concrete structure presented no damages.

No trace on the terrain has been found of the building e, about 60 × 12 m, the protected passage to the building or anti-tanks trench f and the excavation m (**Figure 10**).

4. Discussion

The re-evocations of Rear Admiral Howard-Johnson refers to the days of the operation Aerial in which British and allied forces were evacuated from 15th to

Figure 18. Bouchemaine oil terminal—present main entrance.

25th June 1940 from west France harbours, after the conclusion of the evacuation operations Dynamo from 26th May to 4th June 1940 from Dunkirk and Cycle from 10th to 13th June 1940 from Le Havre and vividly reflects the chaotic atmosphere of those days.

A French air recognition image of 13th August 1944 (**Figure 4**), few days after the conclusion of the Saint-Malo battle, reveals many details of the Talards oil terminal. It was composed by a 1st area a comprising a first group of 11 main tanks, a second group of 2 smaller tanks and a third group of 9 still smaller tanks located close one to the other, a 2nd area b comprising 4 tanks, a 3rd area c comprising 2 tanks and a 4th area d comprising 4 tanks. The tanks of the first group, burned by the Howard-Johnson's group, stored the most required fuel in the region of Saint-Malo, probably gasoline for car and trucks. The fuel supply was ensured by barges and tankers moored to the mooring peer e (**Figure 2**, **Figure 4**). After the Battle of Britain no important *Luftwaffe* unit stationed at the Dinard-Pleurtuit airfield. Therefore, the tanks surviving the burning certainly stored fuels for the *Kriegsmarine* ships in stop or stationed at the harbour and the *Kriegsmarine* and *Heer* vehicles. A pumping station was certainly located on or near the mooring dock e. Because crossing the Channel by oil tankers was dangerous due to the RAF surveillance, it is possible that the fuel came mainly by train, probably from the refinery of Le Havre. A railway contoured the terminal second and third areas b, c; therefore it is possible that the fuel arrived by train was discharged somewhere there, although **Figure 4** does not show a railway depot as in the railway station of Bouchemaine (**Figure 10**). **Figure 4** shows that the Germans did not constructed walls for protecting the terminal tanks surviving the burning and that the allied bombardments of Saint-Malo failed to touch the terminal.

The questions about: the possible German oil terminal requisition, the volumes and oil kinds actually dealt with at the terminal during the war, the reason for which the oil terminal was not dynamited by the Germans during the battle of Saint-Malo, and many other possible questions concerning the Talards oil terminal remain to be answered.

A French air recognition image of 17th September 1944 (**Figure 10**), exactly

one month after the conclusion of the Saint-Malo battle, reveals many details of the Bouchemaine oil terminal. As the Talards oil terminal, it was composed by a 1st area a comprising, in this case, a first group of 4 main tanks each protected by an octagonal wall and a second group of 10 smaller tanks located close one to the other and all protected by a six sides wall. The fuel supply was ensured by trains, which parked in the railway depot s and by barges and tankers coming from the refinery of Donge, which moored at the oil dock d. The main columnar bollards were so big and high for a sure mooring of barges and tankers in the Maine stream also during the Maine floodings, in which the dock platform was covered by water. The pumping station on the top of columnar bollard c permitted oil pumping also during the floodings. Because no sign of German masonry was remarked, the dock platform and its bollards were of French construction. The small bunker h at the terminal entrance was probably a guardhouse and the bunker i a refuge for the personnel lodged in the building e or an ammunition and material depot bunker. The excavation m inclined with respect to the *SNCF* railway (**Figure 10**) reveals the German intention to expand the railway depot s by constructing a second, protected railway depot opposed with respect to the *SNCF* railway to the depot s. The adaptation of the oil terminal to the *Kriegsmarine* needs and the excavation m were probably directed by the *Organization Todt* supervising the work of French requisitioned firms, workers and vehicles. The oil terminal t and the tank wagons parked in the depot s have not been object of attacks by the French resistance. The nearby suspended bridge on the Maine (**Figure 7(a)**), considered of strategical importance, was dynamited by the Germans in retreat with the loss of one of its two ways (**Figure 5**).

The questions about: why the oil terminal was requisitioned by the *Kriegsmarine* and not by the *Heer* or the *Luftwaffe*, why the requisition was made in June 1941 and not before, which were the volumes and the oils actually dealt with at the terminal during the war, if the oil terminal supplied in kerosene the *Luftwaffe* fighters and bombers *Stuka* and *Dornier* of the 10 km far away, today disappeared, airfield of Avrillé (Angers), the reasons for which the oil terminal and the oil dock were not dynamited by the Germans in retreat, and many other possible questions concerning the Bouchemaine oil terminal remain to be answered.

5. Conclusion

In previous articles, fundamental emerged the role of witnesses and experts for identifying and explaining surviving or disappeared structures of the Atlantic Wall. In this article, further emerged fundamental the roles of original air recognition images for identifying surviving and disappeared oil terminal components, of visits on the sites for ascertaining their morphology and preservation states, of archive researches for reconstructing the oil terminal histories and of discussions with experts for understanding aspects of the involved technologies. All this shows that the study of the Atlantic Wall should be conducted in an interdisciplinary way with the support of experts in different technical fields.

Acknowledgements

I express my gratitude to Mr. L. Pottier for sharing the results of his researches about the Talards oil terminal in the Archives Municipales de la Ville de Saint-Malo, to Mr. F. Guillaume for sharing his technical knowledge and information about the Bouchemaine oil terminal and for having guided me during the visit on the oil terminal site and to Mr A. Benoit for sharing digitalised original WWII documentation concerning the Bouchemaine terminal.

References

Archives Municipales de la Ville de Saint-Malo (1940). *Registre du Cadasdre N° 2256 et 2257*.

Brichet, O., & Peyle, E. (2005). *La Marine Allemande à Saint-Malo, 1940-1944* (pp. 71, 115). Cancale: Editions du Phare.

Dahiot, D., Dupont, P., Pottier, L., & Tomezzoli, G. (2009). Die Infrastruktur des Fliegerhorstes Dinard-Pleurtuit im II. Weltkrieg. *DAWA Nachrichten. Ausgabe, 53,* 42-61.

Lippmann, H. (2012). Die Flugabwehrsicherung des Fliegerhorstes Dinard-Pleurtuit. *DAWA Nachrichten. Ausgabe, 60,* 4-13.

Oil Terminal Archive Bouchemaine (2018). *Digitaliseddocumentation*.

Pottier, L. (2013). *Personal Archive*.

Tomezzoli, G. (2014). Der Gefechtsstand der Flak Abteilung 912 auf dem Gelände des Fliegerhorstes Dinard-Pleurtuit. *DAWA Nachrichten. Ausgabe, 63,* 20-27.

Tomezzoli, G. (2015). The Kieswerk of Pointe Saint-Mathieu and the Atlantic Wall. *Advances inAnthropology, 5,* 177-182. https://doi.org/10.4236/aa.2015.54017

Tomezzoli, G. T. (2016). The German Base "the Bank" at Mûrs-Érigné (Anjou-FR). *Archaeological Discovery, 4,* 37-47.

Tomezzoli, G. T., & Pottier, L. L. (2016). Journey through the Defences of the Festung Saint-Malo (FR)-2. *Archaeological Discovery, 4,* 143-169. https://doi.org/10.4236/ad.2016.44011

Tomezzoli, G., & Marzin, Y. (2015). The EroVili and the Atlantic Wall. *Advances in Anthropology, 5,* 183-204.

Tomezzoli, G., Pottier, L., & Dahiot, D. (2013). *La logistique et les défenses de l'aérodrome dePleurtuit (Bretagne-FR) pendant la guerre*. L'écho de la Cohue No. 14, Patrimoine du Pays dePleurtuit en Poudouvre.

Archaeological Discovery, 2018, 6, 216-270
http://www.scirp.org/journal/ad
ISSN Online: 2331-1967
ISSN Print: 2331-1959

Fennel (*Foeniculum vulgare*) Rests on the Holy Maria-Magdalena's Hairs, Studied by Scanning Electron Microscopy and Elemental Analysis

Gérard Lucotte[1*], Thierry Thomasset[2], Alain Salmon[3]

[1]Institut d'Anthropologie Moléculaire, Paris, France
[2]Laboratoire d'Analyse Physico-Chimique, UTC de Compiègne, France
[3]Plénan Le Grand, France
Email: *lucotte@hotmail.com

How to cite this paper: Lucotte, G., Thomasset, T., & Salmon, A. (2018). Fennel (*Foeniculum vulgare*) Rests on the Holy Maria-Magdalena's Hairs, Studied by Scanning Electron Microscopy and Elemental Analysis. *Archaeological Discovery, 6,* 216-270.
https://doi.org/10.4236/ad.2018.63012

Received: April 2, 2018
Accepted: June 11, 2018
Published: June 14, 2018

Abstract

As our new contribution to the scientific knowledge of Holy Maria-Magdalena remains, we have studied pollens and several vegetal tissues of fennel adhering to her hairs by optical microscopy and SEM-EDX. Pollen grains, foliar, pedicelar and stem debris found are characteristics of *Foeniculum vulgare*. Detailed examination of these tissue debris shows that the plant involved was carefully processed and cultivated. Fennel symbolism is an important attribute to the Marie-Madeleine worship concerning the French "Tradition des Saints de Provence".

Keywords

Maria-Magdalena's Hairs, Fennel, Pollens and Vegetal Tissues, Optical Microscopy, SEM-EDX, Elemental Analysis

1. Introduction

Holy Maria-Magdalena, named here Ste Marie-Madeleine (3?-63?), is the most abundantly cited (at least twelve citations, without taking account some repeats) women of the four Gospels. According to the French "tradition des Saints de Provence", she landed to the French (the Gaule at this era) Mediterranean shores, in a region corresponding to the current part of Les Saintes-Marie-de-la-Mer. She (and her companions) attained further the towns of Marseilles and Aix-en-Provence, where they evangelized the Provence region. Thereafter, she withdrew for thirty years to the cave of La-Sainte-Baume, where she died (in 63); she was buried in the currently named village of Saint-Maximin-la-Sainte-

Baume.

Her body was exhumed on 19 December 1279 (according to Chronicles of Pope and Emperors, 1320). Bernard Gui, who was an auricular witness of the facts, wrote: "In the year of grace of Jesus-Christ in 1279, the nineteenth day of December, the Prince Charles, son of Charles King of Sicily, Count of Provence and then King of Sicily, had looked for the body of Ste Marie-Madeleine with so much solicitude and as much a devotion in this holy oratory in which St Maximin, one of the seventy disciples of the Seigneur Jésus-Christ, venerated in the (diocese of) Aix formerly, had given (to her) one burial place…"

The precision concerning the fennel is also given by Bernard Gui, who furnished (Franzoni, 2016) some details observed during the exhumation: "It produces then an extraordinary fragrance, as if one had opened a flavoured container… from her holy tongue, even attached to the head and the throat, left a root with a (green) fennel twig (which) extended". **Figure 1** shows a later representation of the scene.

Some relics (cranium, bones and hairs) of Marie-Madeleine were kept in the Saint-Maximin basilica, where a large lock of Marie-Madeleine hair is arranged in a dedicated reliquary. We have obtained some hairs from this lock, for scientific purposes (microscopic examination and chemical analyses). We have published recently (Lucotte, 2016; Lucotte & Thomasset, 2017) the mitochondrial DNA haplogroup found by extracting genomic DNA from the bulb of hair number 10, and also the brown-red observed colour of the hairs by scanning electron microscopic characterization of its melanosomes.

During hair observation studies, we have found some rests (pollens, leaf and stem debris) of fennel (*Foeniculum vulgare*), on or at the vicinity of some hair parts. The present study describes in details these rests, and gives an interpretation of their presences in the frame of the French "Tradition des Saints de Provence".

2. Material and Methods

The material is seven of the about ten of a large lock of Marie-Madeleine's hairs that is kept in a dedicated reliquary in the Saint-Maximin basilica. These hairs, numbered 4 to 10, were loaded on a sticky-paper (**Figure 2**), for SEM examination and EDX analyses. A special characteristic of these hairs is their extreme dryness (Lucotte & Thomasset, 2017); so, when they were loaded (in folding back its) on the sticky-paper, most of the rests (pollen grains, vegetable debris, mineral and metallic particles…) adhering to hairs were dropped on the sticky-paper in their immediate neighbouring respective hair environments. The circled areas of the sticky-paper examined here are areas P1 (in the vicinity of some part of hair number 6) and P2 (at the basis of hair number 4), which contain pollen grains; areas A (in the vicinity of some part of hair number 9), B (located up to some part of hair number 10) and C (in the vicinity of another part of hair number 6), contains vegetable rests.

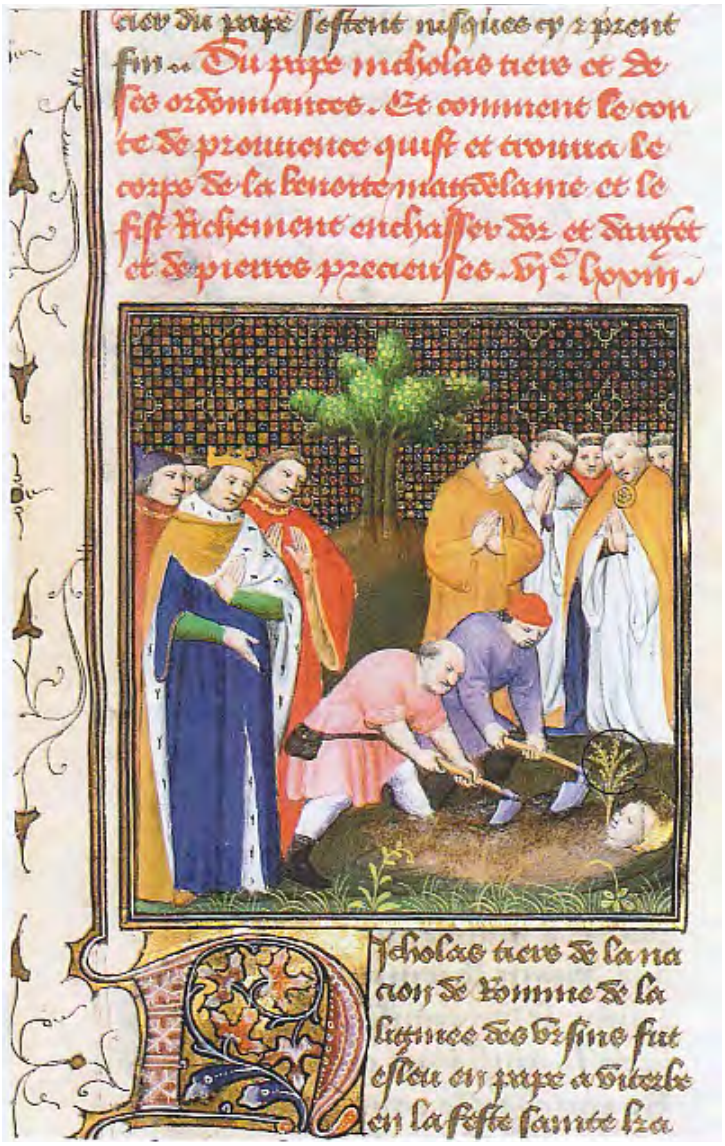

Figure 1. A 1415 representation of the discovery of the Marie-Madeleine body (by Maître Boucicaut, who was active in Paris between 1408 and 1418). In that illumination one can see at the left part the Prince surrounded by his counsellors and a clerk's group at the right part; Marie-Madeleine's face (with a fennel plant—circled—emerging from the right part of her face) is cleared by two labour workers.

Optical microscopy studies were realized using a confocal stereoscopic microscope.

The SEM (Scanning Electron Microscopy) apparatus used is a FEI model Quanta FEG. Elemental analysis was achieved by using EDX (Energy Dispersive X-Ray spectroscopy), this SEM microscope being equipped with the probe model X-flash 6/30. Both LFD (Large Field Detector) and CBS (Circular Back Scattering) were used, the last one to detect heavy elements.

Each elemental analysis is given in the form of a spectrum, with kiloelectrons/Volts (ke/V) on the abscissa and elemental peaks heights (cps/eV) in

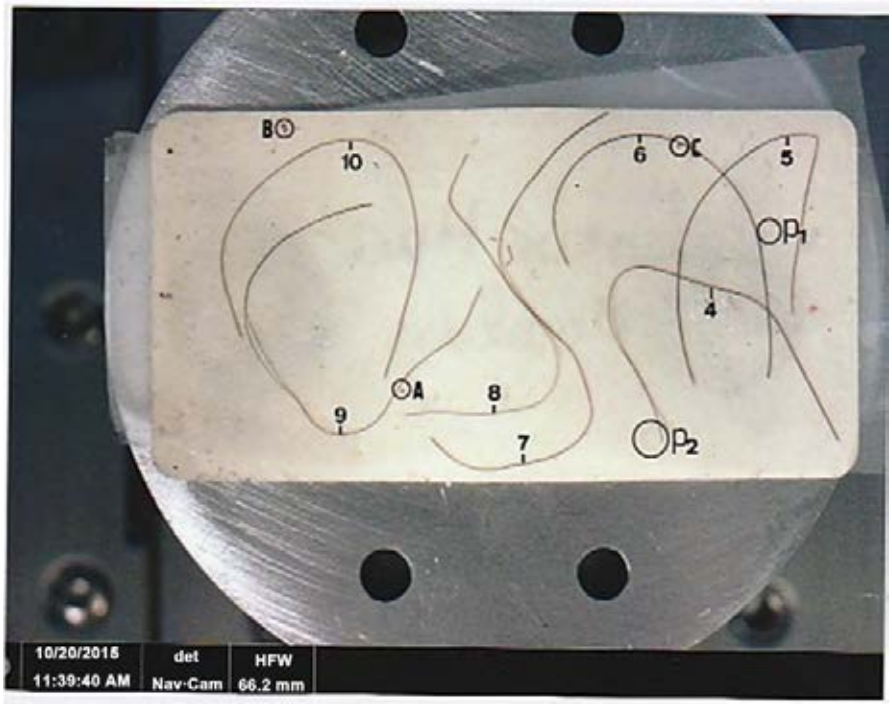

Figure 2. Optical view of seven (numbered 4 to 10) hair fragments of Marie-Madeleine, loaded on a sticky-paper. The P1 circle includes pollens located at the basis of hair number 4. The A circle includes a structure located at the vicinity of hair number 10; The P2 circle includes pollens located at the basis of hair number 9; the B circle includes two structures located up to hair number 10; the C circle includes a structure located at the vicinity of hair number 6.

ordinates. Estimating peak heights, it is possible to obtain some semi-quantitative results.

EDX-mapping was obtained (power: 20 kV; distance: 9.9 mm; acquisition time: 15 min.) for the elements C, O, S, K, Cl, Na, Ca, Si, P, Mg and Al.

3. Results

Results obtained correspond to pollen grains, located near number 6 and at the basis of hair number 4, leaf structures in A and B, and a stem structure in C.

3.1. Pollen Grains

There are about two hundred of pollen grains loaded on the sticky paper, all from the same species. **Figure 3** shows at least twenty visible of them, located inside of the P1 circle. They are seen individually, or lumped together; their orientations differ.

Pollens numbered p1 and p2 are seen (p2 especially) in equatorial views. The enlarged SEM photographs of **Figure 4** shows their characteristics: they are pollen grains of the prolate (of elongated form) type; the p1 length is approximately of 40 μm (its width is about 10 μm). Both p1 and p2 show two longitudinal sulcis, interrupted equatorially by one prominent pore. On the p1 photograph one

Figure 3. A SEM photograph (in CBS, 300×) of pollens (among them, pollen grains numbered p1 and p2) located at the vicinity of some part of hair number 6 (h6).

can distinguish the details of the wall surface, which corresponds to an ornamentation of the reticulate type.

Figure 5 photographs show pollen grains (that taken in optical microscopy is of red colour, which is that of the hair colour) located at the basis of hair number 4; that area corresponds to the most important density of pollen observed on the sticky-paper surface.

Six examples of these pollen grains, or pollen groups, are shown in Figure 6. In equatorial or longitudinal views their length vary from 29.1 to 42.4 µm, depending on orientation; in these views they show at least one longitudinal sulcus, interrupted equatorially by a pore. Some views (as that of photograph 6.2) show a reticulate type of ornamentation. The polar view (photograph 6.3) is triangular. When tightly lumped together, the pollen outline (notably that of the pollen grain in intermediate position of the group of three showed in photograph 6.5) is greatly altered.

What is more of the normal diversity, the variation in shapes and dimensions of these pollen grains is due to their dryness; this dryness intervenes mainly as seen in polar views (where outline is not rounded but triangular, because of extrusion of volumes located between sulcis), but also on width and general outline of these pollens.

A detailed study of the fennel pollens (*Foeniculum vulgare*) was recently published (D'Avila et al., 2016). In the present study, examination of more than fifty pollen grains (seen in equatorial or longitudinal views) confirms this diagnosis. Table 1 summarizes, in accordance to the pollen terminology nomenclature adopted in SEM studies (Hesse et al., 2009), our own characterization.

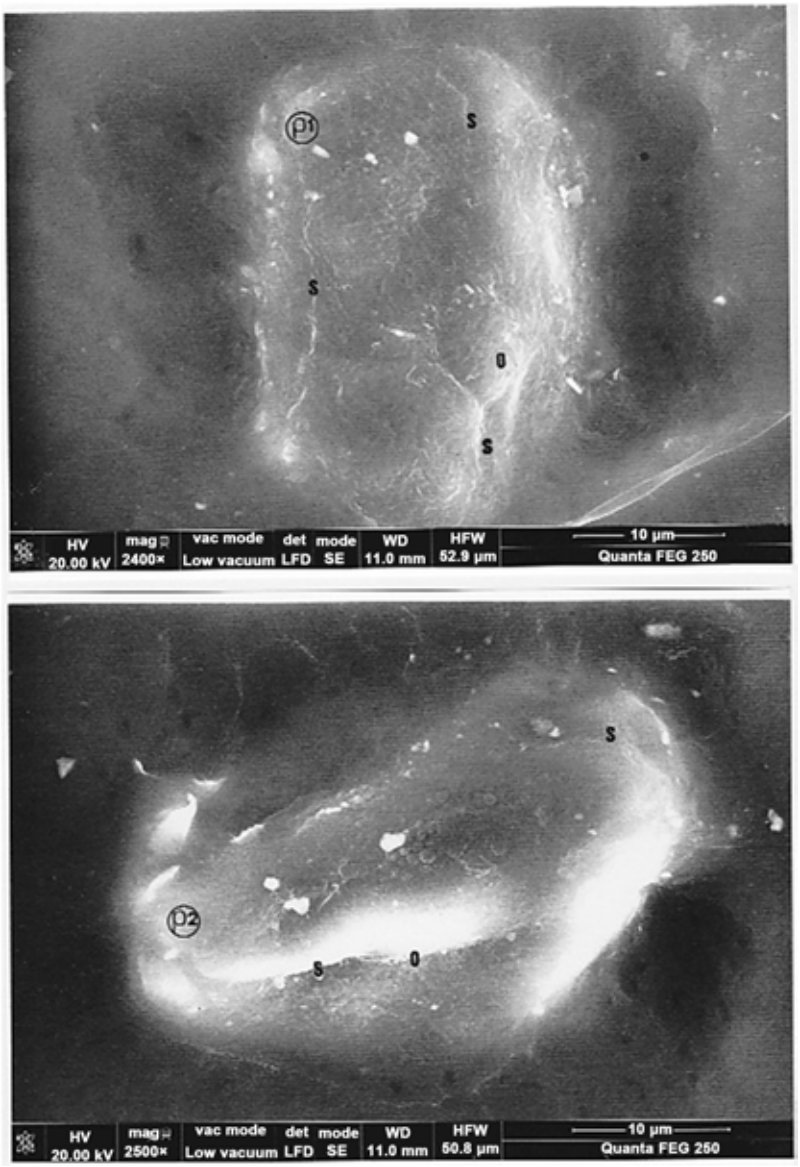

Figure 4. Enlarged views of pollens p1 and p2. *Above*: SEM photograph (in LFD, 2500×) of p1. *Below*: SEM photograph (in LFD, 2500×) of p2. S: sulcis; O: pores.

The mean measurement of lengths—which seems independent of dryness is of about 35 µm; the mean measurement of widths, which is clearly dependent of dryness (and of compression effect) is of about 15 µm. In general, we can say that the observed pollen grains are characterized as follow; prolate, isopolar, triheteroapertured (an additional criterion is the ornamentation, which is of the reticulate type). But these three first characters are valid for all the pollen grains belonging to plants of the Apiacea family (Jones & Jones, 2001), even if you retain additional dimensions criteria.

Supplementary Figure 1 gives some examples of photographs (in optical microscopy and in SEM) of fennel pollens of reference; among them, the SEM photograph was particularly useful for our own study.

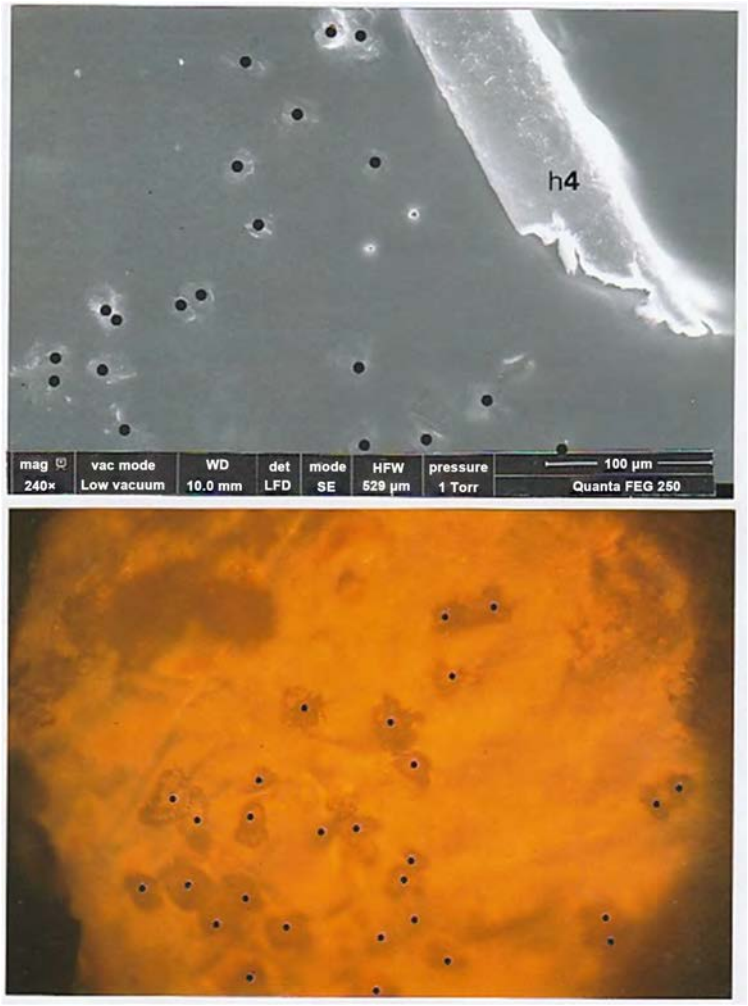

Figure 5. SEM and optical microscopy photographs of pollens located at the basis of hair number 4 (h4). *Above*: SEM photograph (in LFD, 240×) of the pollens. *Below*: some of these pollens seen (in red colour) in optical microscopy (250×); each polllen grains are indicated by a black point.

To be noted is that it is impossible to distinguish (D'Avila et al., 2006) between the pollens of the three aromatic species of fennel (*Foeniculum vulgare*), dill (*Anethum graveolens*) and coriander (*Coriandrum sativum*).

3.2. The Fennel Plant

3.2.1. Background

The fennel, named *Foeniculum vulgare* (taxonomically *F. vulgare* Mill), is a medicinal plant belonging to the Apiaceae (previously Umbelliferae) family, known and used by humans since the Antiquity (Badgujar et al., 2014).

Foeniculum vulgare is an upright, branching perennial herb (**Supplementary Figure 2**) with soft, feathery, and almost hair-like foliage growing up to two metres tall. It is typically grown in vegetable and herb gardens for its anise-flavoured foliage and seeds, both of which are commonly harvested for use in cooking.

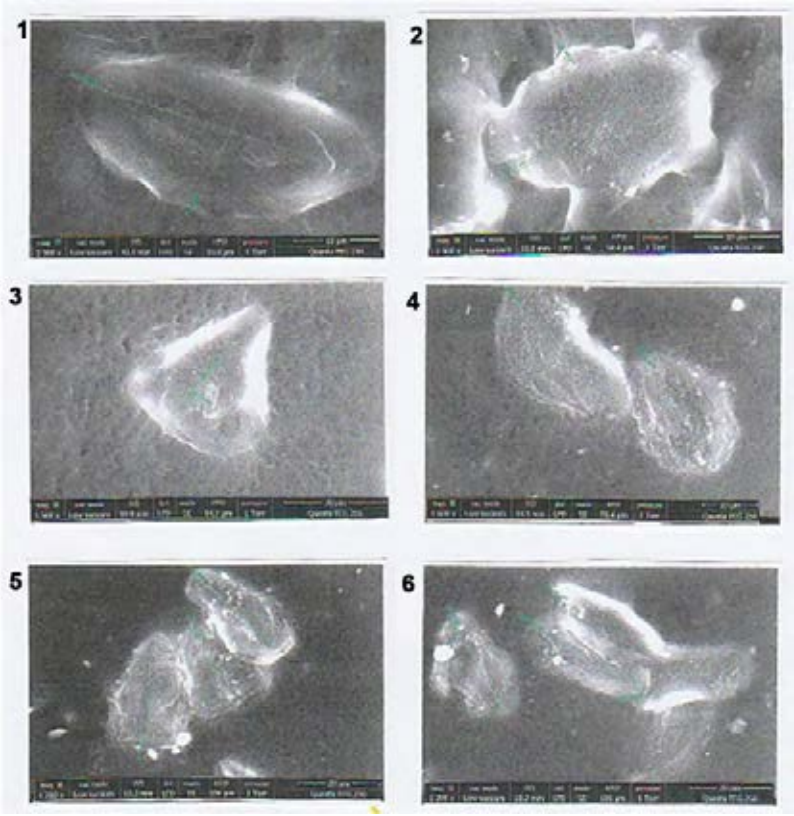

Figure 6. SEM photographs of some examples of these pollen grains. **1**: SEM photograph (in LFD, 2500×) of a pollen grain (42.4 × 19.3 μm) seen in equatorial view. **2**: a pollen grain (29.1 × 20.5 μm) seen (in LFD, 2500×) in longitudinal view. **3**: a pollen grain (39.2 × 33.3 um) seen (in LFD, 1500×) in polar view. **4**: two pollen grains (35.3 and 28.6 um of lengths, respectively) seen (in LFD, 1600×) in longitudinal views. **5**: three pollen grains (34.3, 27.7 and 35 μm of lengths, respectively) seen (in LFD, 1200×) in longitudinal views. **6**: a group of five pollen grains (32.3, 39, 36.6 and 36.2 μm of length, respectively for the four firsts) seen (in LFD, 1200×) in longitudinal views.

It is erect and cylindrical, bright green, and smooth as to seem polished, with multiple branched leaves cut into the finest of segments. The leaves grow up to 40 cm long; they are finely dissected, with the ultimate segments filiforms (threadlike) of about 0.5 mm wide. The bright golden flowers are produced in large and flat terminal umbels (with thirteen to twenty rays) bloom in July to August.

Stem is striated; leaves are 3 - 4 pinnated, with base-segments filiforms (of up to 4 cm long). Leaf basis is sheeted; it has a green, sleek and slippery stem with upright stiff branches and much divided leaves in linear segments.

Foeniculum vulgare is a very polymorphic species (Badoc et al., 1995). The *vulgare* variety (*F. vulgare vulgare*) corresponds to wild, or cultivated, plants. *Foeniculum vulgare* "Purpureum", or "Nigra", or "bronze-leaved" fennel, is widely available as a decorative garden plant. The Florence fennel variety (*Foeniculum vulgare* var. *azoricum*) is a cultivar group with inflated leaf bases which

Table 1. Ten nomenclature criterias for pollens used in our characterization.

Criterias	Nomenclature	Commentaries
1	monad	when they are tightly lumped together , it is mainly due to their proximities on the stick paper
2	**form**: prolate	elongated in form; the main measured length is about 35 µm
3	isopolar	anisopolarity, when it exists, is an artefact due to differential dryness or compression effect
4	medium	their lengths are between 26 and 50 µm
5	perprolate	the mean measured width is of about 15 µm, but this measurement is greatly dependent on dryness. The ratio between polar (DP) and equatorial (DE) diameters = 2.3
6	**sulcus**: sulcate	at least one long longitudinal sulcus is observed in equatorial views
7	trisulcated	three sulcis, for observations in combination
8	**porus**: pore	one voluminous pore in equatorial position, located on the corresponding sulcus
9	tripored	one such pore, for each sulcus
10	heteroapertured	because it is trisulcated and tripored

form a bulb-like structure. It is of cultivated origin and has a mild anise-like flavour, but is sweeter and more aromatic; Florence fennel plants are very much smaller than the wild type. The inflated leaf bases are eaten as a vegetable, both raw or cooked. Several cultivars of the Florence fennel are also known by several other names, notably the Italian name "finocchio".

3.2.2. *Foeniculum vulgare azoricum* Is Used for Comparative Purposes in Our Study

It is a today fennel plant of the variety *azoricum*, the bulbous form (Figure 7), that was used for comparisons. This figure shows macroscopic and microscopic aspects of some pedicels and leafs of the sample. The SEM photograph summarizes the distinctive arrangements of stomates on the epidermis surface: typically they are aligned for the pedicel and in a staggered arrangement for foliar 'leaf'.

Longitudinal cuts of stems were also practised, to compare vessel structures and arrangements.

The SEM photograph of Figure 8 shows that, for the today fennel specimen studied, leaves have both foliar and pedicelar (at the basis) parts. The below spectrum shown is a typical one of both of these parts, EDX analyses being realized at several leaf points. This spectrum shows carbon and oxygen peaks (that constitute the organic part majority) and little peaks of minerals; among them the potassium peak predominates, an essential characteristic of most vegetables in general, and of the fennel plant specially.

3.3. A Foliar Structure in A

Figure 9 shows the structure located inside circle A. It is round in form, with a maximal diameter of about 350 µm; its spectrum is that of a vegetable.

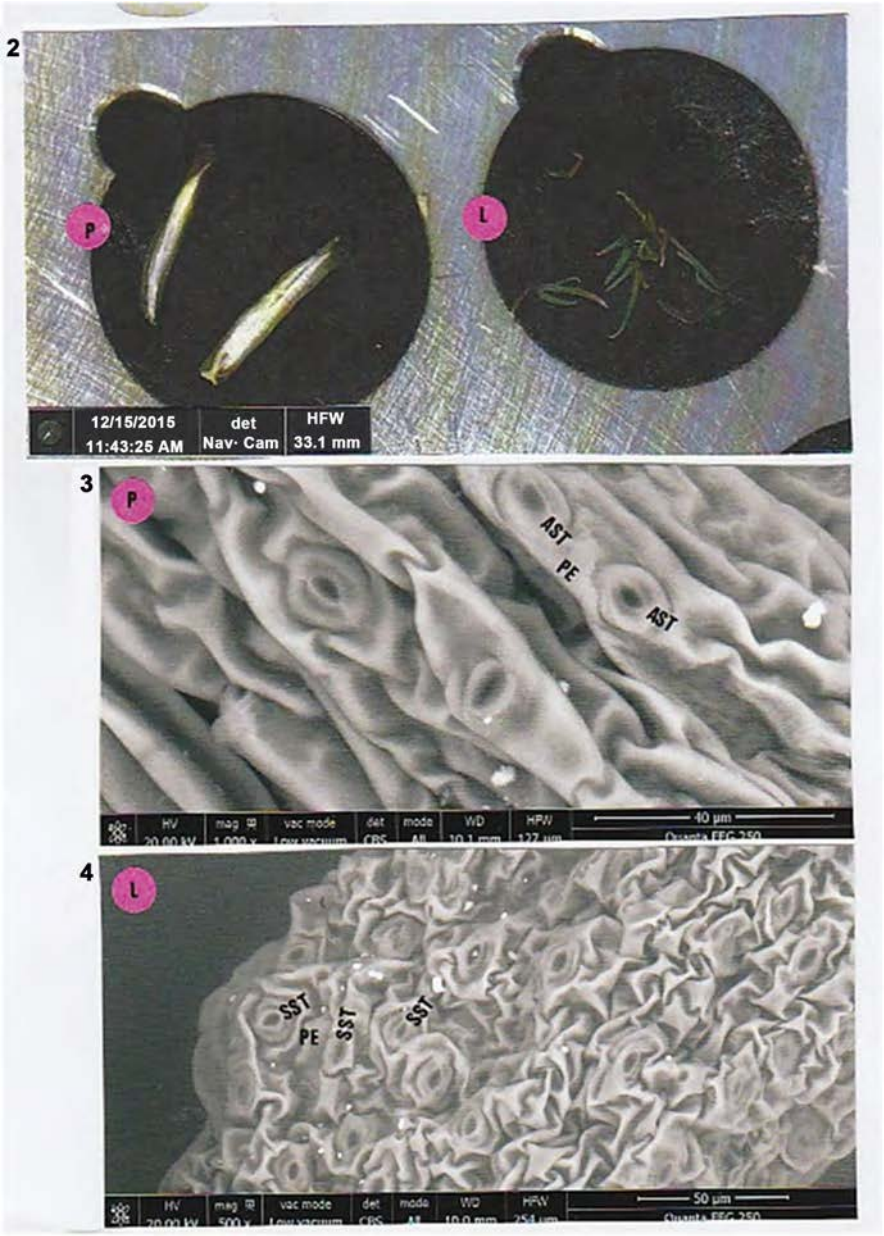

Figure 7. A today plant of fennel. **1**: the fennel sample (L: leaf; P: pedicel; S: stem; B: bulb). **2**: Optical microscopic view of P and L. **3**: SEM photograph (in CBS, 1000×) of some part of the pedicelar (P) epidermis. AST: two aligned stomates; PE: folded epidermis. **4**: SEM photograph (in CBS, 500×) of some part of the foliar leaf (L) epidermis. SST: three adjacent stomates, in a straggered arrangement.

There are numerous stomates on its surface, mainly located at the rounded periphery. As these adjacent stomates are staggered (like to those shown on photograph 4 of Figure 7) and the epidermis between them is highly folded, that establishes that the vegetable structure observed is a fragment of a fennel leaf.

Figure 10 compares stomate dimensions of two of them to those of a today fennel leaf stomata. Although their partial dimensions differ, their proportional sizes (as well for ostiol measurements) for total stomate length (including or not

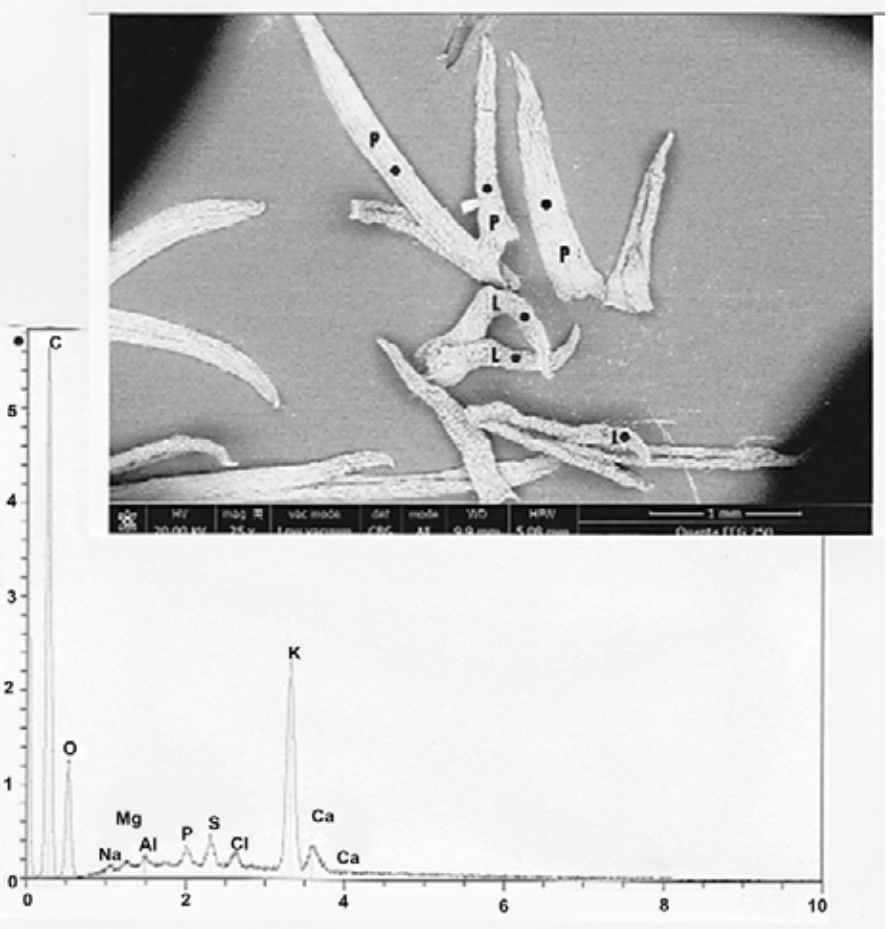

Figure 8. Elementary analyses of pedicelar and foliar parts of leafs of the today sample of the fennel plant. *Above*: SEM photograph (in CBS, 25×) of pedicelar (P) and foliar (L) parts of leafs (black dots indicate the locations where EDX analyses are realized). *Below*: a representative EDX spectrum at the black dots. C: carbon; O: oxygen; Na: sodium; Mg: magnesium; Al: aluminium; P: phosphorous; S: sulphur; Cl: chlorine; K: potassium; Ca (two peaks): calcium.

guard cells) and height (including sentinel or annex cells) are the same for the today fennel leaf and for the structure studied. In general similarity is very great between stomates of this type, said as "low-triangular" (Ellis, 1979).

Figure 11 gives elemental compositions of two sorts of particles (**1** and **2**) deposited on the surface of the structure examined (see Figure 9). Particle **1** is a calcium carbonate that, because of its high calcium content, is a lime; numerous other particles of similar aspect are deposited on the leaf surface. Particle **2** is rich in rare earths (cerium and lanthane).

The calcium carbonate is a very common deposit, that of this of rare earth micro-marble is very unusual. It is in fact an artefact due to the use of one such product (we have documented proofs of that) for the cleaning (http://www.ampere.com/polissage-terres-rares) of the posterior face of the reliquary glass. Supplementary Figure 3 shows another example of this sort of rare earth micro-marble, found at the proximity of hair number 3.

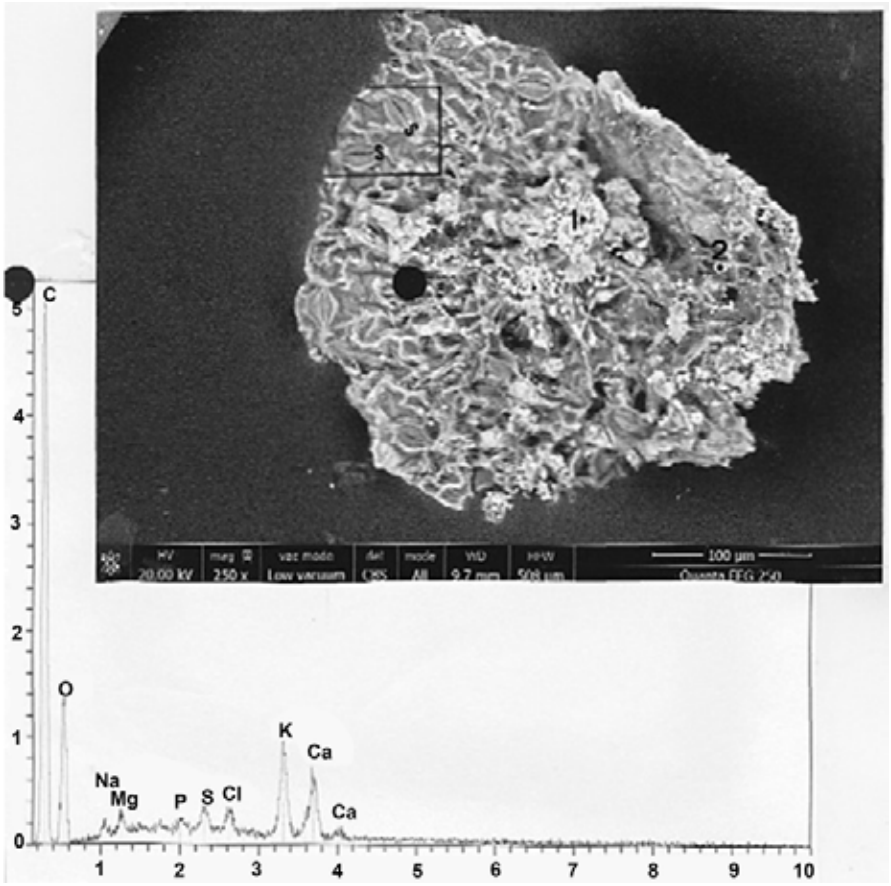

Figure 9. Morphology and composition of structure A. *Above*: SEM photograph (in CBS, 250×) of this structure. The rectangular area containing two stomates (S) is enlarged in the following photograph (1: particles number 1; 2: particle number 2); the big black spot indicates the location where EDX analysis is realized. *Below*: spectrum at the black spot.

3.4. Foliar and Pedicelar Structures in B

Figure 12 shows the two structures (piece **1** above, piece **2** below) located inside of circle B. They are elongated in forms, with a greatest dimension of about 330 µm. Its spectras are that of vegetables.

The stomates of piece **1** (Figure 13) are struggered; so it appears as a foliar part of a fennel leaf. On the three studied particles (**1**, **2** and **3**) deposited on the surface of this piece (Figure 14), the two firsts are mineral particles of silica (with a very elevated peak of silicium).

The third particle is a potassium sulphate, in fact a sulphate double of potassium and of calcium). We have found such a product several times on Marie-Madeleine hairs; for example, Supplementary Figure 4 and, Supplementary Figure 5 show particles (both of micro-needles and micro-plaques) of sulphate double of potassium and calcium located on the surface of some part of hair number 1.

Because that stomates of piece 2 (Figure 15) are mainly aligned (like to those shown on photograph 3 of Figure 7), it appears as a pedicelar part of a fennel

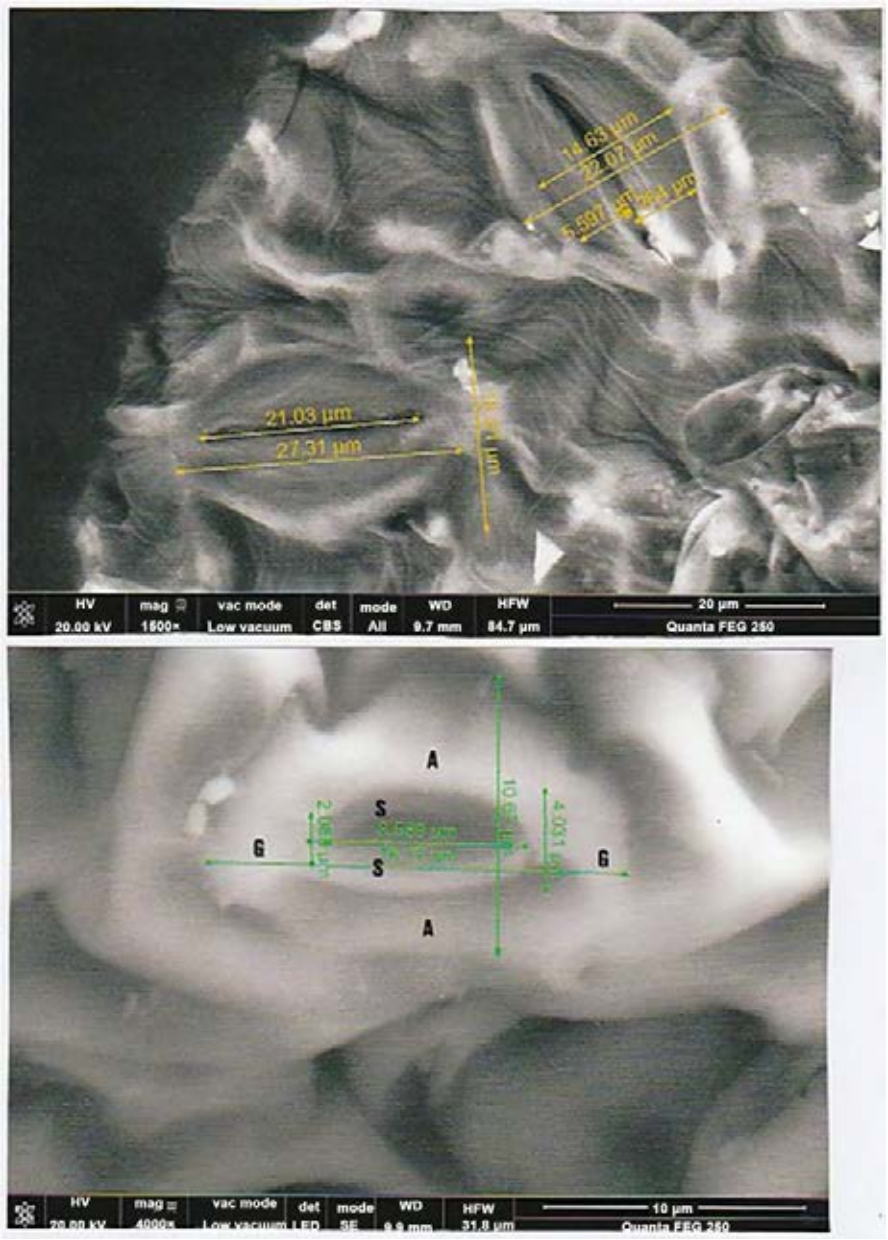

Figure 10. Comparison between stomates of structure A to those of the fennel leaf. *Above*: SEM photograph (in CBS, 1500×) of two adjacent stragered stomates of A. *Below*: SEM photograph (in LFD, 4000×) of one stomate of the today fennel leaf. Dimensions (in µm) are, horizontally, those of the ostiols and of the sentinel cells (S); vertically, those of the stomate cells (S) and those of annex cells (A); G are the guard cells.

leaf. On the two studied particles (**1** and **2**) deposited on the surface of this piece (**Figure 16**), the second is another sulphate double of potassium and calcium.

The first one is a clay mineral particle of an alumino-silicate of the montmorillonite/illite type, relatively iron-rich; because of its elevated content in iron oxide, it must appear as red in optical microscopy.

Supplementary Figure 6 shows another example of montmorillonite/illite mineral particles deposited on some part of the hair number 2 surface. As we

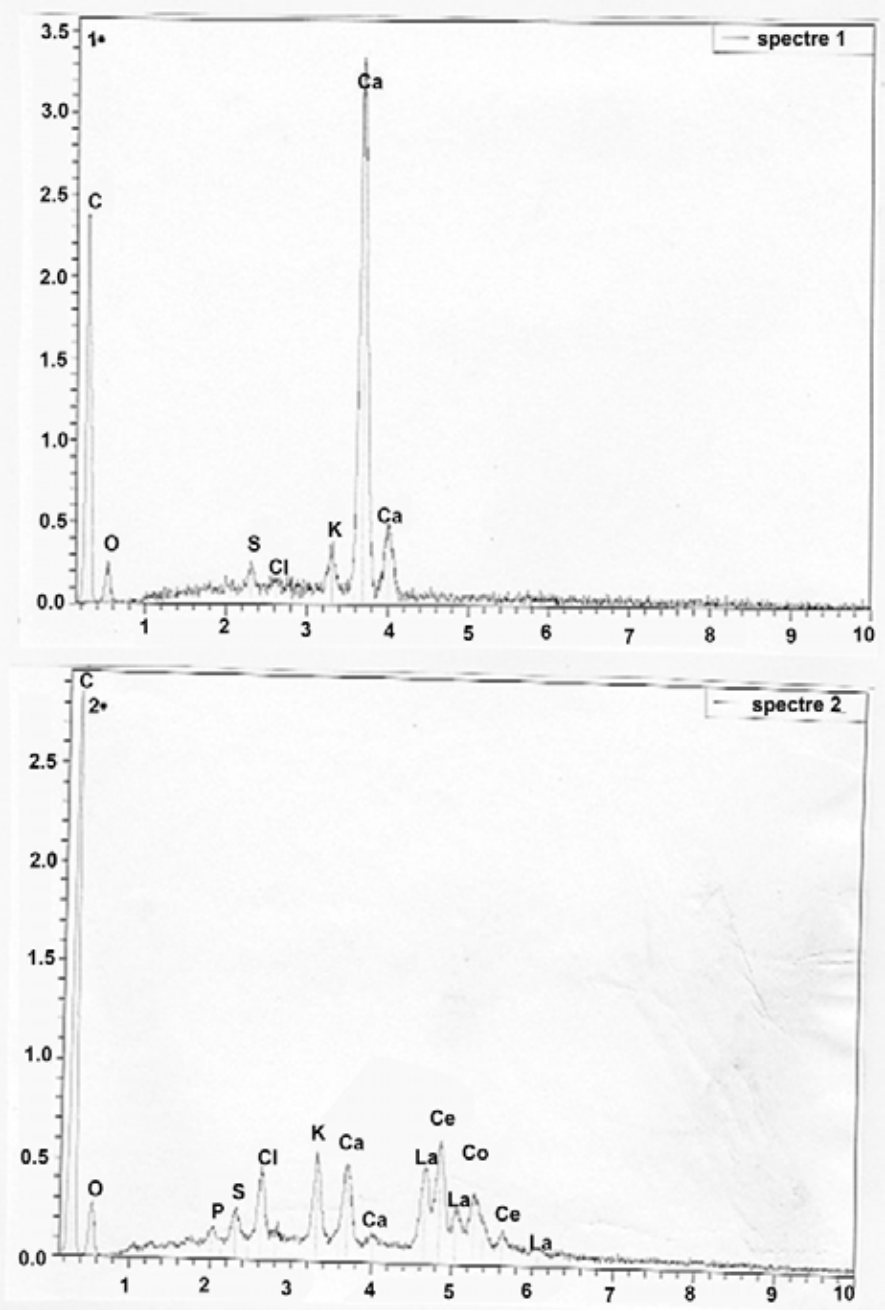

Figure 11. Spectras of particles 1 (spectre 1) and of particle 2 (spectre 2), as indicated on the **Figure 1** photograph. *Above*: spectrum of particles 1. *Below*: spectrum of particle 2; La (three peaks): lanthane; Ce (three peaks): cerium.

found previously there is a mean of about 5/6 of such particles (of relatively great sizes) only per hair, so these clay-mineral particles cannot be responsible for the red hair colour observed (Lucotte & Thomasset, 2017).

3.5. A Stem Structure in C

Figure 17 shows the structure located inside of circle C. It is a piece of triangular form (height of about 360 μm); its spectrum is that of a vegetable.

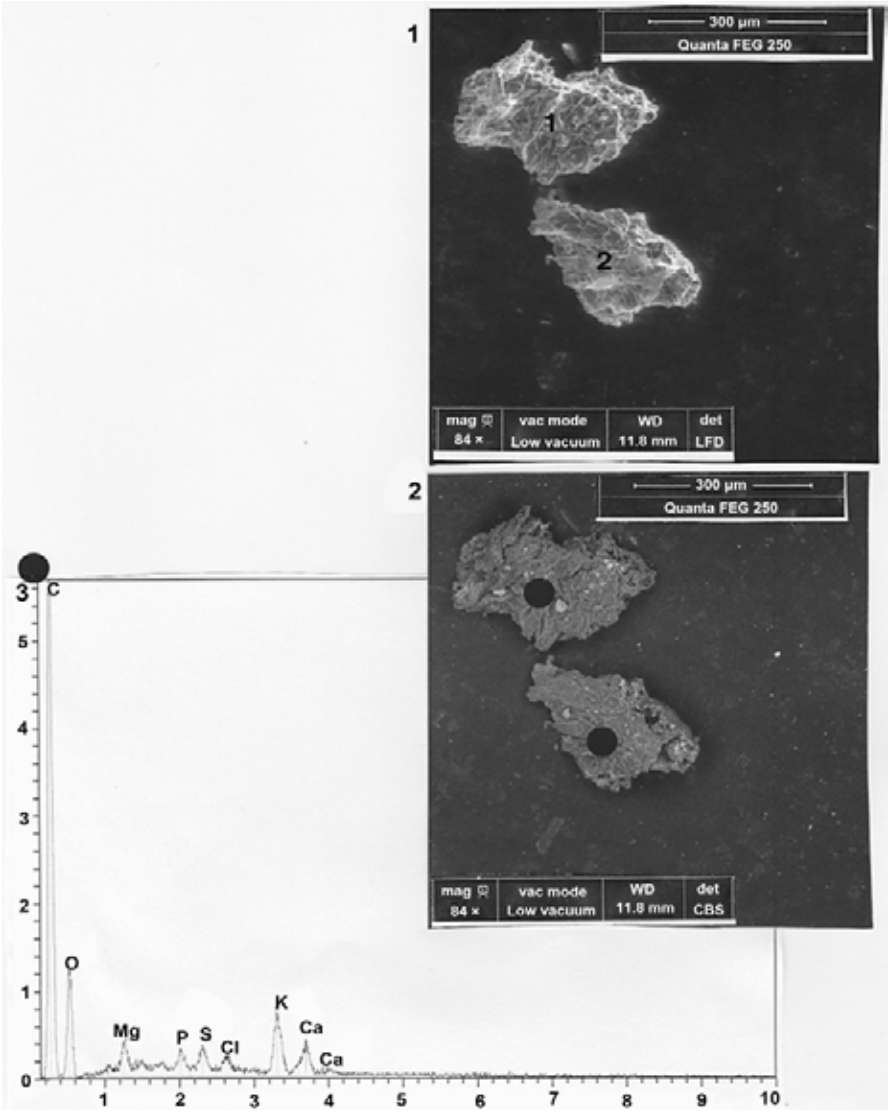

Figure 12. Morphology and composition of pieces one (1) and two (2) of the structure B. **1**: SEM photograph (in LFD, 84×) of pieces 1 and 2. **2**: SEM photograph (in CBS, 84×) of pieces 1 and 2 (black spot indicate the locations where EDX analyses are realized). **3**: spectrum at the black spots.

Angular outlines observed at the piece periphery (Figure 18) corresponds to flutes of the stem. Careful examination shows that the piece had some complexity; so, several peculiar aspects of it are further explored: the pores (circles **1** and **2**); some peculiarities of the epidermis surface (circles **3** and **4**); a cribled tube (circle **5**) and (circle **7**) aspect of a scalariform vessel. The greatest degree of complexity is observed inside the rectangular area indicated as **6**, that was studied in details.

3.5.1. Pores

There are no stomates on the piece surface, but circular pores. Figure 19 shows enlarged views of two of them (p1 and p2); p2 is a well delimitated circular pore, of an internal diameter of about 4 µm.

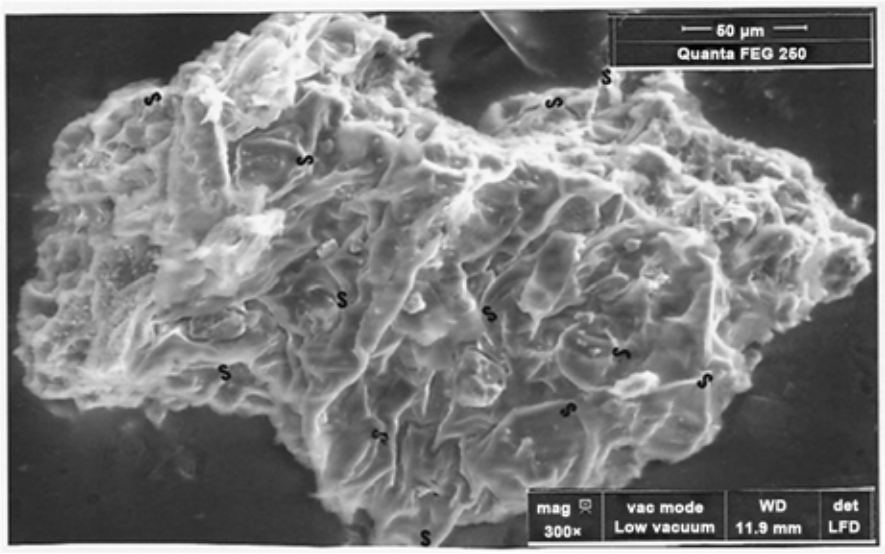

Figure 13. SEM photograph (in LFD) of piece **1**. S (orientated among ostiol cracks) indicate twelve stomates.

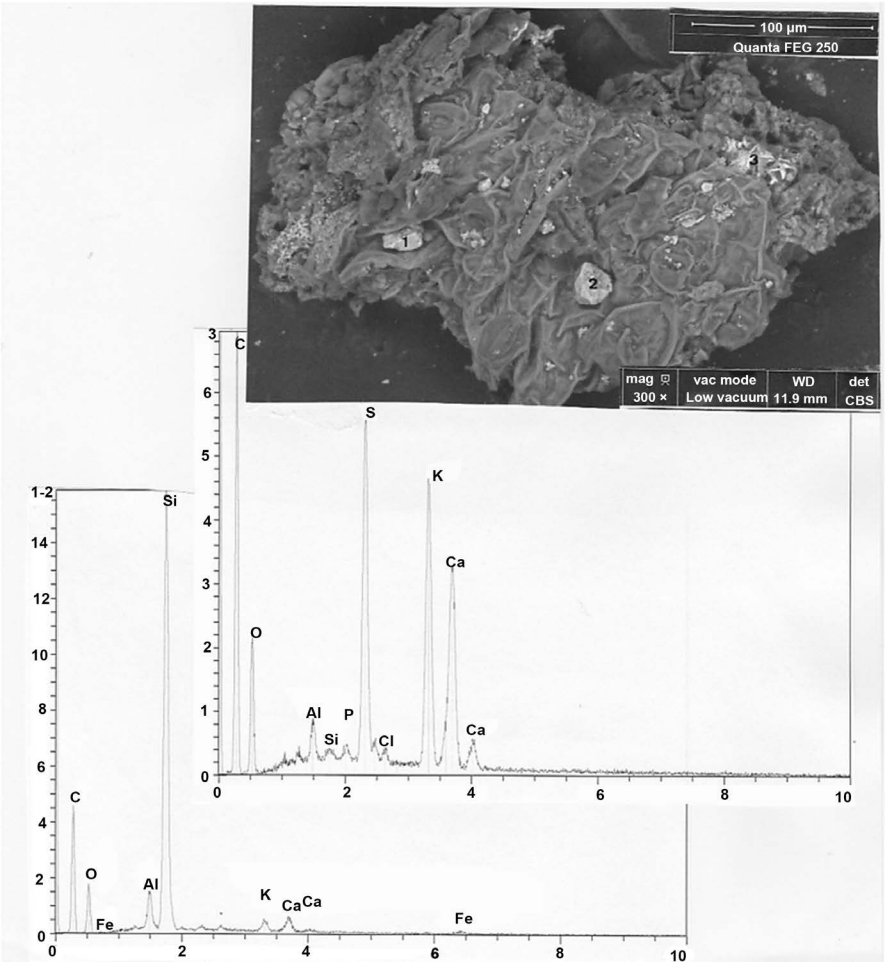

Figure 14. *Above*: SEM photograph (in CBS, 300×) of piece **1** (1, 2 and 3 indicate three mineral particles). *Below*: upper, spectrum of particles number 3; lower: spectras of particles numbers 1 and 2 (there are traces of iron: Fe).

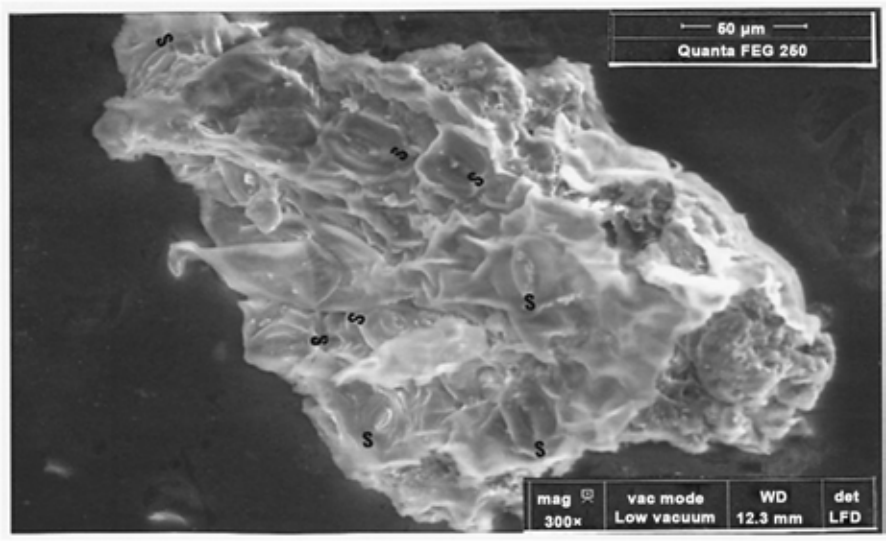

Figure 15. SEM photograph (in LFD, 300×) of piece **2** (S: eight stomates).

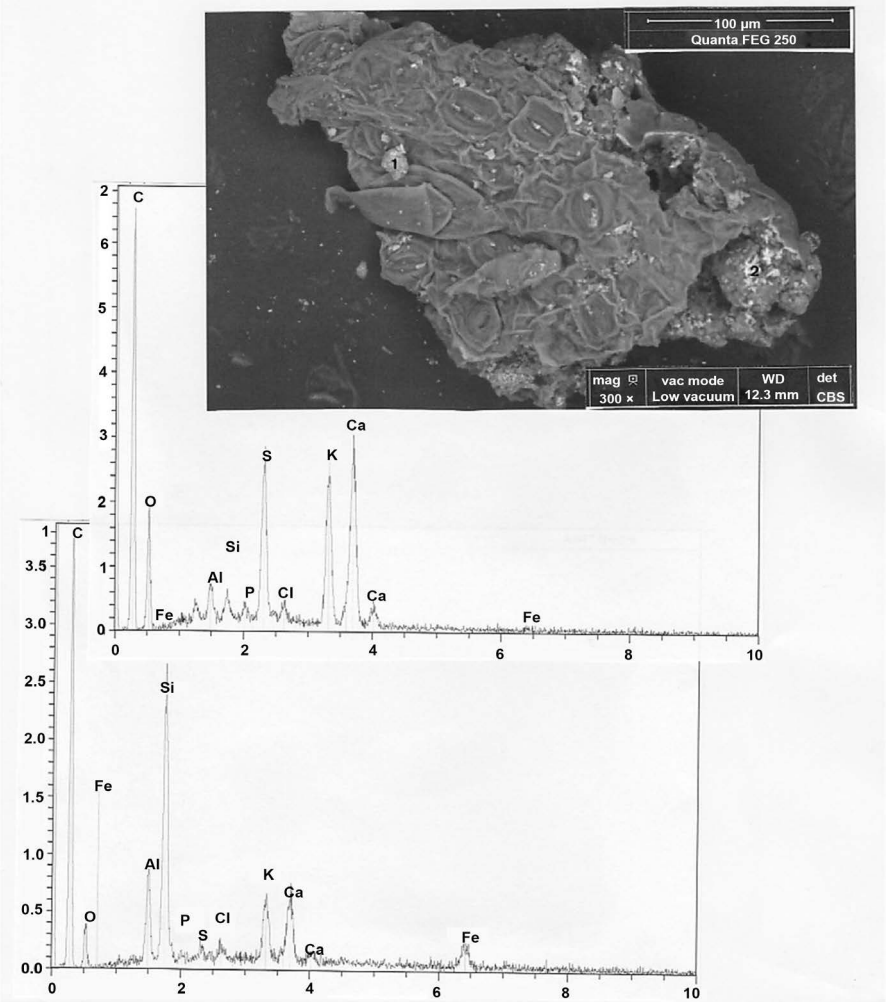

Figure 16. *Above*: SEM photograph (in CBS, 300×) of piece 2 (1 and 2 indicate two mineral particles). *Below*: upper, spectrum of particles number 2; lower; spectrum of particle number 1 (where the main iron peak appears).

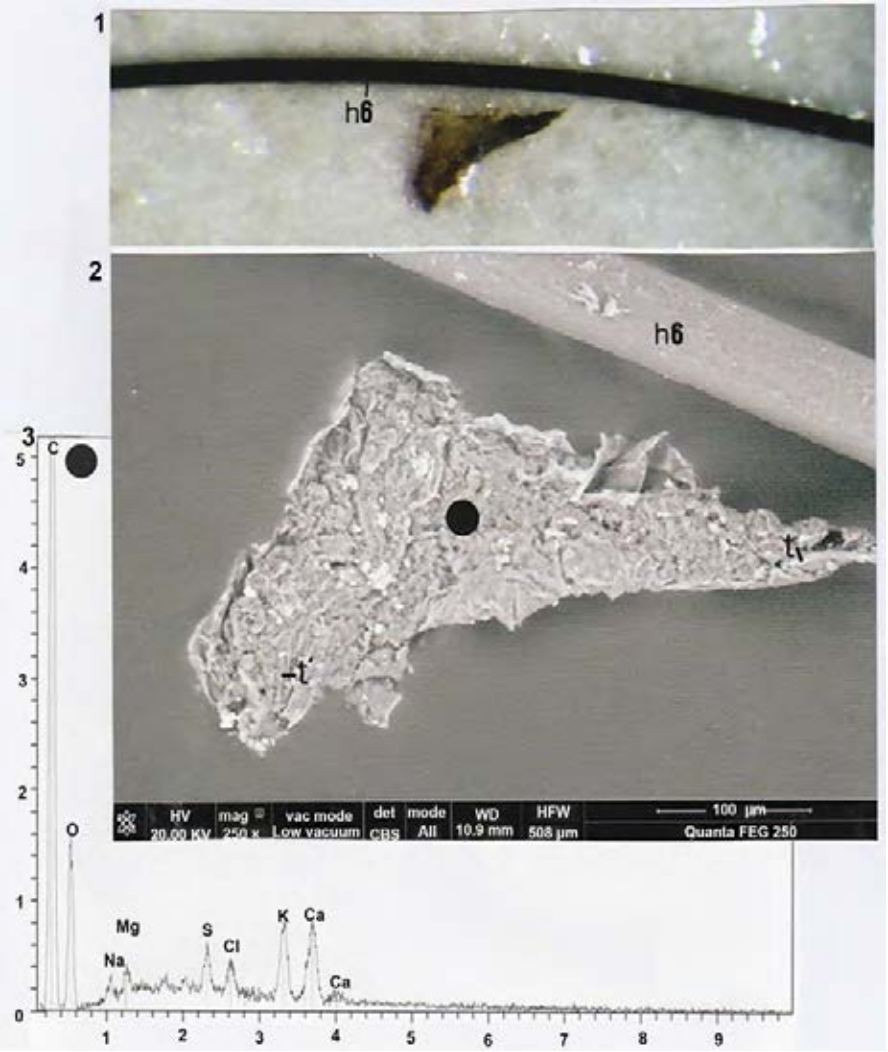

Figure 17. Morphology and Composition of C. **1**: their structure, in optical microscopy (20×); h6 is some part of hair number 6. **2**: SEM photograph (in CBS, 250×) of the structure (black spot indicates the location where EDX analysis is realized). **3**: spectrum at the black spot.

These pores are similar to classically described "wood holes" (Speranza & Galzoni, 1996). That indicates some degree of xylemation of the epidermis studied.

3.5.2. Epidermis

Figure 20 photographs show some aspects of this sclerified epidermis in some places. Its aspect inside of circle **3** shows that the epidermis plaque limits are orientated transversally (or in diagonally) in comparison to the stem longitudinal axis. The exfoliated aspect of some plaques (shown inside of circle **4**) located at the exterior limit of the piece testifies that they overcome in fact strates of previous epidermis layers.

Both these peculiarities are compatible to the stem epidermis aspect of a perennial plant.

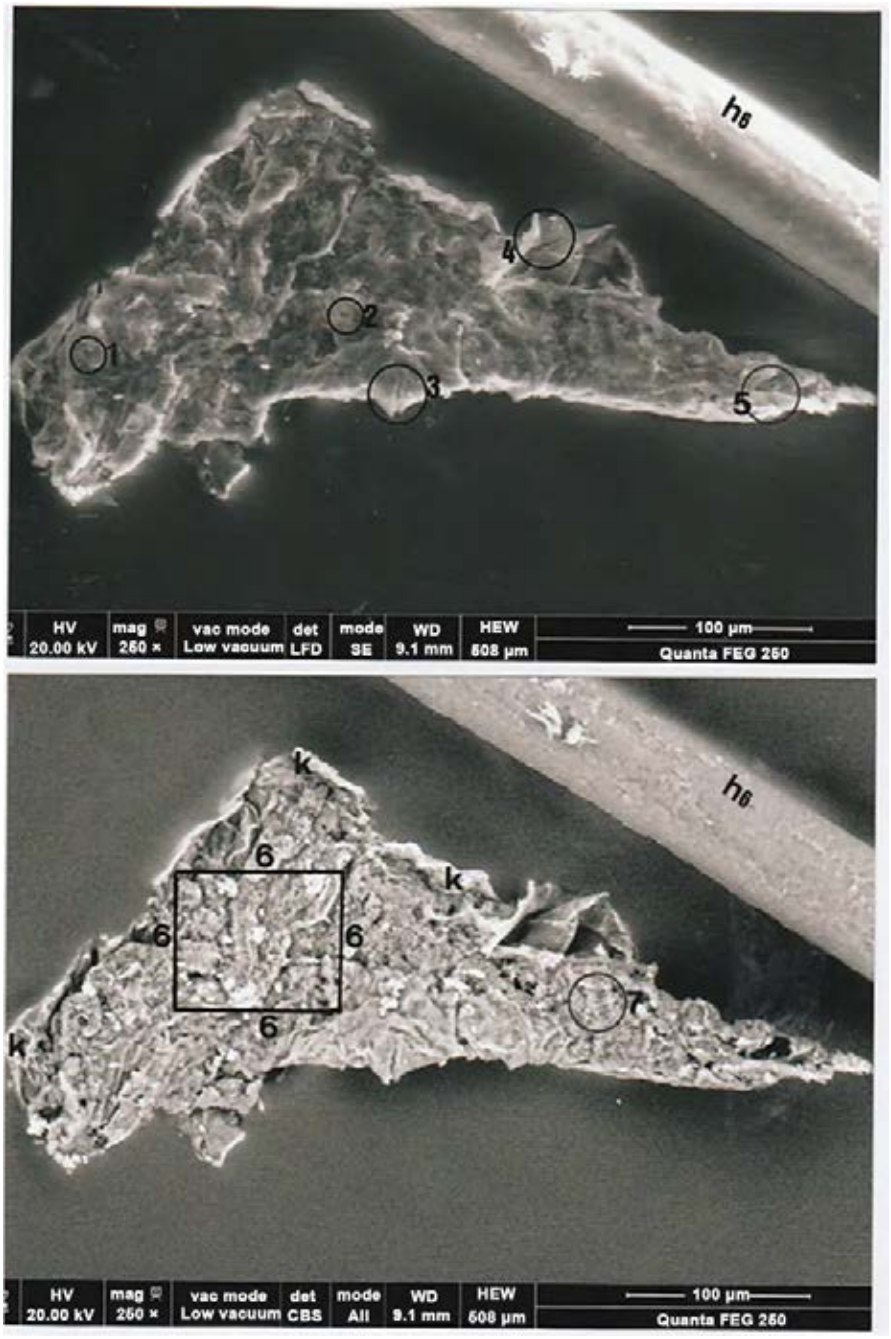

Figure 18. *Above*: SEM photograph (in LFD, 250×) of structure C (circles 1 and 2 indicate holes; circles 3 and 4 indicate regions of exfoliation of the epidermis; circle 5 indicates a vessel. *Below*: SEM photograph (in CBS, 250×) of structure C (the rectangular area 6 shows inside numerous evidence of vascularisation; circle 7 indicates a scalariform vessel). K: two angles (indicating the fluting of the stem) and one abrupt border.

3.5.3. A Cribled Tube

Figure 21 shows inside of circle **5** the external aspect of a segment of a cribled tube. Its form is roughly cylindrical (length of about 42 µm, on about 5µm of thickness). Its right extremity is broken and a cribbled plaque is visible at its other extremity. It is orientated along the stem longitudinal axis (one can see on

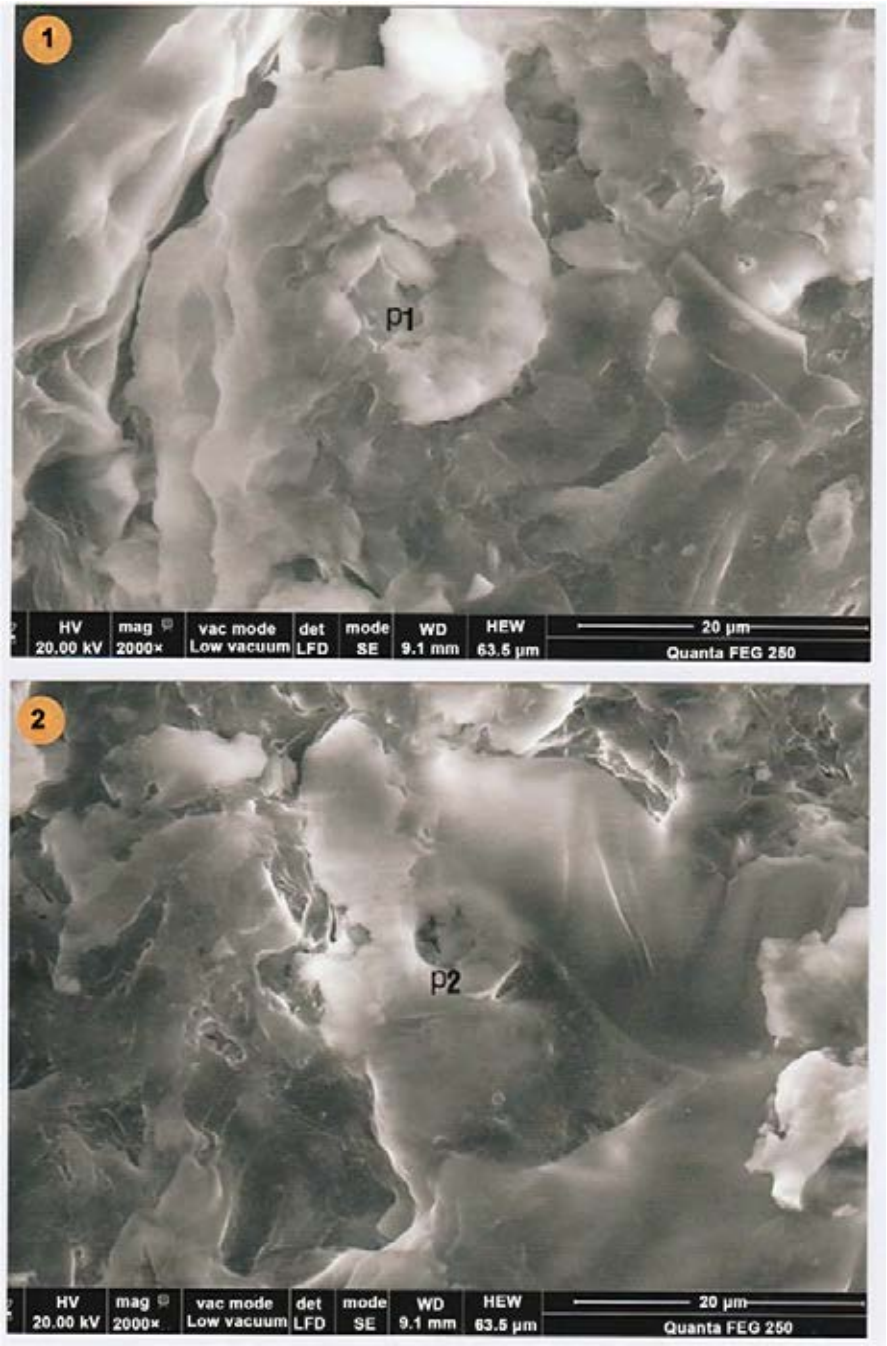

Figure 19. *Above*: SEM photograph (in LFD, 2000×) showing a first pore (p1) inside of circle 1. *Below*: SEM photograph (in LFD, 2000×) showing a second pore (p2) inside of circle 2.

the SEM photograph of **Figure 17** another segment of a cribbled tube (t') that is in orthogonal orientation compared to that described here). Cribled tubes are peculiar vessels of the liber specialized in the transport of the elaborated seve (Speranza & Galzoni, 1996).

Figure 22 photographs are enlarged views of the rectangular area shown on **Figure 21**. One can see on it a relatively voluminous (6.3 µm of length) spore.

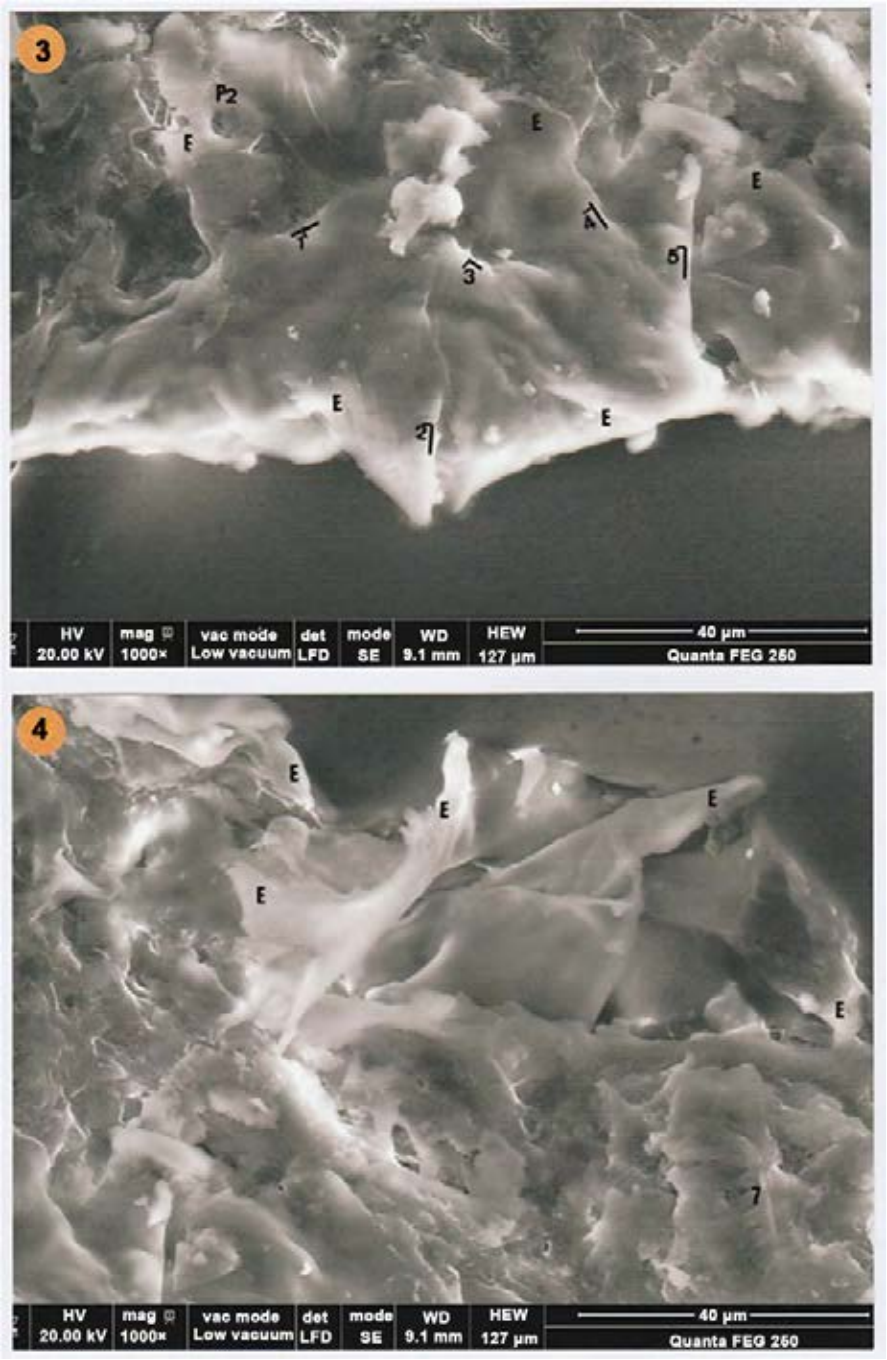

Figure 20. *Above* : SEM photograph (in LFD, 1000×) showing angular limits (1, 2, 3, 4 and 5) of the epidermis plaques (E) inside of circle 3 (p2: the second pore). *Below*: SEM photograph (in LFD, 1000×) showing the exfoliated epidermis plaques inside of circle 4 (7: circle 7).

This spore, of ellipsoid form and organic composition, is an ascopore (Rodeva & Gabler, 2011); it is associated to micro-filaments of a mycelium, visible at the step outline limit.

Three other more little (about 3 µm of length) aligned ascopores, of another species, are seen inside of a stem micro-cavity.

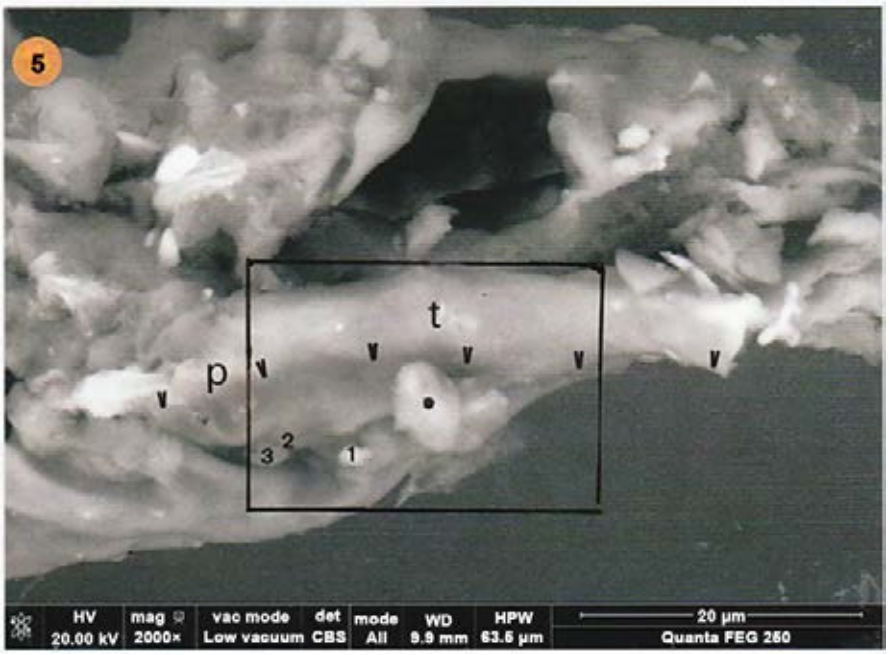

Figure 21. SEM photograph (in CBS, 2000×) showing the external wall of a cribbled tube (t), its inferior limit being indicated by several arrow points (p: cribled plaque), inside of circle 5. The little black point indicates the biggest spore, and numbers 1, 2 and 3 three little spores. The showed rectangular area is enlarged in the following photograph.

All that proves that the stem studied were infected by at least two different sorts of mould species.

3.5.4. Vessels

Figure 23 shows vessels located inside of the rectangular area **6**. The upper photograph of this figure shows a fragment of bilayer epidermis and three different sorts of vessel fragments (enlarged on the lower photograph): of a scalariform vessel, of a vessel with distant rings, and of areoled vessels; this photograph shows also double helix detached elements. All these vessels are grouped in one unit, orientated orthogonally from the stem axis.

Figure 24 shows, for comparison, two parts of a longitudinal (axial) cut of the stem of a today fennel. This comparison permits us to establish firstly fennel stem fragment under study and the today one are delimitated by the same sort of bilayer epidermis.

But it is above all the various vessel forms and their associations that are highly characteristic in plants (Sporanza and Galzoni, 1996). Comparison concerning now the vessel characteristics between the ancient and the today stems of fennel, shows that they have three characters in common:

The presence of scalariform vessels,

The simultaneous presence of the both forms of ringed (with distant, or bringed rings) and double helix vessels,

The presence of double helix detached elements.

In both cases also, areoled vessels are relatively rare.

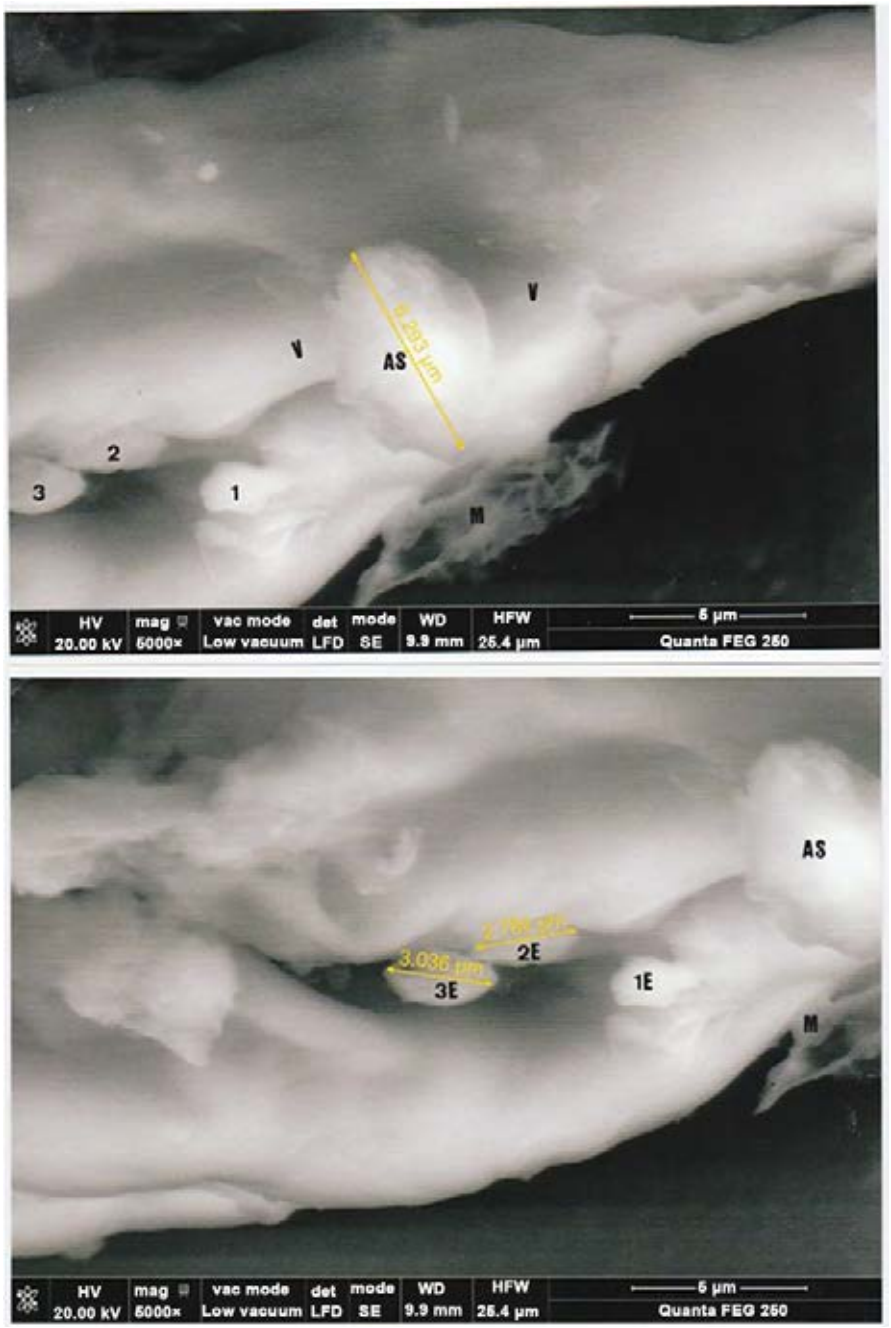

Figure 22. *Above*: SEM photograph (in LFD, 5000×) is an enlargement of the previous photograph (AS: ascopore; M: mycelium). *Below*: SEM photograph (in LFD, 5000×), shifted to the left from the previous one; 1^E, 2^E and 3^E indicate three little spores (dimensions are in µm).

3.5.5. A Scalariform Vessel Fragment

Figure 25 shows a fragment of scalarifrom vessel inside of circle **7**. There is a quasi-identity (concerning scale' pattern and spacing, scale dimensions, width of the scalariform vessel and wall limits arrangement at each side of the vessel) between this observed vessel fragment and that of a scalariform vessel of the today fennel stem.

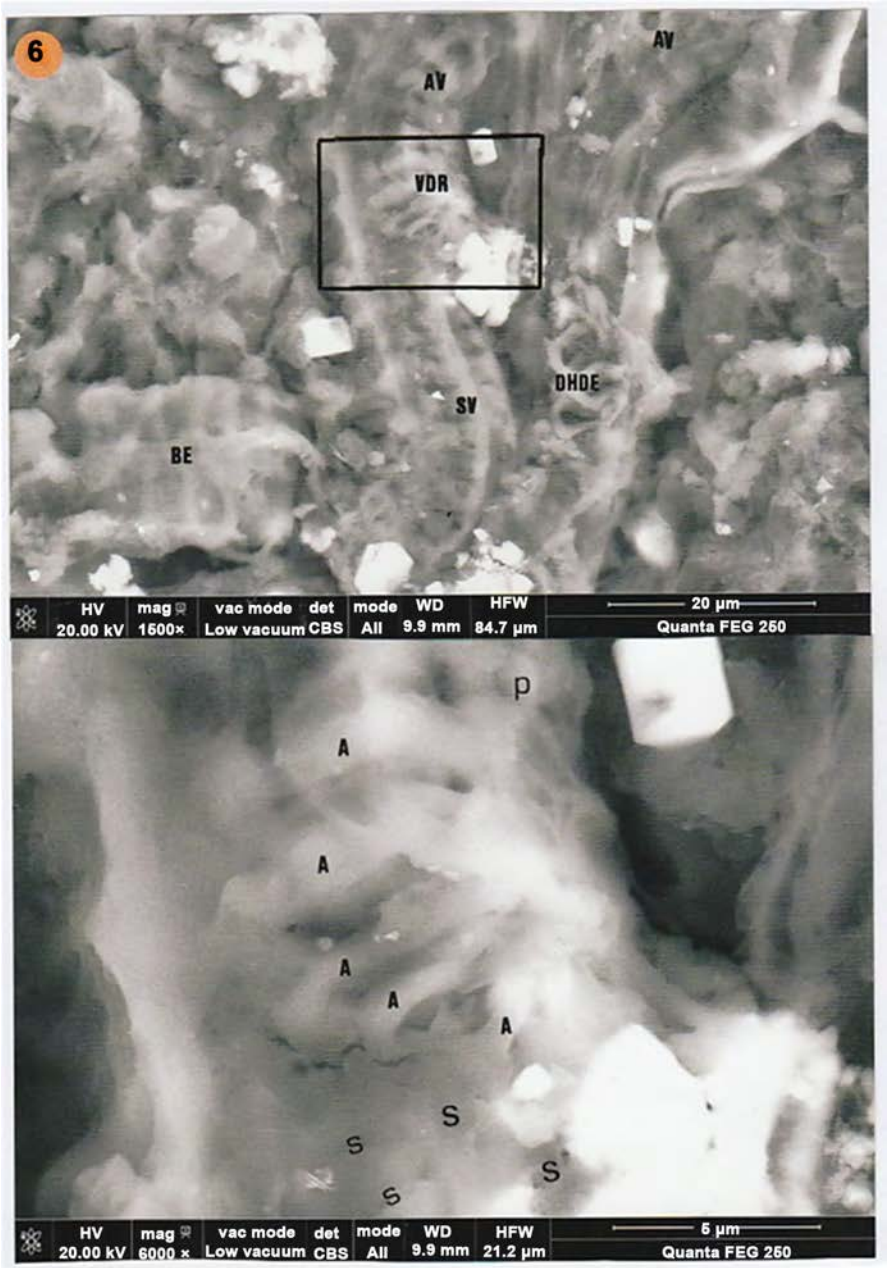

Figure 23. Vascular and epidermis structures inside of the rectangular area 6. *Above*: SEM photograph (in CBS, 1500×) of area. BE: bilayer epidermis; AV: areoled vessels; VDR: vessel with distant rings (the rectangle sub-area is enlarged in the below photograph); DHDE: double helix detached elements; SV: scalariform vessel. *Below*: SEM photograph (in CBS, 6000×) of the enlarged above sub-area. A: rings of vessel with distant rings; p: areole of the areoled vessel; S: scales of the scalariform vessel.

3.5.6. EDX Mapping of the Stem Fragment

Map and EDX general spectrum of the stem fragment (structure C) are shown on **Figure 26**. Carbon and oxygen (main peaks) correspond to the organic matter, and the sulphur peak is relatively elevated; as expected, the potassium peak is the highest among the little peaks of minerals. **Table 2** shows the normalized (carbon and oxygen excepted) composition of elements of C.

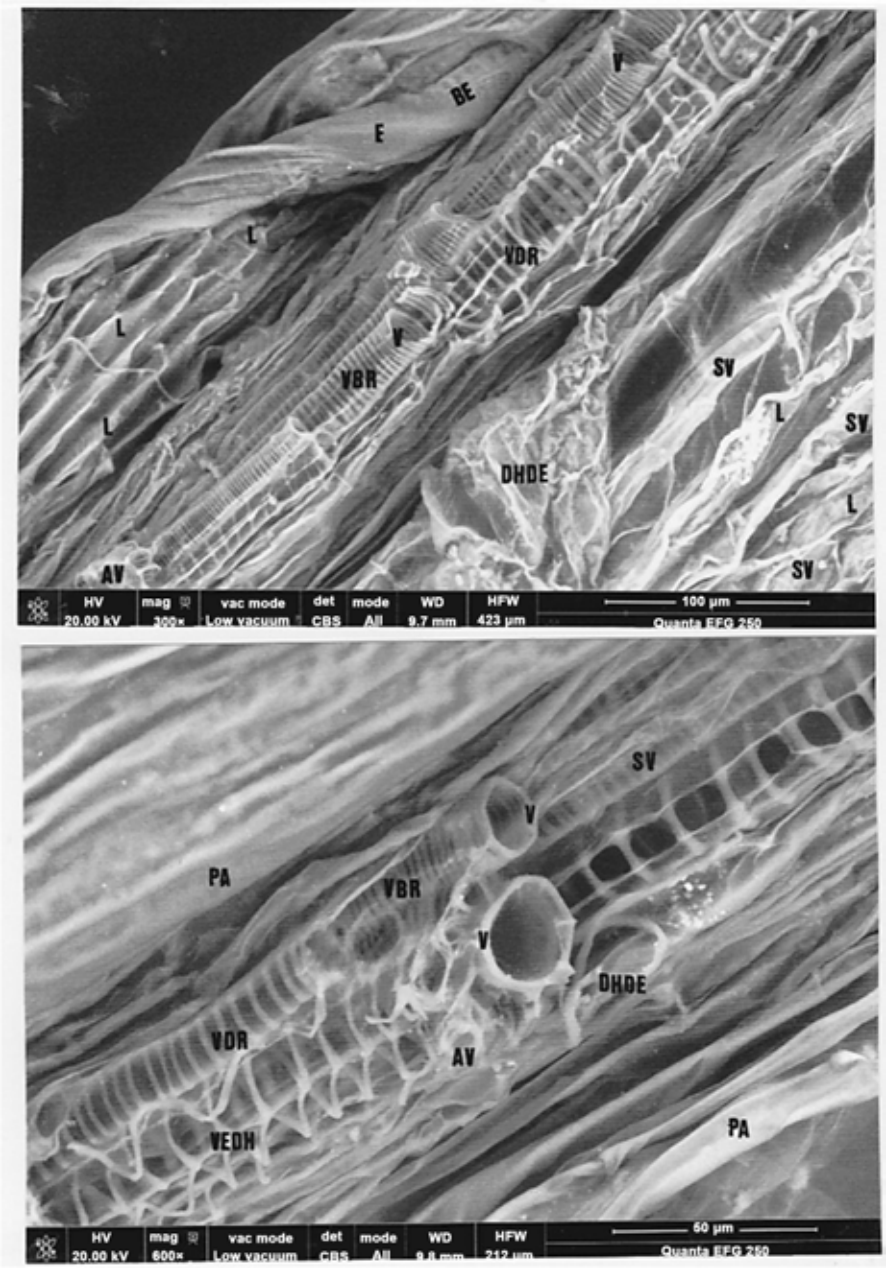

Figure 24. Vascular and epiderm structures in a longitudinal section of a today fennel stem. *Above*: SEM photograph (in CBS, 300×) of some part of the fennel stem cut. E: epidermis; BE: bilayer epiderm; V: two vessel apertures; AV: areoled vessel; VDR: vessel with distant rings; VBR: vessel with bringed rings; DHDE: double helix detached elements; SV: scalariform vessels; L: vessels of the liber. *Below*: SEM photograph (in CBS, 600×) of another part of the fennel stem cut. V: two vessel apertures; SV: a scalariform vessel; VBR: vessel with bringed rings; VDR: vessel with distant rings; VEDH: vessel elements with double helix; DHDE: double helix detached elements; AV: areoled vessel; PA: the two layers of the parenchyme, at each side of the vessels unit.

Figure 27 shows EDX mapping of elements of the stem fragment C. Carbon and oxygen are regularly present in piece C; sulphur is more plentiful in the hair than in the piece.

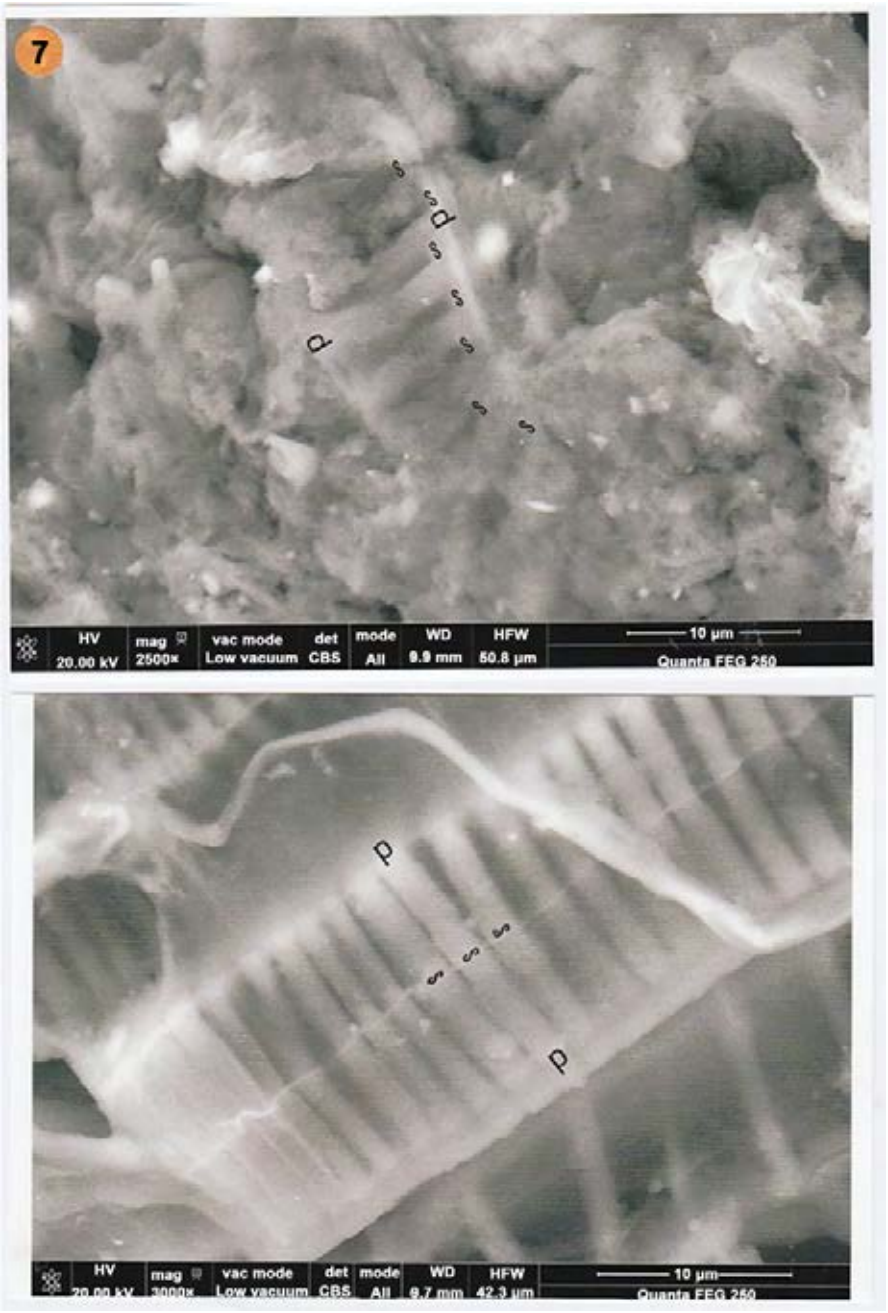

Figure 25. Comparison between a scalariform vessel of piece 7 to that of a today fennel stem. *Above*: SEM photograph (in CBS, 2500×) of the scalariform vessel of piece 7 (s: scales; p: the two walls of the vessel). *Below*: SEM photograph (in CBS, 3000×) of a scalariform vessel of a today fennel stem (s: scales; p: the two walls of the vessel).

Chlorine, sodium and aluminium are spread out regularly in the piece, but at low signal' level. Contrary to, calcium and silicium show packty distributions due to the presence of the corresponding mineral particles of calcium carbonate on the one hand and of silica and of amino-silicates on the other hand. Phosphorus and magnesium are particularly spread out in the central part of the piece.

Figure 26. Map and general spectrum of structure C. *Above*: map of C (the general spectrum is taken in the rectangular area indicated); h6: the part of hair number 6. The coloured code of each element is indicated in the lower part of this map. *Below*: general spectrum of C (the upper limit of the lower red area indicates the background noise).

3.5.7. Exploration of the Central Part of Piece C

Figure 28 shows this central part of piece C, enlarged on the below photograph. Twelve particles (numbered 1 to 12), of relatively great sizes, are shown in the enlarged photograph.

Figure 29 shows spectras of some of them. Particles numbered as 1, 3, 5 and 6 have a typical spectrum of vegetable; they are vegetable debris.

Table 2. Normalized composition of elements in the general spectrum of Figure 26 (measured by rays of the K-serie).

Elements	Atomic numbers	Normalized mass (%)
Sulphur	16	24.33
Potassium	19	17.49
Calcium	20	16.51
Sodium	11	15.52
Magnesium	12	10.15
Aluminium	13	6.89
Chlorine	17	3.64
Silicium	14	3.19
Phosphorus	15	2.28

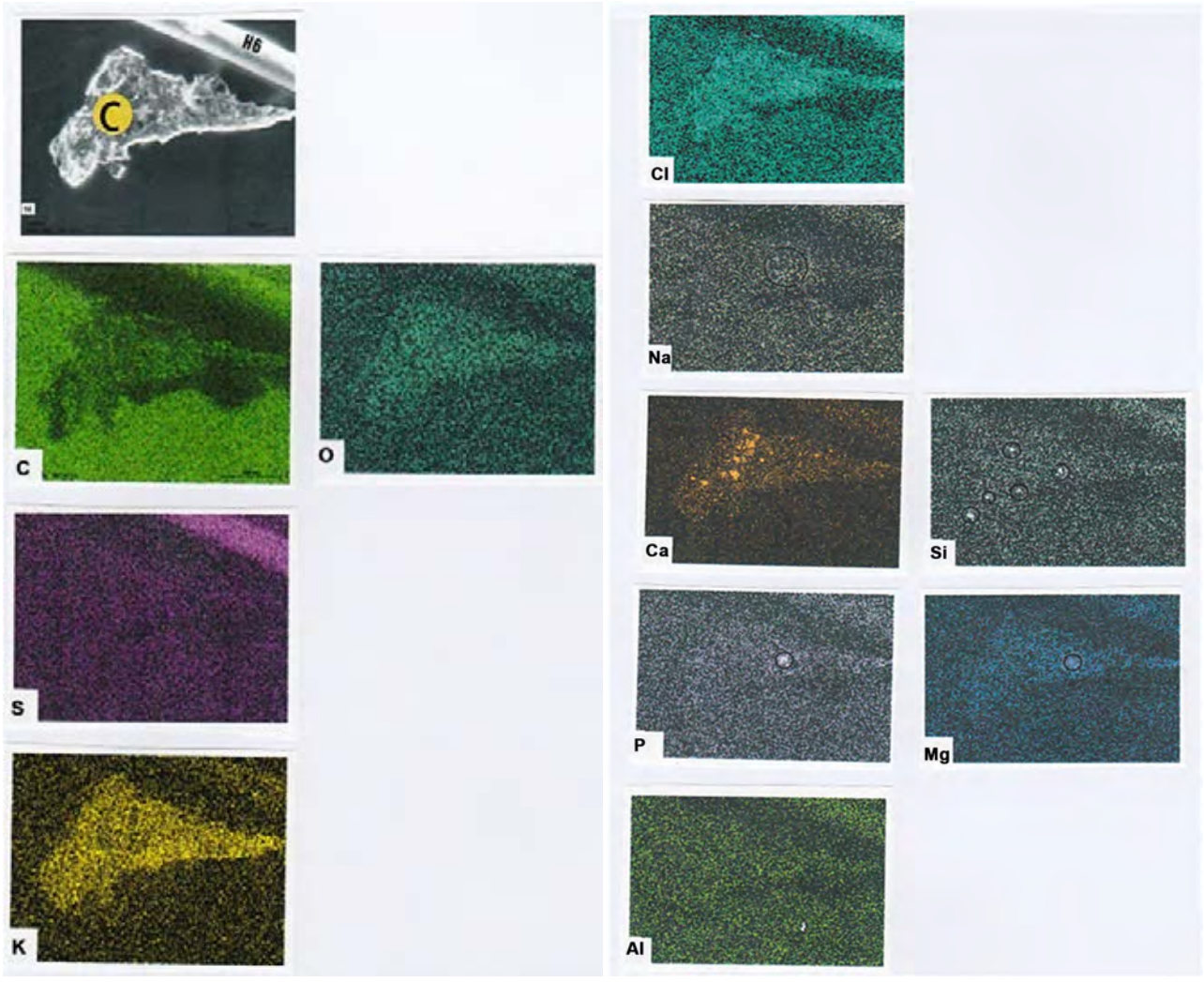

(a) (b)

Figure 27. Mapping of structure C. First row: general map of structure C (h6: hair number 6). Second row: C, carbon mapping, O oxygen mapping. Third row: S, sulphur mapping. Fourth row: K, potassium mapping. Fifth row: Cl, chlorine mapping. Sixth row: Na, sodium mapping. Seventh row: Ca, calcium mapping. Eight row: P, phosphorous mapping, Mg, magnesium mapping. Ninth row: Al, aluminium mapping.

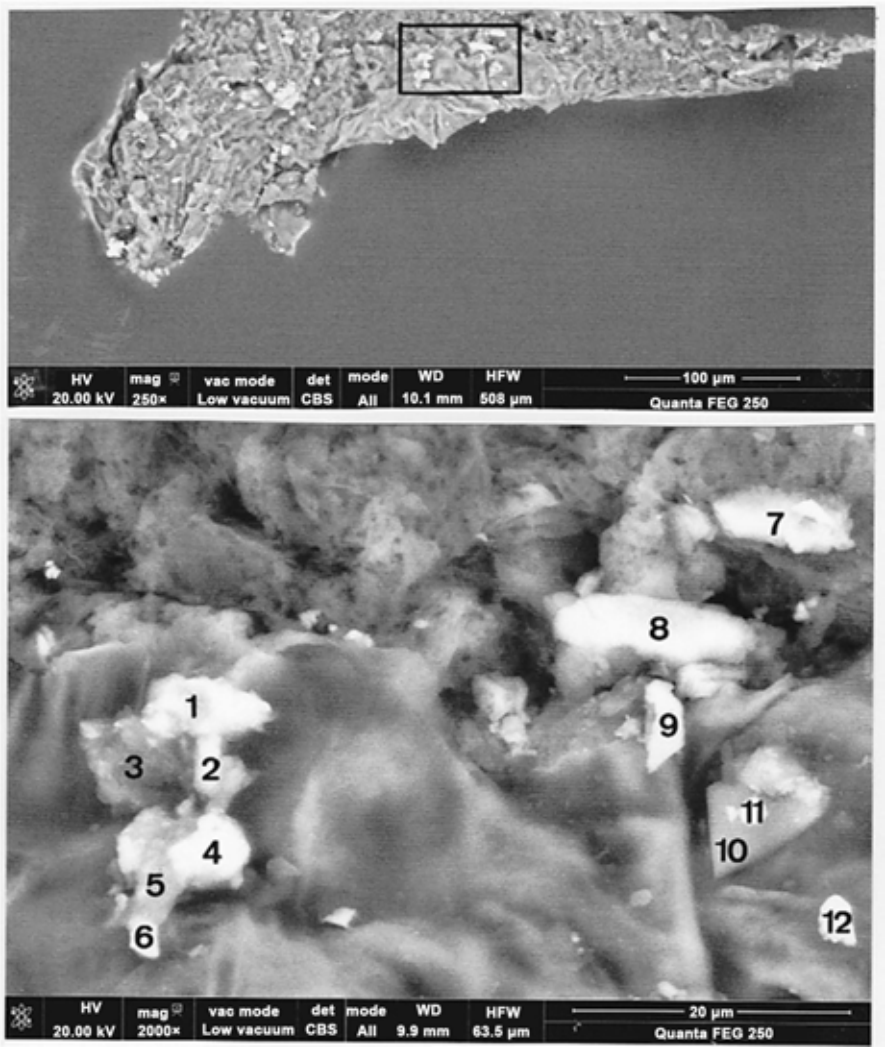

Figure 28. Photographs of the central part of structure C. *Above*: partial SEM photograph (in CBS, 250×) of C (the area in the rectangle is enlarged in the below photograph. *Below*: SEM photograph (in CBS, 2000×) of the enlarged rectangular area. Particles studied are numbered 1 to 12.

Particles numbered as 7, 8, 9, 10 and 11 have a spectrum where the oxygen peak is relatively elevated. Among the smaller peaks, those of magnesium phosphate Mg (H_2PO_4) 2. All the particles numbered as 7, 8, 9 and 10 (**Figure 30**) are of magnesium phosphate; but the little particle number 11 is a calcite, stacked on the magnesium phosphate particle number 10.

Figure 31 concerns spectras of other particles shown in the below photograph of **Figure 28**. Particle number 2 is another silica; particle number 4 is another clay mineral of the montmorillonite/illite type, relatively iron-rich.

Particle number 12 is a potassium chloride (in fact a chloride double of potassium and magnesium): a marine salt (KCl). Some other particles of such type are found elsewhere on the sticky-paper; for example, **Supplementary Figure 7** shows two potassium chloride crystals located at the external border of some part of hair number 1.

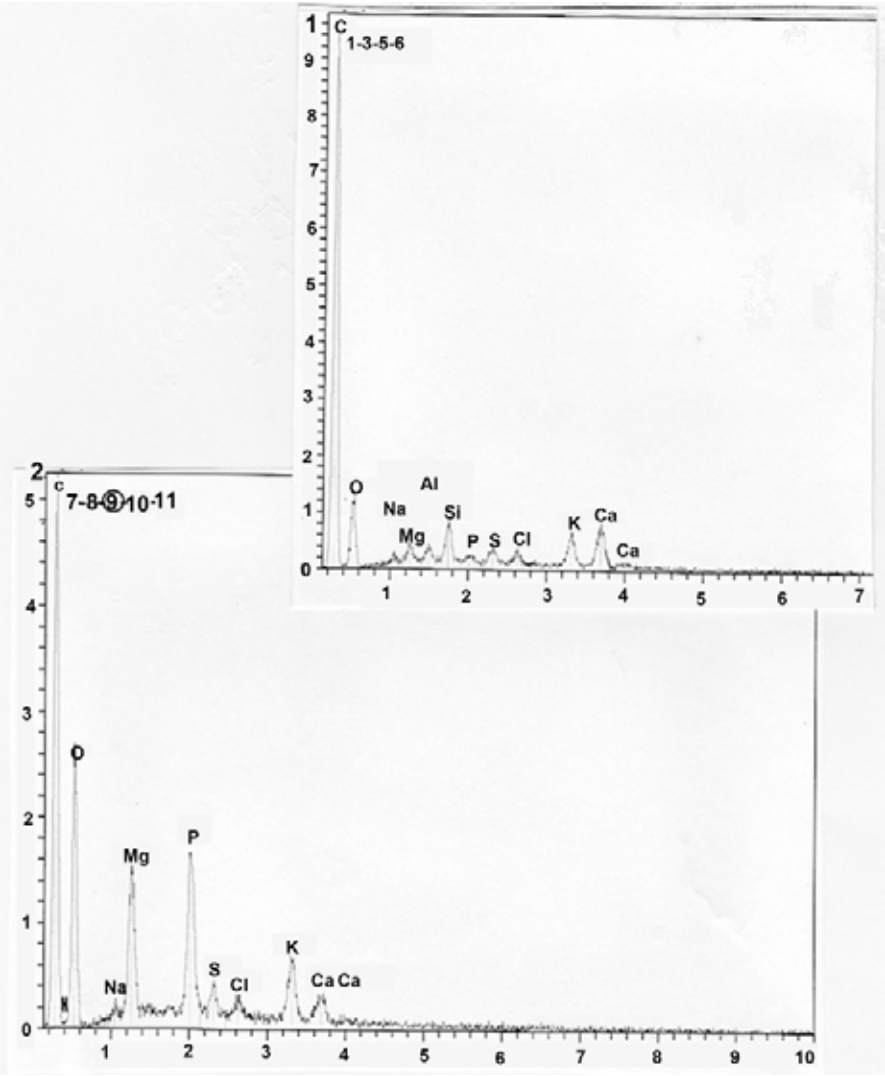

Figure 29. Spectras of some particles located inside of the rectangle of **Figure 28**. **1**: spectrum in common to particle numbers 1, 3, 5 and 6. **2**: spectrum (in fact of particle number 9) in common to particle numbers 7, 8, 9, 10 and 11. The position of the N (nitrogen) peak, located between those of carbon and oxygen, is given (in the below spectrum) as indicative.

Table 3 summarizes compositions of the twelve particles studied.

4. Discussion

We have found numerous fennel rests (pollen grains, leaf and stem debris) at the vicinity of some studied Marie-Madeleine's hairs. That confirms some wordings concerning the Ste Marie-Madeleine's discovery on 19 of December 1279.

But this "extraordinary fragrance" reported by Bernard Gui (that of the fennel smell) do not correspond to the usual notion of "odour of sanctity": the odour of sanctity (Yerby, 1969)—that appears to have emerged in the Middle Ages—according to the Catholic Church, is commonly understood to mean a specific

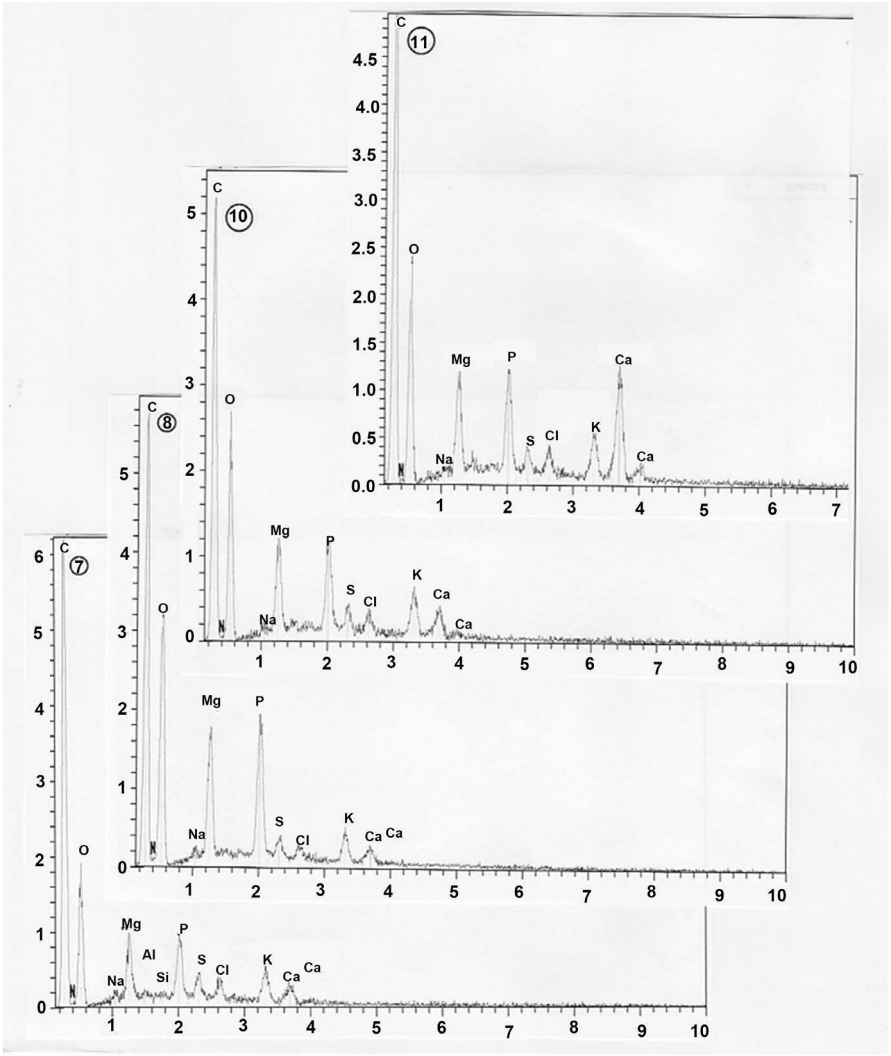

Figure 30. Spectras, from bottom to high, of particles numbers 7, 8, 10 and 11.

scent that emanates from the bodies of saints. This odour of sanctity (a religious term) is a concept occurring at the person's death that carried some weight in convincing the local ecclesiastic authority to "canonize" the saint (at that time, many saints were raised to that status by acclamation of faithful). There are many known examples of saintly men and women who have emitted agreeable fragrances having a strong odour of flowers during a very prayful time; but these flower odours were usually those of the rose and the violet, not of the fennel.

Another important point of the Bernard Gui story that must be taken in consideration is that the "green fennel twig" (*ramusculo funiculi*) come out of the mouth (the tongue being even attached to the osseous palate). Such a singularity must be simply explained if we admit that some fennel seeds (also sweet-smelling), that have grown further, have been implanted at the interior of the mouth of the corpse.

The different steps of the Marie-Madeleine's exhumation process are precisely described (Trouillet, 2016). In fact, if the date of the 19 of December 1279 is well

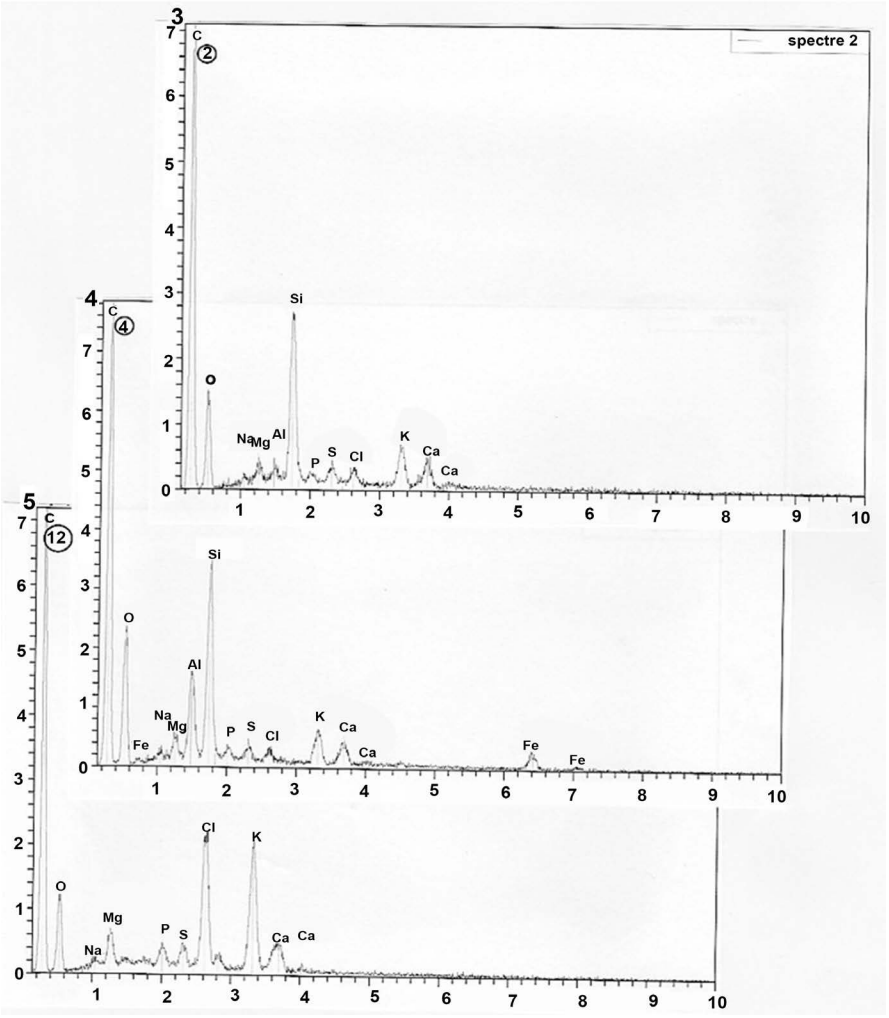

Figure 31. Other spectras of some particles located inside of the rectangle of Figure 28. **3**: spectrum of particle number 2. **4**: spectrum of particle number 4. **5**: spectrum of particle number 12.

Table 3. Compositions of the twelve particles found inside of the rectangular area of photographs of Figure 28.

Particle numbers	Compositions
1	vegetal debris
2	silica
3	vegetal debris
4	montmorillonite/illite
5	vegetal debris
6	vegetal debris
7	magnesium phosphate
8	magnesium phosphate
9	magnesium phosphate
10	magnesium phosphate
11	calcite
12	potassium chloride

that of the exhumation of the Marie-Madeleine's body, it was preceded by a first step(on 9 of December) of the "invention" (*inventio*): Charles-Prince of Salerne—and his farm workers founded the Marie-Madeleine sarcophagus, opened her cover, and contemplated the Marie-Madeleine's rests (Franzoni, 2016); on the same day, Charles shut again the sarcophagus cover and appened seals on it. After that the second step (on 18 of December) was that of the "elevation" (*elevatio*): archbishops and bishops of Provence were convened by the Prince; the sarcophagus was open again, and they certified (it is *the canonic verification of the contain*) the rests: the entire body but the mandible and one leg; hairs surrounded the cranium.

The "ceremonial exhumation" (*revelatio*) of Marie-Madeleine's body was on the 5 of May 1280, at Saint-Maximin, in front of a considerable crowd (Franzoni, 2016). The ceremony was given around the little oratory of Saint Maximin, where the relics were found. To be noted is that—in his process—the Prince of Salerne scrupulously followed the successive steps of the previous relic inventions (Gronnier, 2015).

Who and what determines Charles of Salerne to search for Marie-Madeleine's body at that place (in this oratory)? By a sort of "divine inspiration" (*inspiratione divina*), or because that "in a dream, Marie-Madeleine herself had declared to him that her body was buried in a field, near the Villata church, where a green plant fennel indicated the place"? As reported by Trouillet, the prince was very much involved—both in time and money—(*cum magnis laboribus et expensis*) in the discovery of these relics: he went to Aix for consultation of historical books and annals, and questioned ancients about local traditions concerning that subject.

Charles' s father, as the King Louis IX (Saint-Louis), married to Béatrice, one of the four daughters of the Count of Provence. She was probably influenced by her son Charles (who became Charles II of Anjou) in his engagement to the Provencal origin of Marie-Madeleine; at that time, it existed another possible location of Marie-Madeleine's body in Vézelay (in Burgundy). Among another source, it is King Louis IX himself, sometime after one of his pilgrimage to La-Sainte-Baume, that put in charge his nephew Charles to find Marie-Madeleine's relics in Provence.

We have already signalled the considerable importance taken by the olfactory fennel fragrance at the early stage of the *inventio*. Some confusion has been maintained later on this subject, between this particular fragrance and that of the previous perfume (the "nard") which Maria-Magdalena covered feet and/or Jésus' head (Matthew: 26, 6-13; Mark: 14, 3-9; Johan: 12, 1-8).

But the fennel plant itself intervenes in the *inventio*; we have already given the Bernard Gui 'description of the fennel green ramus that extruded from the mouth of the Marie-Madeleine rests. According to some sources (Franzoni, 2016), that have guided the prince in the relic discovery.

So, the fennel is very tightly associated to the Marie-Madeleine of the Provence tradition. Consequently symbolism of fennel

(http://www.dictionnairedessymboles.fr/article-le-symbolisme-du-fenouil-53869699.html) is a Ste Marie-Madeleine's attribute. Today in Marseilles, in the crypt of Saint-Victor (Notre-Dame-de-la-Confession), is again given the religion of "Notre-Dame-du-Fenouil", named at the origin as
"Notre-Dame-du-Feu-Nouveau" (that was contracted in provencal language as "feu mou", that means new fire).

Fennel (*Foeniculum vulgare*) is native to southern Europe and the Mediterranean area. The name comes from the Greek word for marathon, because of the famous battle at Marathon (490 B.C.) against the Persians was fought on a field of fennel. *Foeniculum* is a roman name, from the latin word *foenum* ("hay"), that was corrupted to *fanculum* in the Middle Ages.

Fennel was well known to the Ancients, and was cultivated by the ancient Romans for its aromatic fruits and succulent edible shoots. Pliny had much faith in its medicinal properties, according no less than twenty-two remedies to it.

Fennel perennial herb is a native to the Meditteranean region. It is now widely cultivated as an annual, biannual or perennial in various European countries (Muckensturm *et al.*, 1997): in Bulgaria, Romania, Hungary, Greece, Italy and France.

What we know about the story of fennel in West Europe, and particularly in France, is a follows:

Wild fennel was a common aromatic herb in Provence, where it grows everywhere.

The growing of fennel became more common in West Europe after Charlemagne (*capitulare* of Willis, end of the VIIIth Century) enjoined its growing on imperial farms.

Fennel cultivation began to develop in the south of Italy in the XVIth Century. The Florence (the bulbous form) fennel variety was introduced in France by Catherine de Médicis (1519-1589), by seed exchanges between Italian and Provencal gardeners.

At the early times of the Middle Age in France, fennel was cultivated mainly because of its medicinal properties. It was (with other medicinal plants and herbs) cultivated in reserved gardens (named now "medieval gardens"), that were always in relationship to monasteries, abbeys and priories. We know that, since the beginning, these monastic gardens were cultivated by religious (mainly those monastic communities belonging to the order of Benedictines); their gardens supplied by herbs which were considered to be so precious for the treatment of various human ills. Fennel particularly, were credited with the power to soothe stomach problems, improve eyesight and cure rheumatism.

As shown in the present study, many fennel pollen grains were found: that proves that it was at least one cycle of annual reproduction for the corresponding plant. Observations about epiderm alterations of the studied stem fragment seems to indicate some perennial herb. Probably because of the time when it was dated, the fennel involved belonged to some wild ancient variety.

But, more surprising, we have found that the tissue fennel debris we have studied correspond to those of plants that were cultivated and processed.

Table 4 gives the characterizations of the fourteen mineral and chemical particles we found on the tissue debris surface. Among the seven first lime and clay minerals could correspond to those of a fertile ground.

At the Middle Age period, farmers only had a rudimentary knowledge of fertilizers; but some farmers did have methods for fertilizing their soil (http://www.thefinertimes.com/Middle-Ages/farming-in-themiddle-ages.html). A common fertilization technique for farming at the times was called marling: for marling farmers spread clay containing lime carbonate onto their soil; this process restored the nutriments needed to grow crops.

Fennel, in its natural habitat, prefers sunny and clayey grounds. A special fennel demand that modern days fennel cultivation establishes (Polese, 2006) is it needs lime (that increases the pH of the soil) for its development; probably the lime particles observed testify of this empirical knowledge at this period.

More surprising is the discovery of two potassium sulphate (both in pieces 1 and 2 in B) and of five magnesium phosphate (all on the structure in C) particles on the fennel debris surface.

They look like, for the two first, to those of modern fertilizers named as potassium sulphate (obtained by the action of sulphuric acid H_2SO_4 on KCl) and—to a lesser degree—as sulphate double of potassium and magnesium. In fact potassium sulphate is, although rare enough, a natural mineral product (arcanite). It is known since the Antiquity and before, and had received very numerous names. We are informed that it was produced commonly, at least since 1300 (alchemists used it for various purposes: in technical chemistry—in lapidary-therapy, dying, and even in symbolic astrology).

The relatively great size and irregular forms of the potassium sulphate deposits (in fact a mixture between potassium sulphate and calcium carbonate) on hair number 1 (see supplementary Figure 4) exclude that there were fine powder particles of such a today industrial product.

Table 4. Numbers of minerals and chemical formulaes of particles found on the fennel debris.

Mineral products	Chemical formulaes	Numbers found
Lime	CaO	1
Calcite	$CaCO_3$	1
Clay minerals	montmorillonite[(1)] illite[(2)]:	2
Silica	SiO_2	3
Potassium sulfate	K_2SO_4	2
Magnesium phosphate	$Mg(H_2PO_4)_2$	4
Potassium chloride	KCl	1

[(1)]$(Na, Ca)_{0.3}(Al, Mg, Fe)_2 Si_4O_{10}(OH)_2 . nH_2O$; [(2)]$(K, H_3O)(Al, Mg, Fe)_2 (Si, Al)_4 O_{10}[(OH_2, H_2O)] SiO_2$.

Still more astonishing is the discovery of the four magnesium phosphate particles on the stem debris; it is only recently (Massey et al., 2009) that magnesium phosphate is produced as a fertilizer. Today, magnesium phosphate is an alimentary complement that is used for the treatment of low amounts of magnesium in the blood.

Magnesium phosphate is in fact a general term for salts of magnesium and phosphate; three forms exist: magnesium phosphate ($Mg(H_2PO_4)_2$)itself, and two other forms of dimagnesium phosphate ($Mg\ HPO_4$) and magnesium phosphate tribasic ($Mg_3(PO_4)_2$). The main magnesium phosphate organic form is struvite ($NH_4MgPO_4{\cdot}6H_2O$), discovered in 1845 by the chemist G. Ulex in medieval sewers of the Saint Nicolas church of Hamburg. Struvite is formed for some organic materials, as old dry dungs constituted of cow dung and horse manure or putrefied dejections.

The mineral form (other term: struveite) of struvite (https://www.mindat.org/min-3811.html) is currently studied (Talboys et al., 2016) in the aim to determine whether it could be a component of a sustainable phosphate fertiliser management strategy for arable crops. Struvite is one of the crystalline mineral (named as guanite) found in guano. In humans, struvite participates to the formation of calculus by precipitating an alkaline urine (https://colique-nephretique.fr/calcul-renal-calcul-de-struvite); the formation of struvite calculus is favoured in some bacterial infections (notably by *Proteus*, *Pseudomonas*, *Klebsiella*, *Staphylococcus*, and *Mycoplasma*) that hydrolyse area in ammonia and raise the urine pH to neutral or alkaline values. In the veterinary domain, struvite calculus are intensively studied for the horse http://www.ncbi.nlm.nih.gov/pubmed/725146), the dog http://www.shilohshepherds.info/geneticTaskForce/Uroliths.htm) and the cat (http://www.cliniqueveterinairedegranby.com/les-struvites-chez-le-chat).

The crystal system of struvite is orthorhombic . The crystals, of relatively great sizes in some cases, are colourless, white (when dehydrated), yellow or brownish, or light grey; the various crystal forms are: equant, wedge-shaped, coffin-shaped (when viewed along), short prismatic or thick tabular. **Table 5** gives sizes and forms of the four struvite crystals (see the lower photograph of **Figure 28**) observed on the surface of the stem debris.

Their spectras (see **Figure 29** and **Figure 30**) show two peaks of the same heights for magnesium and phosphorous (it is the equimolarity that indicates magnesium phosphate as the corresponding product). A purified struvite of reference have a very similar spectrum (Suguna et al., 2012). The quasi-absence of nitrogen in our struvite spectras (as well as its presence at a low level in the struvite sample of reference) can be explained by technical problems: briefly, the EDX analyses we practised cannot resolve levels—even elevated—of nitrogen (the detection system used gives a bad response, in general, for light elements—those of atomic numbers < 10)—because there is a protection film of polymers around the crystal analyser). Another interesting possibility to explain the

Table 5. Forms and sizes of the struvite crystals located on structure C (crystal numbers as for those on Figure 28).

Crystal numbers	Forms	Dimensions (in µm)
7	short prismatic	10 on 3
8	thick tabular	16 on 3
9	short prismatic	8 on 2
10	wedge-shaped	10 on 7

absence of nitrogen in the struvite spectras is that our samples could be in fact crystals of newberyite ($MgHPO_4 \cdot 3H_2O$), a tri-hydrated hydrogenophospahte of magnesium that is frequently associated to struvite. This crystalline component (also of orthorhombic form) seems rare in human kidney calculus; but it was found in caves, formed directly from bat guano (http://www.webmineral.com/data/Newberyite.shtml#Woehf9QS_Gg). Despite the fact that technical problems are responsible for nitrogen detection at low levels, very probably the "struvite crystals" we observe are in fact those of newberyite particles.

The only fertilizer known for the Middle Age period was the dung. But this manure was rare at that period, because cows were not so numerous and malnourished; moreover the cattle was scattered in moors (the meadow did not exist at that time).

Pigeon dropping was the best fertilizer of the Middle Age period, hence reserved to needy soils. The main function of Middle Age pigeonniers (http://pigeonniers-de-france.chez-alice.fr/) was the production of the "columbine" (pigeon feces), which was hightly sought after as a fertilizer for demanding crops in vineyards, vegetable gardens and orchards.

But there was not much of it, since it had be collected from under the pigeon coop. The constitution of stone coops were costly, which meant that they were seigneurial (or monasterial) constructions, their "fertilizers" went to the master's garden and orchard.

The potassium chloride-associated to magnesium-particle (found on the stem surface) is a mineral salt. This product is odourless and has a white or colourless vitreous crystal (of crystallographic cubic structure) appearance. Under its solid form, this neutral salt occurs naturally as the mineral named sylvite and in combination with sodium chloride as sylvinite. This solid dissolves rapidly in water, and its solutions have a salt-like taste ("sel amer").

Supplementary Figure 8 summarizes the study of a powder of a today commercial lighted salt product. Of the two sorts of its particles, those (the most numerous) that are rounded in forms are of potassium chloride; those that are with angular outlines are of sodium chloride (NaCl).

In deserted maritime regions, or in sunny salt marshes, it is possible to extract potassium chloride from seawater. Potassium chloride obtained in this way is

more or less (depending on the local composition of the sea water) mixed with magnesium chloride ($MgCl_2$), as for the particle analysed that we found on the stem surface. During the extraction process from the sea-water KCl and $MgCl_2$ appears under the forms of brine and deliquescents salts, that precipitate after the halite (NaCl).

Potassium chlorine is now used in medicine, lethal injections and scientific applications. The majority of the potassium chloride actually produced is used for making fertilizer, since the growth of many plants is limited by their potassium intake. In fertilizer chemistry (http://www.fertilizer-machine.net/solution_and_market/types-of-fertilizer.html) the generic term of potash includes, wineshim potassium chlorite (sylvite), the chloride double of potassium and magnesium (named carnallite, for its hydrated form), the sulphate double of potassium and magnesium, the potassium sulphate K_2SO_4 already cited (obtained by the action of sulphuric acid on KCl), the potassium nitrate (KNO_3) and the hydroxide of potassium (KOH).

There are documented evidence (Venturini, 2006) of salt production in the Middle Age in the South of France. All the coastal line since the Roussillon region to that of Var mouth have favourable conditions (high salinity of the Mediterranean sea water, intense evaporation favoured by both sun and wind, presence in these areas of little-deap ponds near the sea) to salt working. The central region of this coast (corresponding to the Rhone delta) contains, mainly in Camargue, the most active centers of marine salt production ("salines"), particularly around the little town of Aigues-Mortes. Salt production and exploitation were here under the control of abbeys, and we have numerous written accountable documents attesting that (dating at least since the Xth Century).

Brine can be obtained, notably from sea-water. How and why this corresponding new technology was introduced remains a mystery, through it appears the technique possibly spread from southwest France (Lemonnier, 1980). We know that natural brines always contain other substances dissolved along with salt, notably potassium chloride (the most other common of these substances are magnesium chloride, magnesium sulphate, calcium sulphate, magnesium bromide and calcium carbonate). These substances of brines may be as commercially valuable at the salt itself.

Immersing fresh vegetables and other foods in a liquid solution of salt brine was a common practice in Medieval Europe. For example, the simplest pickling was done with water, salt and herb or two; a variety of spices and herbs as well as the use of vinegar, verjuice or (after the XII th Century) lemon led to range of pickling flavours (https://www.thoughtco.com/medieval-food-preservation-1788842). Pickling might require boiling the food in the salt mixture, but it could also be done by simply leaving the food items in an open pot, tub or vat of salt brine with the desired flavourings for hours and sometimes days.

We have no firm evidence that brine was used as fertilizer in the Middle Age. Today potassium chloride (KCl) is the more commonly used potassium (K) fer-

tilizer (http://www.cropnutrition.com/potassium-chloride), because it includes more K than other sources (50 to 52 percent K, 60 to 63 per cent K_2O (potash) and 45 to 47 per cent Cl^-). There are regions where plants respond favourably to application of Cl^-, and potassium chloride is usually the preferred material to meet this need. There are no significant impacts on water or air associated with normal application rates of potassium chloride (elevated salt concentrations surrounding the dissolving fertilizer may be the most important factor to consider).

Antiseptic properties of salt were known since the Antiquity. The importance of salt within earlier economies (like that of the Middle Age period) can hardly be overstated; it was in fact essential for the maintenance of life, and also for commerce (*HistoricEngland.org.uk/advice*). In addition to preserving food (most notably fish, but also meat and some vegetables), salt plays an essential role in bread-making and in the manufacture of butter and cheese.

Concerning the studied present case, very probably the fennel was processed by salt. We know (Kaur & Arora, 2009) that *Foeniculum vulgare* controls numerous infectious disorders of viral, bacterial, fungal, mycobacterium and protozoal origin. **Figure 22** shows that at least two ascomycetes species contaminate the fennel plant studied.

Table 6 summarizes that we know concerning the three "fertilizers" (potassium sulphate, newberyite and potassium chloride) that were going on and we found on fennel debris; this term of fertilizer (in fact "pre-fertilizer") used here means that they looked like most modern manufacture fertilizers. The potassium chloride that was used certainly was a by-product of seawater brine. But it is only relatively recently that was found that newberyite is the main constitute of guano (and probably that of pigeon dropping). Concerning now the potassium sulphate used, its utilization at that times necessitates solid knowledge in alchemy.

As already signalled both columbine and seawater brine productions were—since the beginning of the Middle Age—under the control of lords or abbeys respectively.

After the Benedictines, several monastic orders—notably the Cistercians (an order founded in 1100 in Citeaux) and the Chartreux (founded in the XIIth Century by Bruno de Cologne, canon of Reims) continued to do the Saint-Benoït rule concerning monastic gardens and orchards (Fuhrmann, 1990). At that time, monasteries took great care of aromatic plants involved in medieval pharmacy (like mint, rosemary, sage, anise and fennel).

We know (Franzoni, 2016) that, soon after their discovery by Charles in 1279, the Marie-Madeleine relics were untrusted to Benedictines. Since the XIV th Century Dominicans replaced Benedictines, and they are here until now.

The main work on agriculture at that times was *Ruralium commodorum opus*, written between 1304 and 1306 by Petro di Crescenzi (1233-1320, Bologna), an Italian magistrate and agronomist of the University of Bologna (Italy). His book, that resulted from long personal practice (he cultivated his own estate, located at St Nicolas, a little village located near his birthplace), was mainly

Table 6. Compositions and possible origins of three fertlizers found on the fennel debris.

Products	Chemical formulaes	Dominant elements	Origins
Potassium sulfate	K_2SO_4	S	a product of medieval alchemistry
Newberyite	$MgHPO_4.3H_2O$	P	from pigeon droppings
Potassium chloride (in fact, a mixture with magnesium chloride)	KCl	K	from seawater brines

centred on Mediterranean agriculture. This treatise was authoritative during all the three following centuries.

However, contents of the di Crescenzi treatise were based mainly on Greek (Plato, Aristotle, Theophrastus...) and early Roman (Varro, Pliny, Columella...) writings. He added some personal observations and teachings of the Dominican monastery of Bologna. As a consequence, soil fertility and soil amendments practices remained much the same as in the days of the Greeks and Romans, relying principally upon animal manures (notably pigeon manure) and human urine and excreta (lisier), vegetable refuses (manure), wastes from oil press, dregs from wine production, sea products (notably brine), seaweed fish in costal areas, bones and inorganic substances such as ashes, marl and lime kiln.

Historically the term "fertilizer" was modified starting the early 1900's as "chemical manure", "artificial manure", "chemical fertilizers" to "mineral fertilizers" and "commercial fertilizers" (this last term defines the products that are sold through commercial channels with warranted concentration of plant nutrients and physical properties). Commercial fertilizers are mineral fertilizers, mineral-organic fertilizers, organic fertilizers and also special fertilizers applied to foliar fertilization or horticulture.

The usual sources of fertilizer primary nutrients are, for potassium compounds, potassium chloride and potassium sulphate (and also potassium nitrate and potassium phosphate).

The modern era of fertilizers began with Justus von Liebig theory published in 1840 in "Organic Chemistry and its Application to Agriculture and Physiology". The modern definition of fertilizers (Gorecki, 2010) is as follows: fertilizers are materials which supply to plant nutrients and improve soil fertility. Most fertilizers are straight, mixed, or compound products applied as solids (mainly as granules) or liquids (in the form of clear or suspension solutions). These products contain primary (which are required by plants in large amounts) nutrients such as N (nitrogen), P (phosphorous) and K (potassium), secondary nutrients (which are need in smaller but still appreciable quantities) such as Ca (calcium), Mg (magnesium) and S (sulphur) and micronutrients. The main fertilizer products (other than nitrogen fertilizers) include phosphate fertilizers (such as single and triple superphosphates) and potassium fertilizers (potassium chloride and sulphate). All phosphate fertilizers are derived from phosphate rocks (phosphorites and apatites) and potassium fertilizers from deposits of potassium chloride

or from marine brines.

Table 7 summarizes the numbers of particles of each class of pre-fertilizers (in large acceptance) we have found on fennel samples studied.

We have verified that the five locations of the elemental map of the stem (see Figure 27, seventh row, second position) of elevated densities in silicium correspond well to clay mineral particles of montmorillonite or illite (most of them are mixed with calcite particles).

We have also verified that all the numerous locations at the left part of the stem (see Figure 27, seventh row, first position) of elevated densities in calcium correspond well to particles of lime (calcium carbonate particles with an elevated peak of calcium). Numerous of them have forms of cubic crystals.

The four particles (numbers 1, 3, 5 and 6) of fennel debris seen on the lower photograph of Figure 28 are more surprising: they are dessicated parts of fine powder of fennel plant, in accordance with compositions (upper spectrum of Figure 29).

We interpret those as some traces of a naive attempt from farmers to stimulate the corresponding plant growth (by projection of such a fine powder on the plant surface, they think that its favour and accelerate the development of the fennel under cultivation).

The newberyite particles found are detected only in stem elemental zone where phosphorous and magnesium are simultaneously present (see Figure 27, eighth row).

Detection on the elemental map of particles of potassium sulfate (K_2SO_4) and potassium chloride (KCl), other than those already described, is impossible because that the potassium element is uniformly spread out on the stem (see Figure 27, fourth row).

But it is amazing that we do not find salt (ClNa) particles on the stem surface. To find some of them, we explored stem regions where there are some concentrations of chlorine (see Figure 27, fifth row) or of sodium (see Figure 27, sixth row) on the corresponding elemental maps. Supplementary Figure 9 shows an enlarged view of such stem region where there is an apparent concentration of chlorine; the corresponding spectrum indicates some little peaks of sodium and

Table 7. Numbers of pre-fertilizer particles found on the surfaces of fennel samples.

Class numbers	Pre-fertilizers	Numbers of particles found
1	clay	2
2	lime	1
3	fennel debris	4
4	potassium sulphate	2
5	newberyite	4
6	potassium chloride	1
7	salt (ClNa)	0

chlorine, but all the particles observed in this area are of calcium carbonate (Supplementary Figure 10).

Supplementary Figure 11 shows an enlarged view of another stem region where there is an apparent concentration of sodium. The corresponding spectras of two sub-areas of this region indicate both also some little peaks of sodium and of chlorine; but all the particles (even those of cubic forms) observed in these two sub-areas are in fact calcite particles (Supplementary Figure 12).

The necessarily deduction of this research concerning salt particles is that, in the areas explored, ClNa is present in the dissolved form only. In these areas the stem is locally soaked by sea-water.

So, there is some evidence that the fennel plant associated with Marie-Madeleine hairs were specially cultivated (clay, lime, pre-fertilizers...) and processed (salts). In these conditions the plant—which was of the wild type variety—had some vigour; it can easily be taller than one metre, as the cultivated wild variety today.

Initial cultivators of this fennel plant were certainly the Cassianites (who were active between 415 and 1079), a religious Order founded by St Jean Cassien. Cassien was native of Provence (he was born in Cytharista, today Cyreste near La Ciotat) circa 365. He returned to Marseilles in 410, where he urged to spread the monastic ideal of the "Pères du Désert" (beside he lived during a long period) and created at this date the Saint-Victor abbey; it is here that he founded the monastic Cassianite Order, a group of contemplative monks who were settled at many places around Marseilles. He came in 415 to La Sainte-Baume where he installed several of his monks (initially in a simple praying place and then in a monastery), establishing permanent Catholic cult devoted to Marie-Madeleine (they know that she had spent here the last part of her life). At the same year Cassien created a similar "prieuré" in *Castrum Rhodanas* (today Saint-Maximin), where several burial places—notably that of Marie-Madeleine—were already particularly venerated.

5. Conclusion

Some fennel rests (numerous pollens, one stem and three leaf fragments) are kept at the vicinity or on the Marie-Madeleine's hairs studied. They correspond to fennel debris of one fennel plant extruding from the Marie-Madeleine mouth that was signalled at the time (on December 1279) of the Marie-Madeleine exhumation by the Prince Charles, Count of Provence. So, the circumstances of the discovery of the Marie-Madeleine body (described previously only historically) are now scientifically established. Some of these fennel fragments—particularly that of the stem—were covered by minerals (clay and lime), pre-fertilizer products (magnesium phosphate and potassium sulphate) and marine salt (potassium chloride) particles. This indicates that the fennel plant was cultivated and processed (it was not an ordinary wild variety). Cassianites were very probably the cultivators of this plant. In these conditions of cultivation, the fennel plant

attained one metre or more of height; it constituted so for Charles an easily point of reference to locate Marie-Madeleine's burial place.

Acknowledgements

We thank the priest of the Saint-Maximin-la-Sainte-Baume, who furnished to us the Marie-Madeleine's hairs, and Jean-David Malnati for his continuous financial support.

References

Badgujar, S. B., Patel, U. V., & Bandivdekar, A. H. (2014). *Foeniculum vulgare* Mill: A Review of Its Botany, Phytochemistry, Pharmacology, Contemporary Application and Toxicology. *Biomed Research International*. https://doi.org/10.1155/2014/842674

Badoc, A., Lamarti, A., Bourgeois, G., Carde, J. P., & Deffieux, G. (1995). Hybridation Intraspécifique chez le Fenouil, *Foeniculum vulgare* Mill. *Bulletin de la Société de Pharmacie de Bordeaux, 134,* 107-126.

D'Avila, V. A., Aguiar-Menezes, E. L., Gonçalves-Esteves, V., Mendonça, C. B. F., Pereira, R. N., & Santos, T. M. (2016). Morphological Characterization of Pollens from three Apiaceae Species and their Investigation by Twelve-Spotted Lady Beetle (Coleoptera: Coccinellidae). *Brazilian Journal of Biology, 76,* 796-803. https://doi.org/10.1590/1519-6984.07615

Ellis, R. P. (1979). A Procedure of Standardizing Comparative Leaf Anatomy in the Poacea. The Epidermis as Seen in Surface View. *Bothalia, 12,* 641-671. https://doi.org/10.4102/abc.v12i4.1441

Franzoni, A. (2016). *Sainte Marie-Madeleine et les Saints de Provence dans la Tradition Provençale* (Vol. 3 and 4). Plan d'Aups Sainte-Baume: ASTPS.

Fuhrmann, J. (1990). Les Différentes Sources, Caractéristiques et Fonctions des Jardins Monastiques au Moyen-Âge. In *Vergers et Jardins dans l'Univers Médiéval* (pp. 109-124). Presses Universitaires de Provence. https://doi.org/10.4000/books.pup.2975

Gorecki, H. (2010). *Ammonia and Fertilizers*. In *Encyclopedia of Life Support Systems (EOLSS)*; United Kingdom Chemical Engineering and Chemical Process Technology, Vol. V.

Gronnier, E. (2015). *Les Inventions de Reliques dans l'Empire Romain d'Orient* (IVe-VIe s.). Thurnout: Brepols. https://doi.org/10.1484/M.HAG-EB.5.112073

Hesse, M., Halbritter, H., Zetter, R., Weber, M., Buchner, R., Frosch-Radivo, A., & Ulrich, S. (2009). *Pollen Terminology: An Illustrated Handbook*. Wien, New York: Spinger.

Jones, G. D., & Jones, S. D. (2001). The Use of Pollen and Its Implication for Entomology. *Neotropical Entomology, 26,* 341-350.

Kaur, G. J., & Arora, D. S. (2009). Antibacterial and Phytochemical Screening of *Anethum graveolens*, *Foeniculum vulgare* and *Trachyspermum ammi*. *BMC Complementary and Alternative Medicine, 9,* Article 30. https://doi.org/10.1186/1472-6882-9-30

Lemonnier, P. (1980). *Les Salines de l'Ouest: Logique Technique et Logique Sociale*. Presses Universitaires de Lille.

Lucotte, G. (2016). The Mitochondrial DNA Mitotype of Sainte Marie-Madeleine. *International Journal of Sciences, 5,* 10-19. https://doi.org/10.18483/ijSci.1167

Lucotte, G., & Thomasset, T. (2017). Study of the Red Colour of Ste Marie-Madeleine (3?-63?) Hair by Scanning Electron Microscopic Characterization of its Melanosomes. *Journal of Dermatology and Pigmentation Research, 1,* 108.

Massey, M. M., Davis, J. G., Ippolito, R., & Sheffield, R. (2009). Effectiveness of Recovered Magnesium Phosphates as Fertilizers in Neutral and Slightly Alcaline Soils. *Agronomy Journal, 101,* 323-329. https://doi.org/10.2134/agronj2008.0144

Muckensturm, B., Foechterlen, D., Reduron, J. P., Danton, P., & Hildenbrand, M. (1997). Phytochemical and Chemotaxonomic Studies of *Foeniculum vulgare*. *Biochemical Systematics and Ecology, 25,* 353-358. https://doi.org/10.1016/S0305-1978(96)00106-8

Polese, J. M. (2006). *La Culture des Plantes Aromatiques*. Chamalières: Artemis.

Rodeva, R., & Galber, J. (2011) Umbel Browning and Stem Necrosis: A New Disease of Fennel in Bulgaria. *Journal of Phytopathology, 159,* 184-187. https://doi.org/10.1111/j.1439-0434.2010.01728.x

Speranza, A., & Galzoni, G.L. (1996*). Atlas de la Structure des Plantes*. Paris: Belin.

Suguna, K., Thenmozhi, M., & Sekar, C. (2012). Growth, Spectral and Mechanical Properties of Struvite Crystal Grown in Presence of Sodium Fluoride. *Bulletin of Material Sciences, 35,* 701-706. https://doi.org/10.1007/s12034-012-0322-6

Talboys, P. J., Heppel, J., Roose, T., Healey, J. R., Jones, D. L., & Withers, P. J. A. (2016). Struvite: A Slow-Release Fertilizer for Sustainable Phosphorus Management? *Plant and Soil, 401,* 109-123. https://doi.org/10.1007/s11104-015-2747-3

Trouillet, M. C. (2016). *Les Reliques de Ste Marie-Madeleine*. Aix-en-Provence: R.A. Image SARL.

Venturini, A. (2006). Le Sel de Camargue au Moyen Âge. In J. C. Hocquet, & J. L. Sarrazin, *Le Sel de la Baie: Histoire, Archéologie, Ethnologie des Sels Atlantiques* (pp. 365-392). Presses Universitaires de Rennes. https://doi.org/10.4000/books.pur.7636

Yerby, F. (1969). *Odour of Sanctity* (New Impression Edition). William Heinemann LTD.

Supplementary

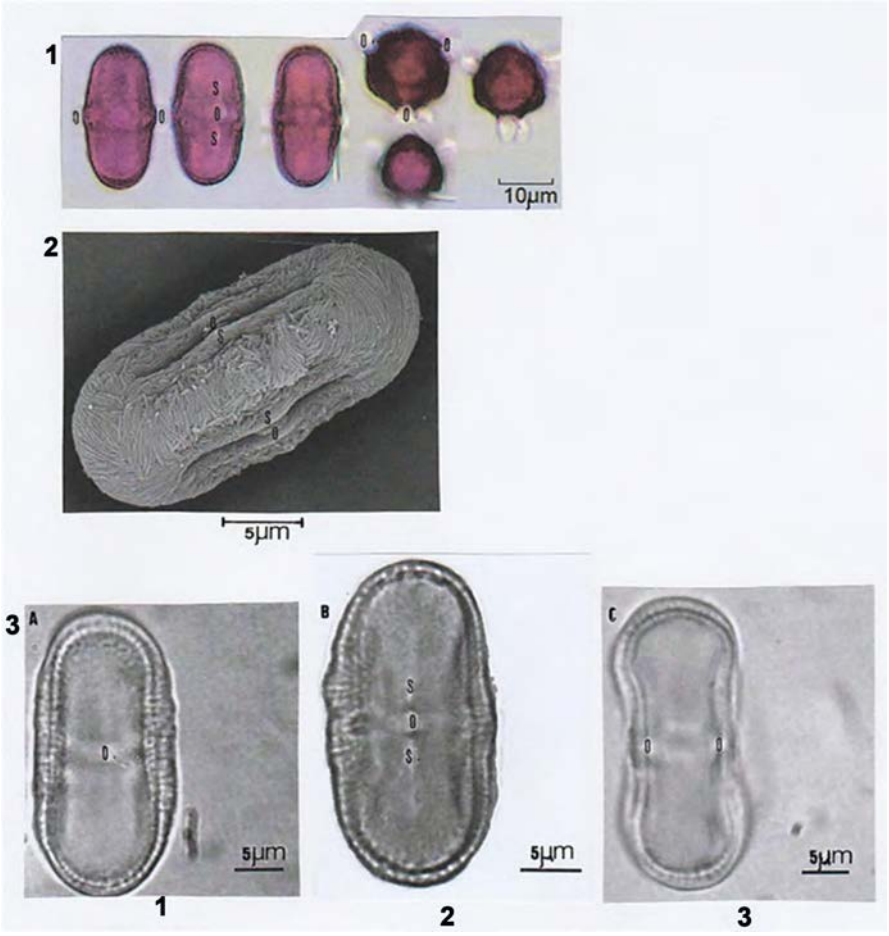

Supplementary Figure 1. Typical pollens of reference. First row: optical microscopy photographs (equatorial and polar views) of pollen grains of *Foeniculum vulgare* (from Aus Pollen-Wiki). S: sulcus; O: pore. Second row: SEM photograph (equatorial view) of a pollen grain of *Foeniculum vulgare*
(from http://remf.Dartmouth.edu/pollen2/pollenimages). Third row: optical microscopy photographs (equatorial views) of pollen grains of *Foeniculum vulgare* (1A: fennel), of *Anethum graveolens* (1B:dill) and of *Coriandrum sativum* (1C: coriander); from D'Avila et al., 2016.

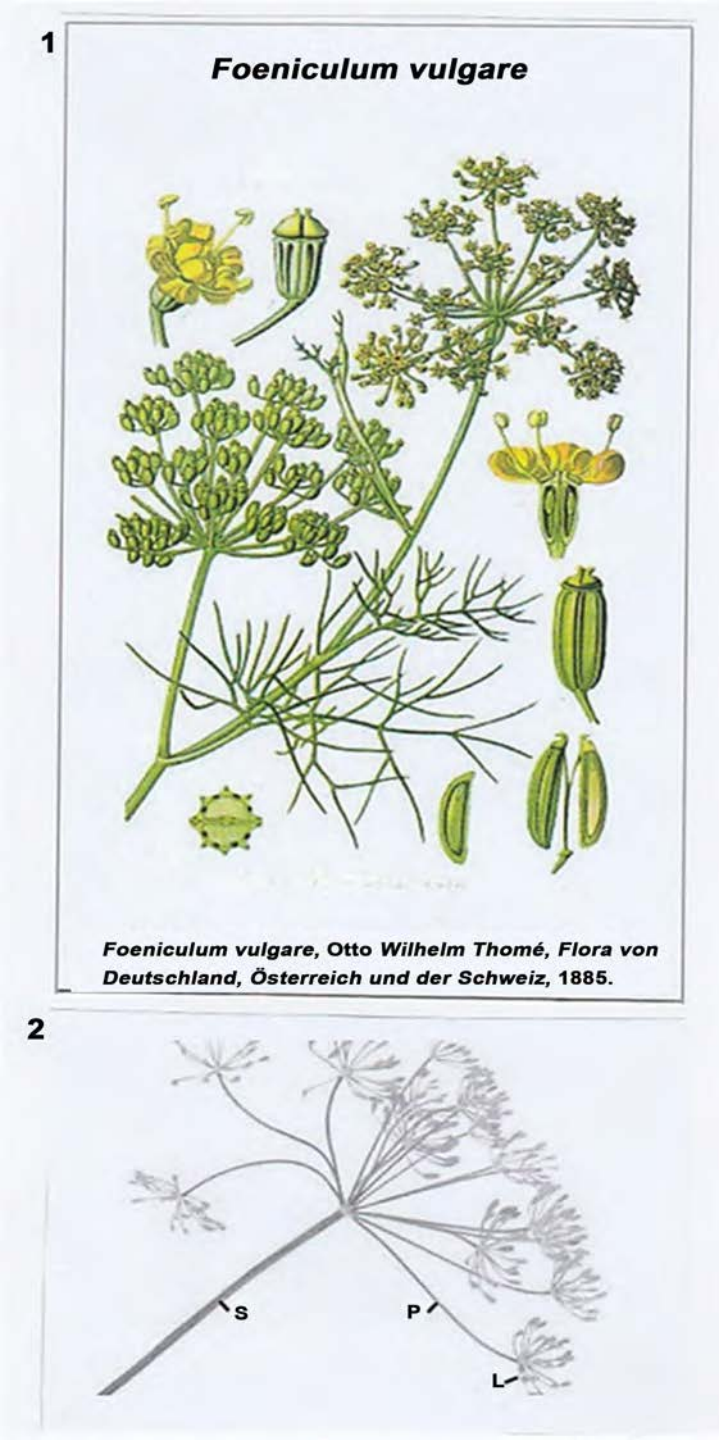

Supplementary Figure 2. Fennel (*Foeniculum vulgare*) images. 1: the different organs of the plant. **2**: details of an umbel (S: stem; P: pedicel; L: leaf).

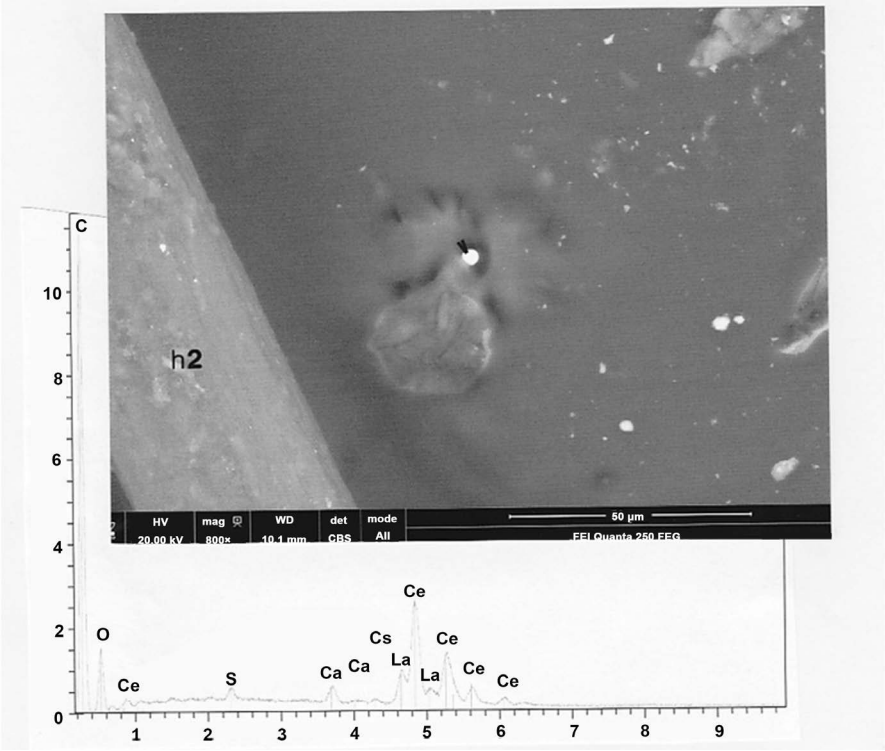

Supplementary Figure 3. An example of a micro-marble of rare earths, located at the vicinity of hair number 2 (h2). *Above*: SEM photograph (in CBS, 800×) of this micro-marble (indicated by an arrow point. *Below*: spectrum of the micro-marble. C: carbon; O: oxygen; Ce (five peaks): cerium; Ca (two peaks): calcium; Cs: cesium; La (two visible peaks): lanthane.

Supplementary Figure 4. SEM photograph (in LFD, 6000×) of micro-needles (1) and micro-plaques (2) of sulfate double of calcium and potassium, deposited on some part of hair number 1 (h1). Black spots indicate the locations where EDX analyses are realized.

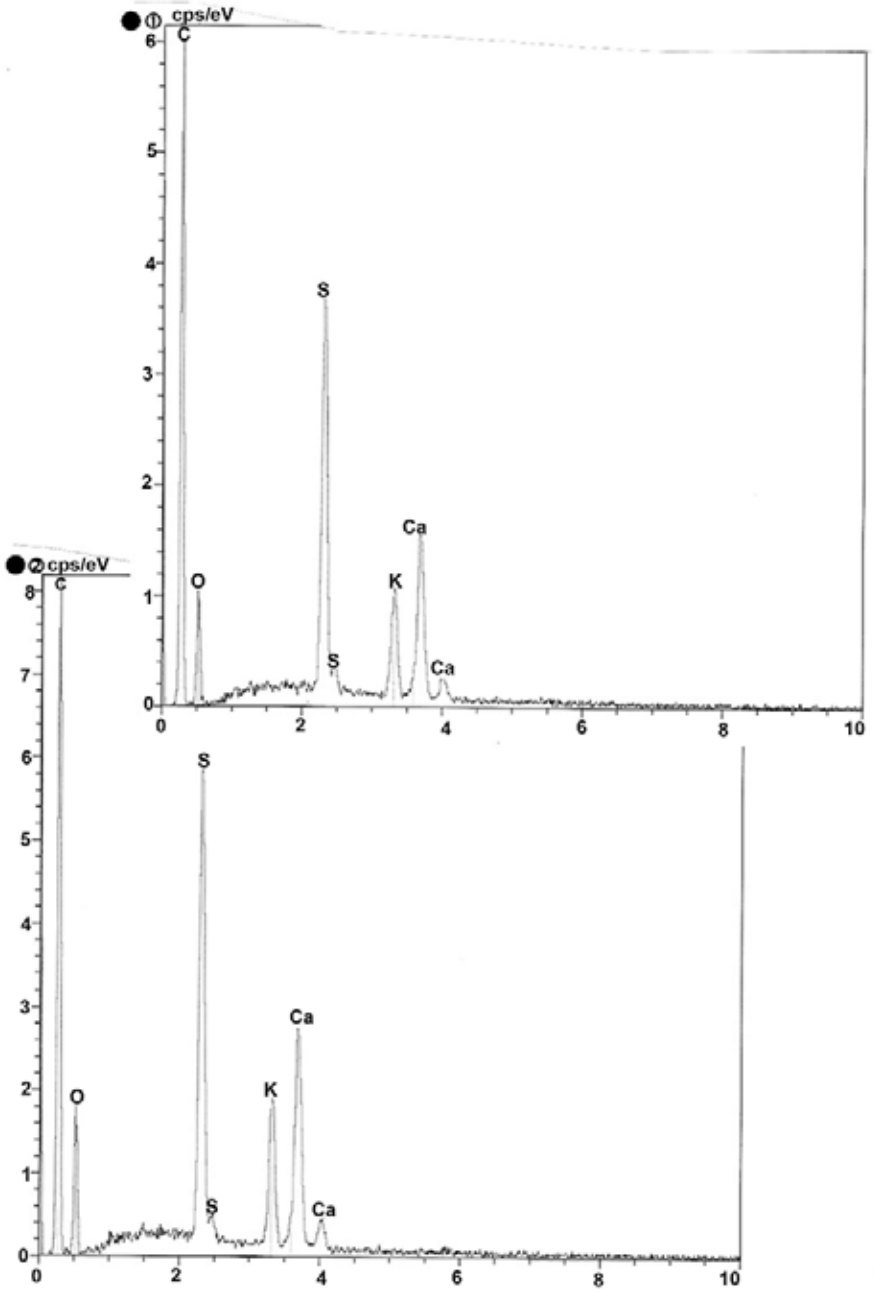

Supplementary Figure 5. Spectras of micro-needles (above) and of micro-plaques (below). C: carbon; O: oxygen; S: (two peaks): sulphur; K: potassium; Ca (two peaks): calcium.

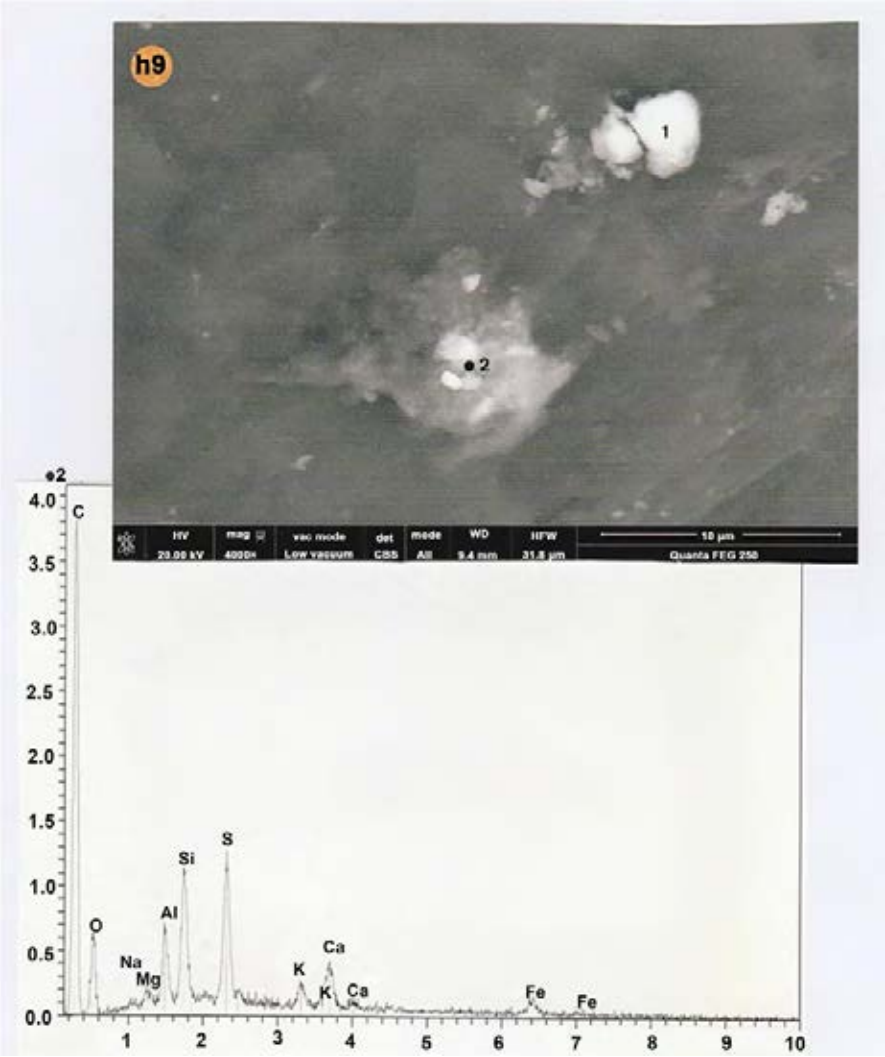

Supplementary Figure 6. An example of deposits of montmorillonite/illite particles on some part of hair number 9 (h9). *Above*: SEM photograph (in CBS, 1000×) of particles of calcium carbonate (**1**) and of montmorillonite/illite (**2**). The black spot indicates the location where EDX analysis is realized. *Below*: spectrum of **2**. C: carbon; O: oxygen; Na: sodium; Mg: magnesium; Al: aluminium; Si: silicium; S: sulphur; K: (two visible peaks): potassium; Ca (two peaks): calcium; Fe (two visible peaks): iron.

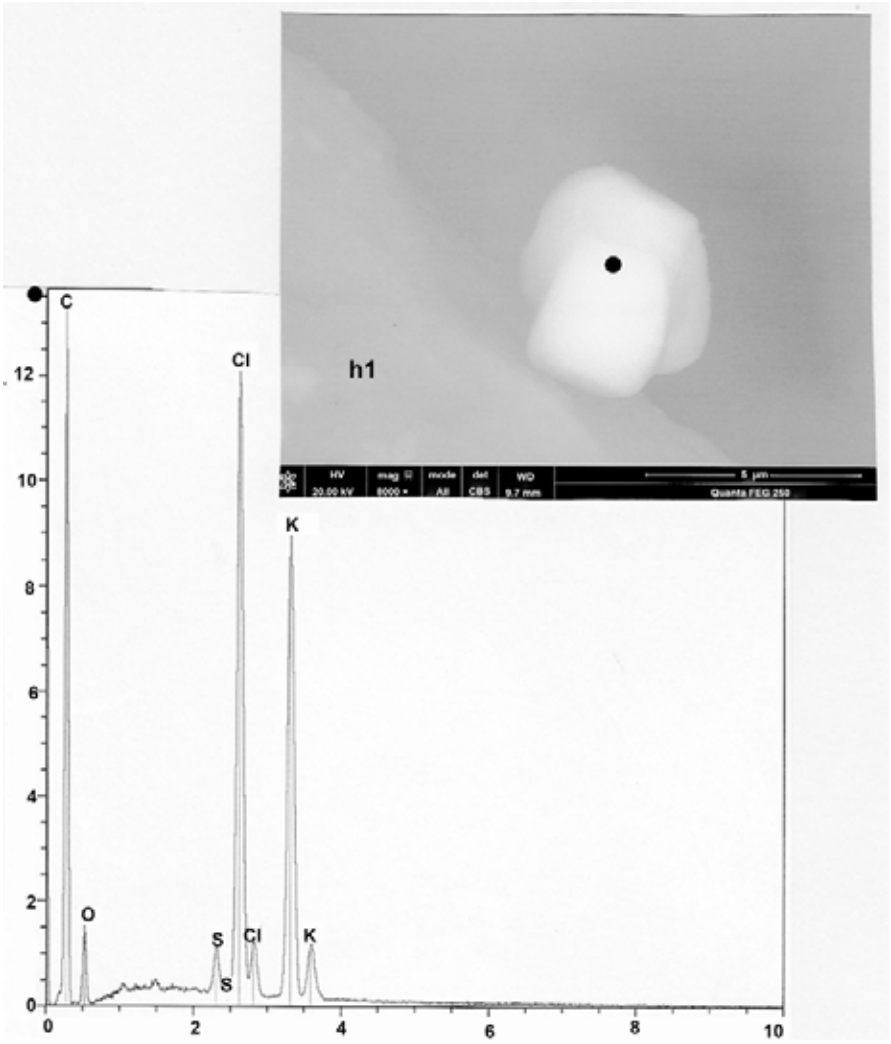

Supplementary Figure 7. An example of crystals of potassium chloride on some part of hair number 1 (h1). *Above*: SEM photograph (in CBS, 8000×) of these crystals (the black spot indicates the location where EDX analysis is realized. *Below*: spectrum at the black spot.

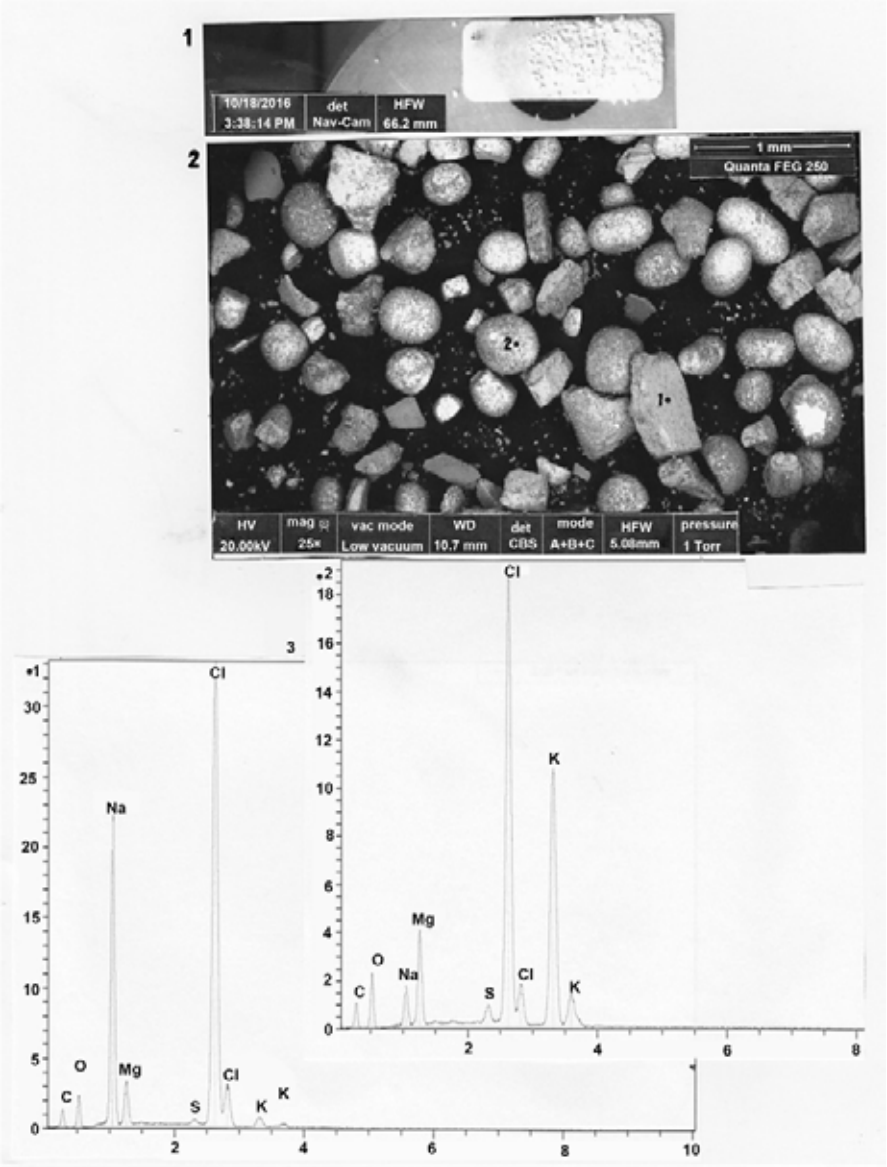

Supplementary Figure 8. Study of commercial lighted salt. **1**: Optical microscopic view (3×) of a powder of the product. **2**. SEM photograph (in CBS, 25×) showing the two different forms of particles from this sample. Some of them (like 2), that are the most numerous, are rounded in form; other (like 1) are with angular outlines. **3**: spectras of 1 (below) and 2 (above).

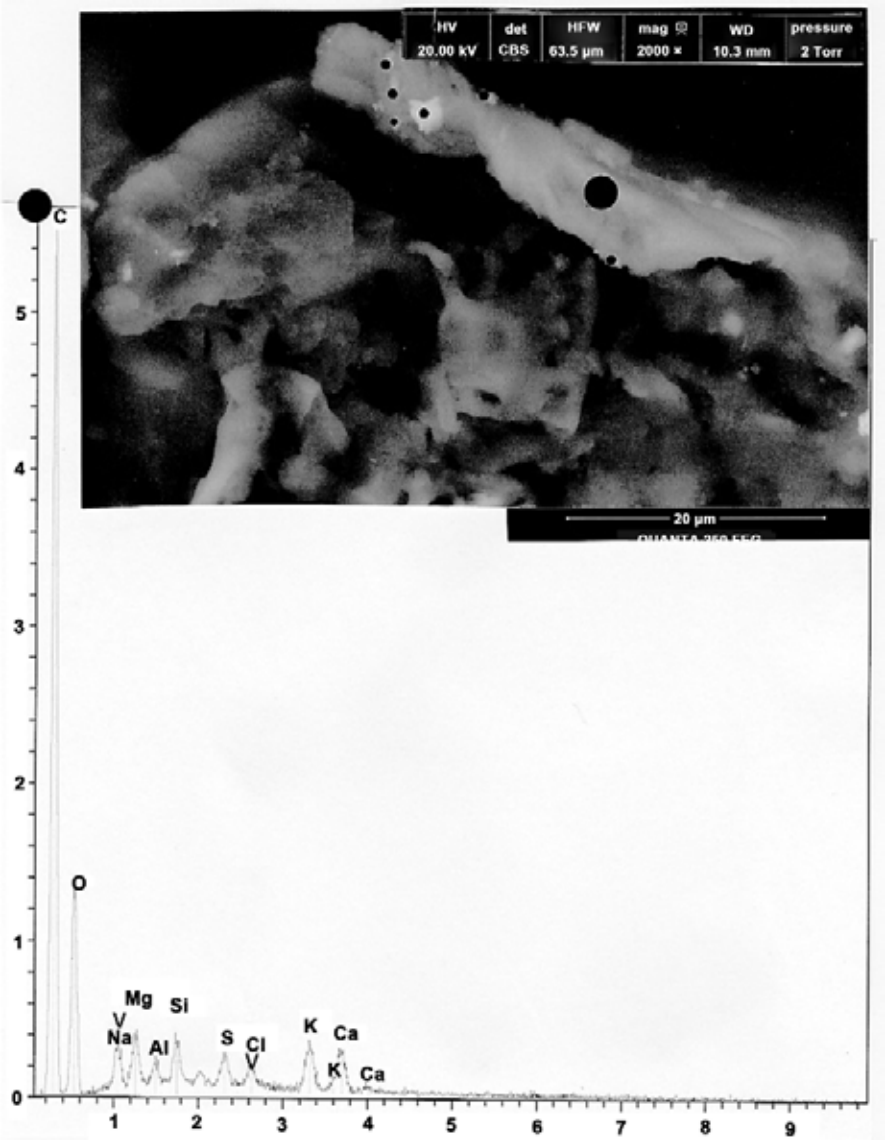

Supplementary Figure 9. Study of one of the superior border of the stem, to detect salt particles composed of chlorine. *Above*: SEM photograph (in CBS, 2000×) showing this border. The great black spot indicates the location where EDX analyses are realized. *Below*: spectrum at the great black spot (arrows indicate peaks of chlorine and of sodium elements).

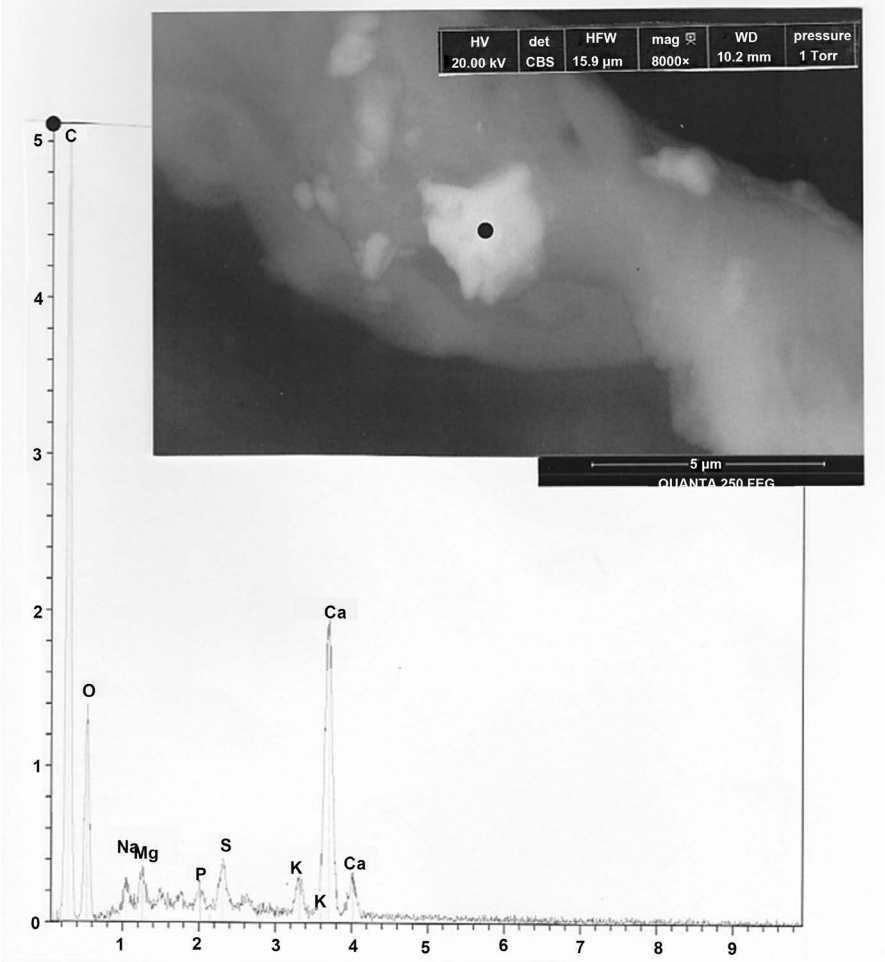

Supplementary Figure 10. *Above*: SEM photograph (in CBS, 8000×) showing an enlarged view of the previous one. *Below*: spectrum of the greatest particle.

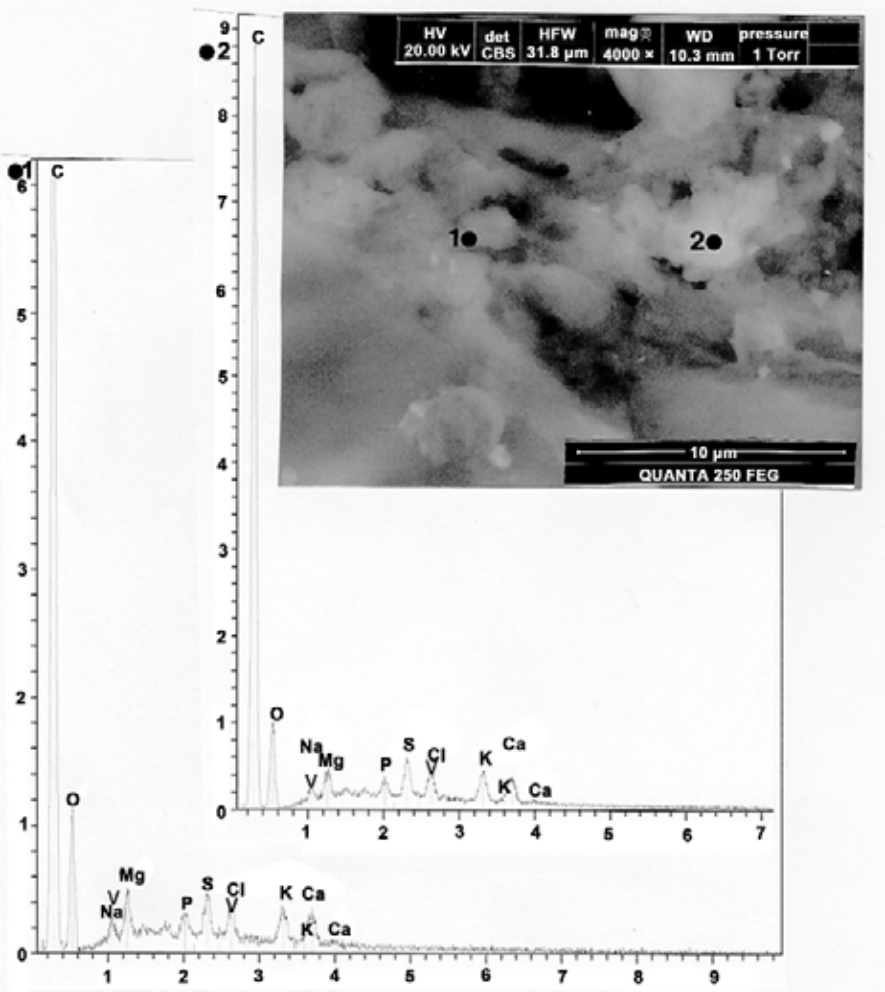

Supplementary Figure 11. Study of the stem part rich in sodium, to detect salt particles composed of sodium. *Above*: SEM photograph (in CBS, 4000×) showing two sub-parts (**1** and **2**) of this part (dots indicate locations of these sub-parts where EDX analyses are realized). *Below*: spectras at dots 1 and 2 (arrows indicate peaks of chlorine and of sodium elements).

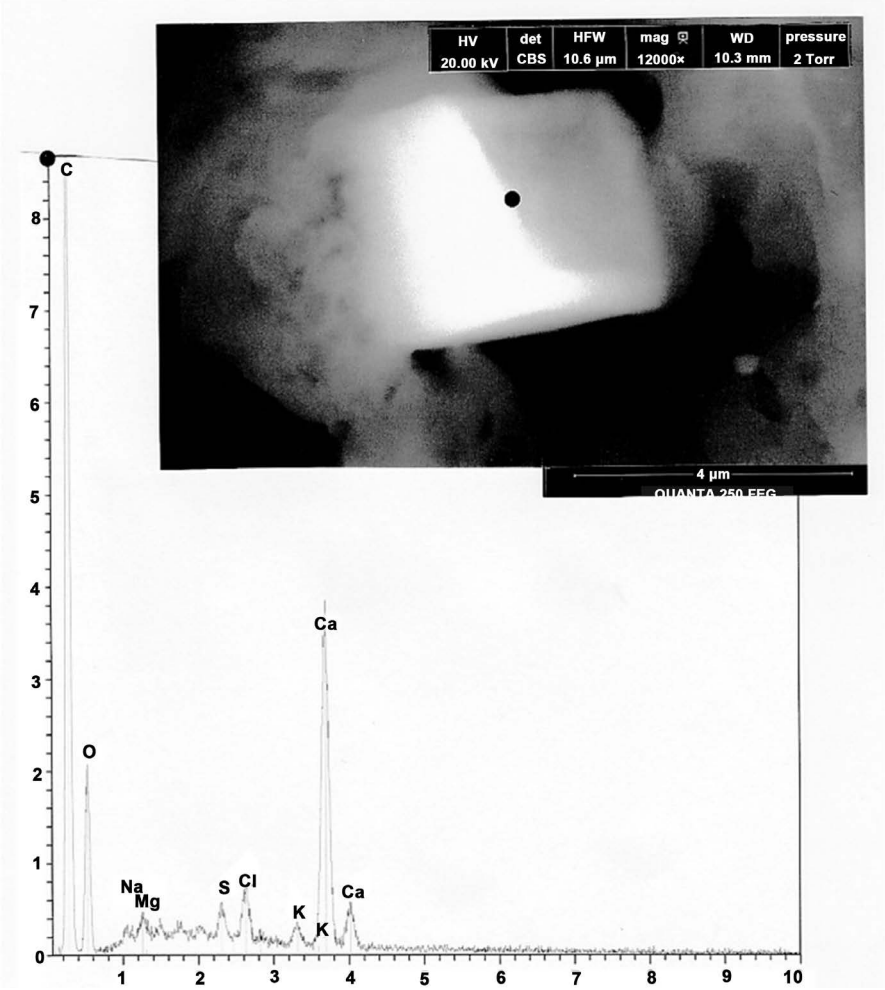

Supplementary Figure 12. An example of an analysis of a cubic particle (crystal) found in the stem area of high concentration of sodium. *Above*: SEM photograph (in CBS, 12000×) of this crystal. *Below*: its corresponding spectrum.

Archaeological Discovery, 2018, 6, 271-277
http://www.scirp.org/journal/ad
ISSN Online: 2331-1967
ISSN Print: 2331-1959

Techniques for the Extraction of Vibrational Signature: A New Method of Pottery Shard Identification

Baxton R. Chen

Foundation for the Advancement of Anthropology & History, Menlo Park, CA, USA
Email: Baxraychen@me.com

How to cite this paper: Chen, B. R. (2018). Techniques for the Extraction of Vibrational Signature: A New Method of Pottery Shard Identification. *Archaeological Discovery, 6,* 271-277.
https://doi.org/10.4236/ad.2018.63013

Received: April 23, 2018
Accepted: June 16, 2018
Published: June 19, 2018

Abstract

Pottery shards are conventionally classified based on their color, surface texture, density, thickness, curvature, material, and shape. We previously reported a method of identifying pottery shards based on their vibrational characteristics with ultrasound stimulation. We now detail the experimental procedure necessary for the extraction of such signatures. With the method of rapid and inexpensive vibrational signature extraction and comparison to a known database library, the technique provides a potential method of onsite shard identification.

Keywords

Pottery, Vibration, Identification, Algorithm, Signature

1. Introduction

The history of pottery echoes the history of human civilization. Ever since fire was first used, man has found the hardened soil around the fire useful for molding into figurines or containers (Renfrew & Bahn, 1991). As mankind evolved and mastered fire, different cultures around the world independently developed their own sophisticated styles of pottery, often with distinctive shapes, colors, and styles based on local soil and other materials, technology, and artistic expression. The variety of pottery developed has proven helpful when studying past cultures and civilizations. Due to the nearly indestructible hardiness of pottery shards, they have been consistently uncovered from many excavation sites. Overtime, the excavation of items of a particular pottery style alongside other known objects helped to establish pottery shards as a useful tool to chronologically date excavation sites. Pottery shard identification has thus become an im-

portant discipline in the field of Archaeology. Archaeologists have traditionally relied on color, surface texture, density, thickness, curvature, material, and shape to identify pottery shards (Historical Archaeology at the Florida Museum of Natural History, 2018; Hunt, 2017). This method of pottery shard ientification requires years of training, and disagreements among experts are not unusual. It would be useful to have a physical method of identifying pottery shards.

As a general principle, all materials vibrate when exposed to sound waves (MIT News, 2014). Pottery is made of dense material that transmits sound and vibrations easily, with distinctive harmonic waves that are characteristic of the material since soils from different parts of the world have different characteristics, they possess unique vibrational signatures (Parikh et al., 2014; Gazetas, 1982). For example, different concentrations of clay soil can influence vibrational signatures (Kitovas, Stelmokaitis, & Doroševas, 2016). The unique vibrational characteristics of North American soil has long been documented (Jacobsen, 1930), and recent studies list European soil vibrational patterns (Eddine, Lenti, & Semblat, 2017). The vibrational signatures of soil around Scotland were also carefully catalogued in a recent report detailing the responses to infrared and x-ray (Robertson, Shand, & Perez-Fernandez, 2018). Since pottery made in each region comprises different soil compositions, each has unique vibrational characteristics. We previously reported using ultrasound-triggered vibrational analysis to automatically differentiate pottery (Chen, 2017). We now detail the technique necessary for extracting such vibrational signatures.

2. Materials and Methods

The system consists of a source for energy stimulation, a holding system for the pottery shard, a system for vibration detection, and a system for vibrational analysis. A number of energy sources have been utilized, including radiofrequency, ultrasound, or mechanical force. At the simplest level, one can strike a shard of pottery with a tuning fork or a small jeweler's hammer to generate a simple and reproducible stimulus. The stimulus is absorbed by the pottery shard, which will then vibrate in accordance to its internal harmonic frequency, which is characteristic of the pottery composition. Alternatively, one can use signal sources such as medical grade Dermatology treatment machines, such as Mini RF Bipolar Radio Frequency (**Figure 1(a)**; UPC code 710280118370, Mychway, Hong Kong, China) or D'Arsonval High Frequency Device (**Figure 1(b)**; Napalabscience, China). At a higher price point, one can use medical grade ultrasound machines such as the VScan pocket ultrasound (GE Healthcare, Little Chalfont, United Kingdom). This type of device produces extremely precise frequencies of ultrasound that are routinely used for medical imaging, and generates high resolution signatures.

The pottery shard specimen is held in place with a simple clamp, which may or may not need to be anchored to a stand for stability. A number of different clamps can be used to hold the pottery shard. The most important precaution is

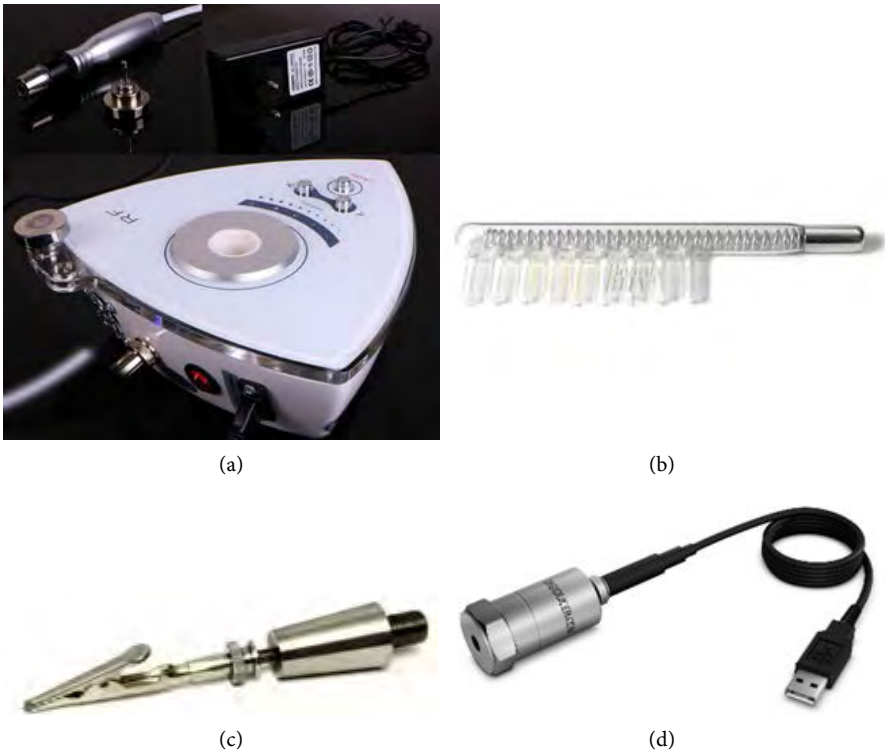

(a) (b)

(c) (d)

Figure 1. (a) Mini RF Bipolar Radio Frequency; (b) D'Arsonval High Frequency Device; (c) Screw-mounted micro-clamp; (d) USB Digital Accelerometer.

to find a clamp that can hold the shard tightly so as to prevent the shard's wobbling, which can produce distracting background vibrations. The clamp can reduce vibration at the point of contact, soit is important to choose a clamp with as small of a clamp footprint as possible in order to prevent damping of the vibrational signature. One should be sure to use clamps that are non-crushing in order to prevent damage to the pottery shards.

The vibration detection system consists of an USB Digital Accelerometer (Model 333D01, Digiducer, Mission Viejo, CA). The accelerometer is connected to the pottery shard via a screw-mounted micro-clamp (Figure 1(c); SCP-MICRO, SnakeClamp Products, Riner, VA). The small profile clamp can transmit signals from the pottery to the accelerometer with minimal signal loss or distortion of signal integrity. The Accelerometer is then connected to an iPad, iPad Mini, or to an iPhone via the Lightning-to-USB Camera Adapter (Apple, Cupertino, CA).

The vibrational analysis system utilizes apps such asVibroChecker Pro (ACE Control Inc, Farmington, MI) or SignalScope (Faber Acoustical, LLC, Lehi, Utah). Both softwares can interpret the signal received from the accelerometer and display them as waveforms that can be easily visualized and recorded.

3. Results

The signal source and the accelerometer are placed approximately one inch apart for standardized signal capture (Figure 2). Pending on the source of stimulation

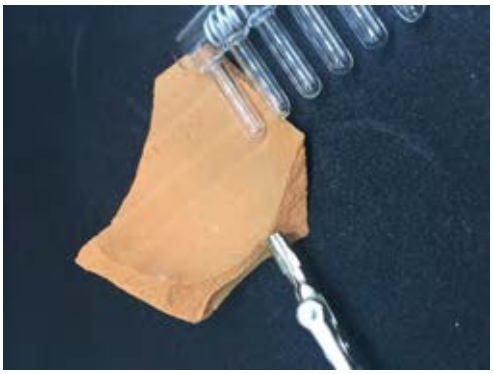

Figure 2. The signal source and the accelerometer are placed approximately one inch apart for standardized signal capture.

and the shape of the pottery shard, additional clamps may be necessary for sample stabilization. It is important to record the exact signal-capturing setup, as the setup may interfere with the vibrational signal. In order to facilitate accurate comparisons, all pottery shards in the database library should be tested and recorded with specified settings.

Here we show the results from a commercially available, common 20th century unglazed, lead free pottery shard made in Mexico (**Figure 3(a)**). The recording is shown in **Figure 3(b)**. One can see the vibrational profile with spikes in the 9K, 6K, and 1K Hz range. In addition, one sees low frequency vibration in the below 10 Hz range. It is important to record and compare the full spectrum of spikes, including the low frequency vibrations plateau. The plateau represents the summation of low frequency spikes which may not be apparent as individual spikes, yet represent a part of the pottery shard's vibrational profile.

Figure 4(a) shows a similar 20th century glazed pottery piece, also from Mexico. The corresponding recording in **Figure 4(b)** showed spikes in the 4K, 1K, and 300 Hz range. In addition, one also sees low frequency vibration, although this one has a peak vibration frequency in the 30 Hz range. These two pottery samples are from similar regions in Mexico, but one can see the vibrational profiles can differentiate based upon different techniques of preparation.

4. Discussion

Big data analytics have had significant recent advances, with many algorithms developed for face recognition as a means of classifying photos uploaded on social media networks. The extraction of a unique signature for each image facilitates the identification of an individual by matching the signature to a database set of known of signatures (Yang et al., 2017). We previously reported the ability to identify pottery shards via a similar method of signature matching. Known pottery shards identified by archaeologists as representative samples from each time period and region can be analyzed, with vibrational signatures stored as a pottery vibrational signature library. Any new pottery shard can be compared to

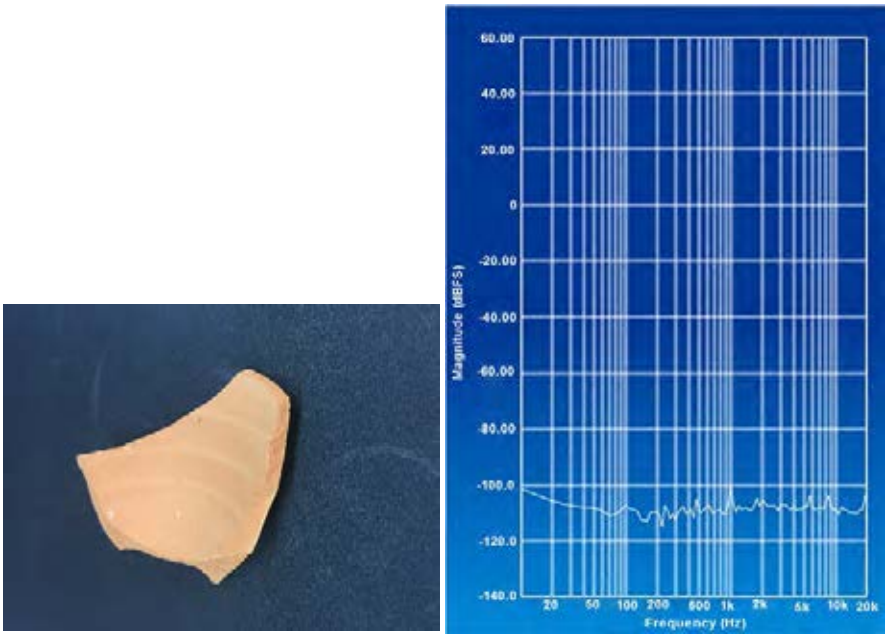

(a) (b)

Figure 3. (a): A commercially available, common 20th century unglazed, lead-free pottery shard made in Mexico; (b) the corresponding vibrational profile, with spikes in the 9K, 6K, and 1K Hz frequencies, and low frequency vibration in the below 10 Hz range.

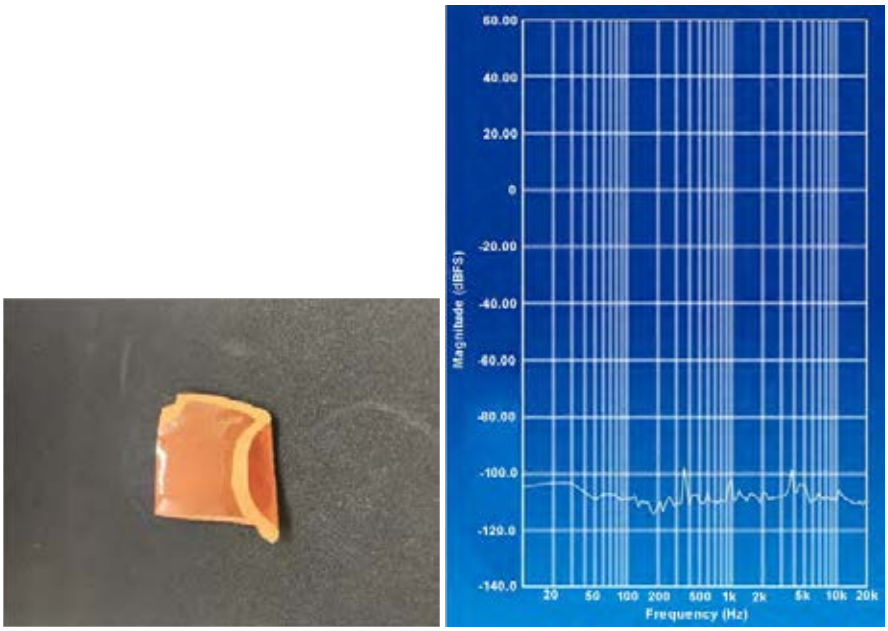

Figure 4. (a). A 20th century glazed pottery shard from Mexico; (b) the corresponding vibrational signature, with spikes in the 4K, 1K, and 300 Hz range, and low frequency vibration, with a peak at the 30 Hz range.

the signature library to identity the new shard. The vibrational signatures will be compared by time analysis, amplitude analysis, dampening analysis, and frequency analysis in order to find the best match (LDS, 2003).

In this article we detail the experimental set-up and procedures necessary for

such signature extraction. The system is designed to be portable so that it can be easily setup in a field lab for on-site, real-time analysis. The paper also shows the vibrational profiles from 20th century commercially available pottery shards, and such vibrational profiles can serve as calibration markers for researchers setting up a new system. This particular brand of pottery is common and commercially available. Once a new researcher has assembled the suggested setup for capturing vibrational signatures, one should start by recording the signature from the above standard pottery shard to ensure one can capture the standard wave form displayed in the article. We were able to observe unique vibrational patterns on two pottery shards manufactured in Mexico with similar soil composition, with the main difference being the firing technique and glazing finish. The fact that their differences can be reflected in their distinctive wave patterns is useful, and confirms the pathway of differentiating pottery from other areas.

In the current setup, all of the necessary equipment is commercially available, relatively affordable, and easy to assemble. It is the hope that, with this article, other archaeologists can benefit from the system and utilize the vibrational method of pottery shard identification.

Different energy sources can be used, and this paper details just three of the current options. Researchers are recommended to explore the vibrational patterns from other energy sources, such as microwaves, X-rays, or infrared waves. It is expected that each type of pottery will register a unique signature with each energy source. All of these vibrational waves can be compiled into a shared library to allow for collaboration and research cooperation.

References

Chen, B. (2017). *Pottery Shard Analysis Using Matching Vibration Signatures.* https://patents.google.com/patent/US20170307570A1/en

Eddine, A. K. J., Lenti, L., & Semblat, J.-F. (2017). Vibrations in Soil: A spectral Prediction Method. *Procedia Engineering, 199,* 2675-2680. https://doi.org/10.1016/j.proeng.2017.09.546

Gazetas, G. (1982). Vibrational Characteristics of Soil Deposits with Variable Wave Velocity. *International Journal for Numerical and Analytical Methods in Geomechanics, 6,* 1-20. https://doi.org/10.1002/nag.1610060103

Historical Archaeology at the Florida Museum of Natural History (2018). *Introduction to Ceramic Identification.* http://www.floridamuseum.ufl.edu/

Hunt, A. (2017). *The Oxford Handbook of Archaeological Ceramic Analysis.* Oxford: Oxford University Press. https://doi.org/10.1093/oxfordhb/9780199681532.001.0001

Jacobsen, L. (1930). Motion of a Soil Subjected to a Simple Harmonic Ground Vibration. *Bulletin of the Seismological Society of America, 20,* 160-195.

Kitovas, V., Stelmokaitis, G., & Doroševas, V. (2016). Investigation of Vibrations Influence on Clay Soil Parameters. *Journal of Sustainable Architecture and Civil Engineering, 4,* 60-67.

LDS Dactron Application Note (2003). *Basics of Structural Vibrational Testing and Analysis.* https://www.calpoly.edu/~cbirdson/Publications/AN011%20Basics%20of%20Structura

l%20Testing%20%20Analysis.pdf

MIT News (2014). *Extracting Audio from Visual Information Algorithm Recovers Speech from the Vibrations of a Potato-Chip Bag Filmed through Soundproof Glass.* http://news.mit.edu/2014/algorithm-recovers-speech-from-vibrations-0804

Parikh, S., Giyne, K. et al. (2014). Soil Chemical Insights Provided through Vibrational Spectroscopy. *Advances in Agronomy, 126,* 85-91. https://doi.org/10.1016/B978-0-12-800132-5.00001-8

Renfrew, C., & Bahn, P. (1991). *Archaeology: Theories, Methods, and Practice.* London: Thames & Hudson.

Robertson, A. H. J., Shand, C., & Perez-Fernandez, E. (2018). *The Application of Fourier Transform Infrared, near Infrared and X-Ray Fluorescence Spectroscopy to Soil Analysis.* https://www.spectroscopyeurope.com/article/application-fourier-transform-infrared-near-infrared-and-x-ray-fluorescence-spectroscopy

Yang, J., Luo, L. et al. (2017). Nuclear Norm Based Matrix Regression with Applications to Face Recognition with Occlusion and Illumination Changes. *IEEE Transactions on Pattern Analysis and Machine Intelligence, 39,* 156-171. https://doi.org/10.1109/TPAMI.2016.2535218

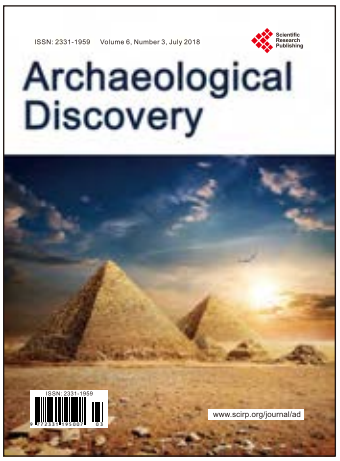

Call for Papers

Archaeological Discovery

ISSN Print: 2331-1959 **ISSN Online: 2331-1967**

http://www.scirp.org/journal/ad

Archaeological Discovery (AD) is an international journal dedicated to the latest advancement in the study of Archaeology. The goal of this journal is to provide a platform for scientists and academicians all over the world to promote, share, and discuss various new issues and developments in different areas of Archaeological studies.

Subject Coverage

All manuscripts must be prepared in English, and are subject to a rigorous and fair peer-review process. Accepted papers will immediately appear online followed by printed hard copy. The journal publishes original papers covering a wide range of fields but not limited to the following:

- Aerial Archaeology
- Archaeological Method and Theory
- Archaeological Science
- Archaeometry
- Art Archaeology
- Environmental Archaeology
- Ethnoarchaeology
- Experimental Archaeology
- Field Archaeology
- Geoarchaeology
- Historical Archaeology
- Island and Coastal Archaeology
- Lithic Studies
- Maritime Archaeology
- Prehistoric Archaeology
- Religious Archaeology
- Social Archaeology
- Underwater Archaeology
- World Archaeology
- Zooarchaeology

We are also interested in: 1) Short reports — 2-5 page papers in which an author can either present an idea with a theoretical background but has not yet completed the research needed for a complete paper, or preliminary data; 2) Book reviews — Comments and critiques, special peer-reviewed issue for colloquia, symposia, workshops.

Website and E-Mail

http://www.scirp.org/journal/ad **E-mail: ad@scirp.org**

What is SCIRP?

Scientific Research Publishing (SCIRP) is one of the largest Open Access journal publishers. It is currently publishing more than 200 open access, online, peer-reviewed journals covering a wide range of academic disciplines. SCIRP serves the worldwide academic communities and contributes to the progress and application of science with its publication.

What is Open Access?

All original research papers published by SCIRP are made freely and permanently accessible online immediately upon publication. To be able to provide open access journals, SCIRP defrays operation costs from authors and subscription charges only for its printed version. Open access publishing allows an immediate, worldwide, barrier-free, open access to the full text of research papers, which is in the best interests of the scientific community.

- High visibility for maximum global exposure with open access publishing model
- Rigorous peer review of research papers
- Prompt faster publication with less cost
- Guaranteed targeted, multidisciplinary audience

Scientific Research Publishing

Website: http://www.scirp.org

Subscription: sub@scirp.org

Advertisement: service@scirp.org